UC Riverside

UC Riverside Electronic Theses and Dissertations

Title

The Rise and Fall of the Stars in the Brain: Astroglia in Disease and Inflammation

Permalink

https://escholarship.org/uc/item/21t1t389

Author

David, Clement Nicolas

Publication Date

2015

Peer reviewed|Thesis/dissertation

eScholarship.org Powered by the California Digital Library
University of California

UNIVERSITY OF CALIFORNIA
RIVERSIDE

The Rise and Fall of the Stars in the Brain: Astroglia in Disease and Inflammation

A Dissertation submitted in partial satisfaction
of the requirements for the degree of

Doctor of Philosophy

in

Neuroscience

by

Clément David

March 2015

Dissertation Committee:
Dr. Emma H. Wilson, Chairperson
Dr. Monica J. Carson
Dr. Todd A. Fiacco

Copyright by
Clément David
2015

The Dissertation by Clément David is approved:

_____

_____

_____

Committee Chairperson

University of California, Riverside

ACKOWLEGDMENTS

I cannot thank my friend and mentor Dr. Emma Wilson enough for the incredible experience I had in her lab over the last 4 years. Dr. Wilson has been an amazing mentor, allowing me to explore my own ideas and execute my own experiments while giving valuable and precise input. She has always encouraged me to present my work at various national and international conferences, greatly contributing to my scientific networking. Furthermore, my research has benefited tremendously from her collaborative spirit and has helped me develop as a scientist. On a personal level, Dr. Wilson has been a great friend, and it was a real pleasure for me to see her family grow as I started mine. I will always cherish the many memories created in her lab.

Although not official, I consider Dr. Monica Carson my co-mentor. She has been extremely generous in her time and resources in helping me develop as a scientist. As the director of our Center for Glial-Neuronal Interactions, Dr. Carson offered me a very fruitful opportunity in helping organize our annual meeting. This resulted in valuable networking exposure and greater involvement in the scientific community. I truly appreciate the constant guidance from this jovial advisor.

Undeniably, my qualification exam and guidance committee members—Dr. Ameae Walker, Dr. Todd Fiacco, Dr. Devin Binder, Dr. Monica Carson and Dr. Peter Hickmott—have contributed greatly to my progress in thinking like a scientist and connecting the dots properly. These advisors have closely mentored me during and after my qualification exam, expanding my knowledge and giving me the tools needed to succeed on my own. I am forever grateful for their time and honest input.

None of this work would have been possible without the daily support of my labmates, both current and past. My initial student mentor, Phil Nance, has been a continuing friend whom I know I can always count on both personally and professionally. I would have never made it through without our occasional “beer lunches”. I want to thank Shahani Noor, Kathryn McGovern, Danielle Worth and Tyler Landrith for all the help, input and support throughout my stay in the Wilson lab. Friends from other labs—Charles Abbott, Matt Valdez, Jacqueline Hubbard, and Jenny Szu have also been the best colleagues one could ask for. Thank you all for the beer, the venting and the support as we all progressed through this journey.

To the most dedicated undergraduate student I know—Elma Frias—you have been a pleasure to work with over the last few years. What started as my mentoring and teaching you basic science techniques ended in a collaborative, exciting and work-filled bond. I truly appreciate your dedication and passion for science and your insatiable thirst for knowledge and work. Your work ethic has helped us finish two wonderful projects and collect novel, exciting data. I will always remember the 2 months we came in on each weekend at 4:00 AM to collect our microdialysis. I see an exciting future for you in science and am eager to work with you again.

To my Mom, Dad and Step-Dad: You guys are to blame for this! I appreciate your high expectations and am grateful for always being held to the highest degree of quality in everything that I do. Having always been there for me, and pushing me to be the best that I could be has defined me and has enabled me to excel personally and professionally: Thank you so very much.

Everyone knows a PhD is hard, and even harder when you have a family. What is often not spoken of is that it is also hard *on* the family. My wonderful fiancée, Meredith and my children—Victoria, Christian, and Everest have had to sacrifice so much for me to succeed. I could have not done any of this without their support. Meredith has been by my side for every high and low, being a steady rock in my emotional and stress roller coaster. The kids have been tremendously helpful, around the house, with the pregnancy and with their new baby sister, taking stress off of my shoulders on work-filled weekends. I cannot express how lucky and grateful I am to have had such an understanding, patient and supportive family as we adventured through this journey.

Chapter 2 and 3 of this dissertation, in part or in full, are reprints of material as it appears in *Brain Research,* 1481:71-78, 2012*;* and *ASN Neuro* (In press) respectively and are used here with permission of the publishers.

DEDICATION

To

My Father,

Thierry André David

ABSTRACT OF THE DISSERTATION

The Rise and Fall of the Stars in the Brain: Astroglia in Disease and Inflammation

by

Clément David

Doctor of Philosophy, Graduate Program in Neuroscience
University of California, Riverside, March 2015
Dr. Emma H. Wilson, Chairperson

The brain is an extremely complex organ composed of neuronal and non-neuronal cells working *en concerto* to maintain what we perceive as emotions, thoughts, memories, speech, movement, and much more. Although neurons, and their networks, are the cells responsible for the functional outcome of the brain; glial cells play a crucial role in maintaining homeostasis and are increasingly thought of as active modulators of neuronal function. Astrocytes are large, star shaped glial cells responsible for a multitude of functions including glutamate homeostasis, potassium buffering, metabolic support and some immune functions. Because astrocytes are so critical for normal brain functioning, a loss of function or a gain of deleterious function can severely alter brain chemistry, cause neurodegeneration or worsen an underlying disease. In this thesis, Chapter 2 and 3 discuss potential therapeutics for glioblastoma multiforme (GBM). GBMs usually occur spontaneously, following severe genetic mutations in astrocytes, which then proliferate uncontrollably and cause large, metastasizing tumors and eventually death. GBMs modify their environment, causing neighboring astrocytes and

other cells to create a permissive environment for tumor growth. Chapter 2 investigates the changing immune environment in GBMs while Chapter 3 focuses on a direct chemical therapeutic. Chapter 4 of this thesis examines the extent of neuropathology associated with a loss in astrocytes' primary function: the control of extracellular glutamate. Although losing a degree of this critical function is associated with many diseases such as Alzheimer's, amyotrophic lateral sclerosis, epilepsy and more; here, we will investigate it in the context of a prevalent chronic infection with the protozoan parasite *Toxoplasma gondii*. Whether gaining a deleterious genetic mutation, or losing a critical homeostatic function; disruption of astrocyte functioning in the brain has profound detrimental effects and should be considered as therapeutic targets.

TABLE OF CONTENTS

CHAPTER 1: Introduction. 1

1.1 The Anatomy and Function of Astrocytes 2
1.2 Astrocytes and Gliomas 4
1.3 SPARC, Stabilin-1 and Astroglia 7
1.4 Astrocytes in Injury, Infection and Immunity 8
1.5 Chronic Infection with *Toxoplasma* 11
1.6 Behavior and Infection 13
1.7 The Regulation of Glutamate by Astrocytes 16
1.8 References 20

CHAPTER 2: Stabilin-1 Expression in Tumor Associated Macrophages. 34

2.1 Abstract 35
2.2 Introduction 36
2.3 Materials and Methods 39
2.4 Results 42
2.4.1 Scavenger receptor stabilin-1 is expressed in early glioma 42
2.4.2 Stabilin-1 expression on macrophages decreases with tumor growth 43
2.4.3 Stabilin-1 expressing macrophages also express CD40, MMR 44
2.5 Discussion 46
2.6 Figures and Legends 49
2.7 References 55

CHAPTER 3: Antitumor activity of a polypyridyl chelating ligand:
in-vitro and *in-vivo* inhibition of glioma. 58

3.1 Abstract 59
3.2 Introduction 60
3.3 Materials and Methods 64
3.4 Results 68
3.4.1 SBP inhibits glioma cell growth *in-vitro* 68
3.4.2 SBP induces GL-26 apoptosis 69

3.4.3 SBP inhibits *in-vivo* glioma growth 70
3.4.4 SBP does not cause overt peripheral pathology 73
3.5 Discussion 74
3.6 Figures and Legends 79
3.7 References 89

CHAPTER 4: *Toxoplasma gondii* infection disrupts CNS glutamate homeostasis and neuronal connectivity: implications for behavioral abnormality. 94

4.1 Abstract 95
4.2 Introduction 97
4.3 Materials and Methods 101
4.4 Results 108
4.4.1 Infection induces profound and chronic astrocytic morphological and molecular changes 108
4.4.2 Infection with *Toxoplasma* causes profound neuronal pathology 110
4.4.3 Glutamate extracellular concentrations increase during infection 111
4.4.4 Ceftriaxone does not alter the immune response to *Toxoplasma* infection 114
4.4.5 Ceftriaxone specifically rescues glutamate transporter GLT-1 115
4.4.6 Ceftriaxone is neuroprotective during infection with *Toxoplasma* 116
4.4.7 Infection with *Toxoplasma* disrupts neuronal networks and changes behavior 118
4.5 Discussion 122
4.6 Figures and Legends 126
4.7 References 148

CHAPTER 5: Conclusion and Perspectives. 154

5.1 Conclusion and Future Directions 155
5.2 References 160

LIST OF FIGURES

Figure 1: Regulation of Glutamate 19

Figure 2-1: Stabilin-1 expression in the tumor environment 50

Figure 2-2: Stabilin-1 expression on macrophages 52

Figure 2-3: Stabilin-1 expressing macrophages change as the tumor progresses 54

Scheme 3-1: Molecular structure of 2,9-di-*sec*-butyl-1,10-phenanthroline (SBP) 80

Figure 3-1: *In-vitro* GL-26 inhibition with SBP 82

Figure 3-2: The compound SBP induces apoptosis 84

Figure 3-3: SBP inhibits *in-vivo* glioma growth 86

Figure 3-4: SBP does not cause peripheral pathology 88

Figure 4-1: Infection induces profound and chronic astrocytic morphological and molecular changes 127

Figure 4-2: Infection with *Toxoplasma* causes profound neuronal pathology 129

Figure 4-3: Glutamate extracellular concentrations increase during infection 131

Figure 4-4: Ceftriaxone does not alter the immune response to *Toxoplasma* infection 133

Figure 4-5: Ceftriaxone specifically rescues glutamate transporter GLT-1 135

Figure 4-6: Ceftriaxone is neuroprotective during infection with *Toxoplasma* 137

Figure 4-7: Infection with *Toxoplasma* disrupts neuronal networks and changes behavior 139

Supplemental Figure 4-1: Infection with *Toxoplasma* induces dynamic changes in essential amino acids 141

Supplemental Figure 4-2: Infection with *Toxoplasma* induces a loss in GLT-1 in the resistant BALB/c mouse 143

Supplemental Figure 4-3: Infection with *Toxoplasma* does not affect motility 145

Supplemental Figure 4-4: Treatment with Ceftriaxone does not alter extracellular amino acid concentrations 147

CHAPTER ONE

Introduction

1.1 The Anatomy and Function of Astrocytes:

The early, neurocentric notion that all brain function such as speech, motor control, emotions, and decision-making was all attributed to neurons and their electrochemical properties has been widely dismissed. Although neurons are obviously an essential component of the brain, an increasingly large amount of studies demonstrate the role of glia in not only supporting neurons, but actively modulating the central nervous system (CNS). Initially termed glia to refer to their postulated role as the "glue of the brain", glia have shown to be much more complex than simply a scaffold for neurons to operate on. The term glia encompasses both macroglia (oligodendrocites, astrocytes, ependymal cells, and radial glia) and microglia, which are the resident macrophages of the CNS. Though the maintenance of myelin by oligodendrocytes and the creation and secretion of cerebrospinal fluid by ependymal cells is clearly vital in the CNS, this dissertation thesis will focus on the function of astrocytes in the CNS in health and disease.

Astrocytes are, as their name implies, star-like cells whose processes cover the entire brain without overlapping their functional domains. They are histologically identified primarily by their positive expression of the cytoskeletal protein glial fibrillary acidic protein (GFAP), although not all populations of astrocytes are GFAP positive (Hertz et al., 1999; Hatton, 2002; Lin and Bergles, 2004; Sofroniew and Vinters, 2010). Astrocytes extend their processes to a multitude of targets: 1) Intimately wrapping around blood vessels in the CNS, thus creating an additional physical obstacle in the blood brain barrier and controlling blood flow (Metea and Newman, 2006; Attwell et al., 2010;

Sofroniew and Vinters, 2010). 2) Astrocyte processes are interconnected via gap junctions composed of connexin-43 and connexin-30 (Ogata and Kosaka, 2002; Nagy et al., 2004) allowing for small molecules such as potassium and glutamate in their cytoplasm to diffuse rapidly from one area of the CNS. This adaptation is critical when considering the role astrocytes play in potassium buffering during heavy neuronal firing (Nedergaard et al., 2003; Nicchia et al., 2005; Ball et al., 2007; Wetherington et al., 2008; Strohschein et al., 2011). 3) Processes also envelop synapses, thus creating a close contact between the astrocyte and neuronal communication (Bergles et al., 1999; Bushong et al., 2002; Ogata and Kosaka, 2002; Lin and Bergles, 2004; Halassa et al., 2007). Furthermore, a recent study has shown evidence for the existence of sandwich synapses, where astrocytic processes are wedged in between the pre and post synaptic neurons and serve as an intermediate in communication (Rozanski et al., 2013a; Rozanski et al., 2013b).

Astrocytes perform many complex functions, which cannot be all described here in detail. Here, we will review a few key functions, mainly pertaining to their capability and critical role in buffering and maintenance of extracellular molecules. Many studies have demonstrated the critical role of astrocytes in buffering potassium following intense neuronal firing, with important implications for seizures and epilepsy (Wetherington et al., 2008; Strohschein et al., 2011; Jin et al., 2013). Astrocytic processes enveloping synapses express at high density the potassium channel Kir 4.1 (Nagelhus et al., 2004) along with the bi-directional water channel AQP-4 (Neely et al., 2001; Amiry-Moghaddam et al., 2003; Furman et al., 2003; Noell et al., 2007; Wolburg et al., 2009;

Nicchia et al., 2010). The co-expression of these channels and transporters, along with others such as the sodium/bicarbonate co-transporter (NBC) (Nagelhus et al., 2004) allows for clearance of the accumulating potassium and CO2 following neuronal firing events (Nagelhus et al., 2004; Eid et al., 2005; Binder et al., 2006; Djukic et al., 2007; Hsu et al., 2007; Strohschein et al., 2011; Binder et al., 2012; Lee et al., 2012; Jin et al., 2013). The increasing intracellular concentration of potassium in astrocytes can then be quickly diffused by the network of gap junction coupled astrocytes (Nagelhus et al., 2004; Nicchia et al., 2005; Strohschein et al., 2011). Another molecule which is critical to remove during neuronal activity is the major excitatory neurotransmitter, glutamate. Glutamate is also taken up by astrocytes following its release at the synaptic level. Astrocytes maintain a tight control on glutamate uptake and are able to efficiently remove excess extracellular glutamate mainly through the activity of the glutamate transporters GLT-1 and GLAST (Rothstein et al., 1996; Bergles et al., 1999; Daikhin and Yudkoff, 2000; Gegelashvili et al., 2000; Danbolt, 2001) . The detailed mechanism of glutamate synthesis and uptake by astrocytes will be discussed in section 1.7.

1.2 Astrocytes and Gliomas:

Glioblastoma multiforme (GBM) is the most common form of CNS tumors. Current therapies include a combination of chemotherapy, radiotherapy and surgical removal (Stupp et al., 2002; Stupp et al., 2005; Mutter and Stupp, 2006; Furnari et al., 2007; Ajaz et al., 2014). However, unless treated in the early stages, GBMs are incurable and have a median survival of less than 1 year (Friedman et al., 2000; Furnari et al.,

2007). In recent years, increase understanding of the molecular and biological mechanisms of GBMs as well as advances in technological genetic tools allows for greater hope in developing therapies to slow or eradicate these fast growing tumors. GBMs are classified histologically as actrocytomas, oligodendrogliomas or oligoastrocytomas (Louis et al., 2007). GBMs arise most commonly from astrocytes and are defined by the very features that make them so deadly: uncontrolled proliferation, resistance to apoptosis, tendency to be necrotic, prolific angiogenesis, and diffuse infiltration. GBMs are classified into different progressive WHO derived scale of I-IV (Louis et al., 2007). Grade I tumors are the only tumors considered to be curable if they can be surgically removed. Grade II tumors are categorized by moderate proliferation and invasion, which may progress slowly but are incurable by surgery. Grade III and IV tumors are rapidly proliferating, increasingly invasive and exhibit increased necrosis and angiogenesis (Louis et al., 2007).

An additional sub-classification has been created for GBMs to differentiate between primary GBMs which appear as grade IV tumors *de-novo*, with no prior indication of lower grade tumors and secondary GBMs which progress through the 4 stages of malignancy (Louis et al., 2007). Primary GBMs are unfortunately more common and appear in older patients while secondary GBMs are rare and are more commonly found in patients under 45 years old (Furnari et al., 2007; Louis et al., 2007). Although the exact etiology of the disease is unknown, recent genetic advances have helped us understand what specific genes are altered in astrocytes and how those are associated with the different stages of the disease. Interestingly, although histologically

indistinguishable, primary and secondary GBMs are characterized by different genetic mutations reviewed in Furnari et al (Furnari et al., 2007).

In addition to being the main cause of CNS tumors, non-tumorigenic astrocytes are also thought to play a role in inadvertently aiding tumor progression and invasiveness. Astrocytes near the GBM display a reactive phenotype, with increased expression of GFAP and are thought to aid in tumor invasiveness, and proliferation (Charles et al., 2011). It has been shown that gliomas directly exploit their neighboring astrocytes to activate MMP-2 and increase their invasive phenotype (Le et al., 2003). Another recent study demonstrated *in-vitro* that glioma contact with non-tumorigenic astrocytes caused a change in the astrocytes' phenotype which resulted in a more permissive environment to glioma invasion with marked increases in extracellular remodeling proteins MMP-2 and SPARC (Gagliano et al., 2009). Furthermore, a study measuring expression of genes associated with movement and migration demonstrated that astrocytes significantly increase the invasion ability of GBM stem-like cells (Rath et al., 2013) in culture. In addition to using astrocytes to increase their proliferative and invasive potential, gliomas can also inactivate astrocyte expression of p53, even in the presence of DNA damage (Biasoli et al., 2014). Although, classically, p53 is thought as having cell-autonomous function, recent evidence suggests that p53 can exert a non-cell autonomous function, mainly through the regulation of secreted factor (Khwaja et al., 2006; Rangel et al., 2014). These studies, and many more, suggest that gliomas actively modify their environment to promote their growth and inhibit their death, making it extremely difficult to eradicate them.

1.3 SPARC, Stabilin-1 and Astroglia:

Secreted protein acidic and rich in cysteine (SPARC), also known as Osteonectin, is an extracellular matrix (ECM) remodeling protein and is highly expressed during development, tissue remodeling and repair (Bradshaw, 2009). SPARC facilitates ECM remodeling by acting as an anti-adhesive and modulating collagen assembly (Motamed and Sage, 1998). Increases in SPARC during GBMs are associated with increased metastasis (Golembieski et al., 1999; Golembieski et al., 2008; Yunker et al., 2008). SPARC can be produced by a variety of cell types including fibroblasts, endothelial cells, vascular smooth muscle cells, macrophages and astrocytes (Brekken and Sage, 2001). During GBM, SPARC released by astrocytes could contribute to increased tumor invasiveness by decreasing cell adhesion. The mechanism by which SPARC decreases cell adhesion is not fully understood; however, it is thought that SPARC disrupts local adhesion and actin fibers (Murphy-Ullrich et al., 1995; Bradshaw et al., 1999). Indeed, early studies have shown that fibroblasts treated with SPARC do not spread and attach incorrectly (Lane and Sage, 1990).

The only known receptor for SPARC is stabilin-1, expressed on macrophages and endothelial cells (Kzhyshkowska, 2006; Kzhyshkowska et al., 2006; Park et al., 2009; Palani et al., 2011; Workman and Sage, 2011). As a scavenger receptor, stabilin-1 binds, internalizes and degrades SPARC through the endosomal pathway (Kzhyshkowska et al., 2004; Kzhyshkowska, 2006; Kzhyshkowska et al., 2006; Kzhyshkowska and Krusell, 2009; Park et al., 2009; Palani et al., 2011). Although SPARC is present in the tumor environment, not much is known about the distribution, expression pattern and density of

its receptor stabilin-1. Infiltrating alternatively activated macrophages expressing stabilin-1 might have the potential of reducing extracellular SPARC concentration and slowing tumor progression. With their proximity within and around the glioma, tumor associated macrophages (TAMs) have the potential of slowing or even killing the glioma. However, TAMs, which comprise up to 50% of the tumor mass (Solinas et al., 2009), create a permissive environment for tumor invasion and proliferation (Talmadge et al., 2007; Mantovani et al., 2011) and are usually associated with a poorer prognosis (Bingle et al., 2002; Zhang et al., 2011). One study confirmed *ex-vivo*, that stabilin-1 is present on alternatively activated infiltrating TAMs early in disease (David et al., 2012). However, as the tumor progresses, stabilin-1 expression decreases and the proportion of alternatively activated macrophages significantly decreases (David et al., 2012). It appears that GBMs modify infiltrating macrophages such that stabilin-1 expression is significantly decreased and a tumor permissive phenotype is produced (Vasievich and Huang, 2011; David et al., 2012). The potential benefit of chronic stabilin-1 expression in GBM remains to be elucidated.

1.4 Astrocytes in Injury, Infection and Immunity:

Far from their passive supportive role initially proposed by early glia research, astrocytes perform not only complex homeostatic functions, but also mount significant immune responses in the CNS. With the presence of the blood brain barrier and low MHCII expression, the CNS has long been regarded as an immune privileged site, with circulating T-cells, B-cells and other leukocytes not actively crossing into the brain

without specific signals (Ransohoff et al., 2003; Carson et al., 2006; Wilson et al., 2010). As cortical neurons do not regenerate (Fitzgerald and Fawcett, 2007), severe inflammation in the CNS can be devastating for the host, as evidenced by CNS autoimmune diseases such as multiple sclerosis (Baxter, 2007; Gonsette, 2008; Giraudon and Bernard, 2009; Bilbo et al., 2012). Although circulating leukocytes do not freely enter the brain without a stimulus (Ransohoff et al., 2003; Wilson et al., 2010), the brain is not left defenseless. Indeed, microglia—the brain's resident macrophage—are constantly surveilling the environment in the brain by extending and retracting their fine processes (Nimmerjahn et al., 2005). Microglia become activated and can mount rapid and powerful immune responses to injury, disease, and infection. Additionally, the phagocytic microglia are key in clearing debris and dead cells (Fischer et al., 1997; Carson et al., 1998; Strack et al., 2002; Carson et al., 2007).

Astrocytes also play a critical role in CNS immunity: they can upregulate and secrete critical cytokines and chemokines, present antigen, modify blood brain barrier permeability and their gap-junction interconnection allows for fast transmission of noxious signals. When reactive, astrocytes undergo profound changes in their morphology, significantly upregulating GFAP and, depending on the insult, swell dramatically (Stenzel et al., 2004; Wilson et al., 2009; Sofroniew and Vinters, 2010; Hyzinski-Garcia et al., 2011). Due to their presence throughout the entire brain, and their intimate relationship with synapses, the blood brain barrier, and each other; reactive astrocytes have the potential to exacerbate the underlying pathology through loss of essential functions or gain of damaging effects (Sofroniew and Vinters, 2010). As briefly

discussed previously, astrocytes have essential functions in ion regulation, glutamate uptake, blood brain barrier maintenance, regulation of synapses, and metabolic support. During a reactive state, the disruption or failure of these functions can exacerbate the existing pathology of various diseases such as infections, trauma, neurodegenerative diseases and others. For example, studies have demonstrated that the loss or disruption in glutamate uptake by reactive astrocytes can lead to neurodegeneration through excitotoxicity in ischemia, amyolotrophic lateral sclerosis, multiple sclerosis, trauma, and others (Rothstein et al., 1996; Obrenovitch and Urenjak, 1997; Danbolt, 2001; Swanson et al., 2004; Yi and Hazell, 2006; Gonsette, 2008; Foran and Trotti, 2009; Lau and Tymianski, 2010). Although losing an essential function can be extremely damaging to the CNS, reactive astrocytes can also gain detrimental functions in response to an insult. Although sometimes undeniably necessary, secretion of cytokines (Fischer et al., 1997; Swanson et al., 2004; Wilson and Hunter, 2004; Ploix et al., 2011; Rath et al., 2013), active release of excitotoxic glutamate (Takano et al., 2005; Bowens et al., 2013; Lee et al., 2013), and production of high levels of reactive oxygen species (Lee et al., 2013) all have the potential to worsen the underlying pathology.

While reactive astrocytes can be damaging in their response to injury, degeneration or pathogens, they are usually necessary in controlling further damage by the underlying disease (Stenzel et al., 2004; Wilson and Hunter, 2004; Drogemuller et al., 2008; Promeneur et al., 2013). For example, in *Toxoplasma* infection, astrocytic release of cytokines such as TNF-α and IL-6, chemokines such as IP-10 and CCL2, and expression of IFN-γ are critical in controlling parasite burden and inflammation (Suzuki

et al., 1989; Gazzinelli et al., 1993; Fischer et al., 1997; Suzuki et al., 1997; Halonen et al., 1998; Halonen and Weiss, 2000; Halonen and Taylor, 2001; Strack et al., 2002; Schlüter et al., 2003; Wilson and Hunter, 2004; Drogemuller et al., 2008; Ploix et al., 2011). Additionally, in a model of traumatic brain injury, ablation of reactive astrocytes caused a substantial increase in neuronal death and inflammation suggesting a protective role for reative astrocytes (Myer et al., 2006).

In healthy CNS tissue, astrocytes perform many homeostatic functions, regulate synapse development, and maintain the blood brain barrier. Following an insult to the brain such as infection, injury, or ischemia, astrocytes respond by becoming reactive and altering their morphology and expression phenotype. These alterations can include loss of function or gain in function, both of which can be detrimental to neurons and can exacerbate the disease. However, these responses are an effort to protect the CNS and are sometimes critical in preventing further damage.

1.5 Chronic Infection with *Toxoplasma*:

Toxoplasma gondii is an obligate intracellular protozoan parasite capable of infecting any nucleated cell in mammals and birds. The stomach of its definitive host—the feline—is where sexual replication of the parasite occurs and results in the highly resistant oocysts secreted in feces. These oocysts can persist in the environment and contaminate soil and water supply (Dabritz et al., 2007). Once ingested, by grazing cattle for example, oocysts convert to fast-replicating tachyzoites, which can infect any nucleated cell and spread through the body quickly (Dubey, 1986a, b; Dubey and Fayer,

1986). The infection is quickly controlled by Th-1 cells producing IFN-γ thus driving the parasite into conversion to slow replicating bradyzoites which can then encyst in any tissue type (Denkers and Gazzinelli, 1998). Although tissue cysts are present in most tissues, they are predominantly found in the brain where they remain for the life of the infected host (Ferguson and Hutchison, 1987; Lambert and Barragan, 2010). The resulting CNS infection requires a delicate balance between an immune response robust enough to control parasite burden but sufficiently restricted to avoid severe CNS damage (Gazzinelli et al., 1992; Suzuki et al., 1997; Denkers and Gazzinelli, 1998; Strack et al., 2002; Schlüter et al., 2003; Wilson and Hunter, 2004; Ploix et al., 2011; Nance et al., 2012). In humans, infection commonly occurs from the consumption of meats infected with tissue cysts or from oocysts contracted while changing cat litter boxes. *Toxoplasma* is considered one of the most successful parasites with seroprevalence rates of 10-20% in the US and upwards of 80% in parts of Europe and South America (Pappas et al., 2009).

In the immunocompetent individual, the resulting Th-1 response prevents uncontrolled parasite replication and the infection usually progresses unnoticed. In immunocompromised individuals however, the lack of an effective Th-1 response results in Toxoplasmosis, the disease state associated with *Toxoplasma* infection. This disease came to the public eye largely in the 1980s with the increase in immunocompromised patients due to the HIV epidemic (Contini, 2008). Toxoplasmosis is characterized by massive parasite replication resulting in large brain ring-enhancing lesions visible by MRI (Antinori et al., 1997), profound neurological symptoms and is often fatal if untreated (Antinori et al., 1997; Contini, 2008).

The CNS Th-1 immune response to *Toxoplasma* has been extensively studied in mice, and it is now understood that successful resistance to toxoplasmosis is a result of a complex and coordinated effort from multiple cell types. Astrocytes play several central roles in this multi-faceted concert: first, astrocyte activation and upregulation of IGTP, and subsequently IFN-γ, is critical for the control of *Toxoplasma* in the CNS (Halonen and Taylor, 2001; Drogemuller et al., 2008). Next, the secretion of chemokines such as IP-10 and CCL2 by astrocytes are vital and ensure entry of T-cells and macrophages, respectively, into the CNS (Halonen et al., 1998; Khan et al., 2000; Strack et al., 2002). The continuous entry into the CNS of activated CD4 and CD8 T-cells is required to protect against parasite reactivation (Gazzinelli et al., 1992).

While around 30% of the world human population is infected with *Toxoplasma*, and thus live with persistent CNS infection and inflammation, no overt signs of pathology or neurodegeneration have been reported in immunocompetent individuals. Considering the strong Th-1 response elicited by *Toxoplasma*, it is surprising that a pronounced phenotype resulting from chronic infection has not yet been apparent.

1.6 Behavior and Infection:

Although *Toxoplasma* infection has not yet been causally linked to any disease or psychiatric disorders in humans, accumulating correlative evidence appears to suggest the involvement of *Toxoplasma* in a wide range of neurodegenerative disease, psychiatric disorders, and behavioral abnormalities. Indeed, *Toxoplasma* is a significant risk factor in Parkinson's (PD) (Miman et al., 2010), Alzheimer's (AD) (Kusbeci et al., 2011), bipolar

disorder (Dickerson et al., 2014) and Schizophrenia (Yolken et al., 2001; Conejero-Goldberg et al., 2003; Torrey and Yolken, 2003; Webster et al., 2006; Torrey et al., 2007; Torrey et al., 2012). Interestingly, the seropositivity rate for anti-*T.gondii* IgG antibodies were 44.1% among AD patients (Kusbeci et al., 2011), 42.3% among PD patients (Miman et al., 2010), and an average of 23.4% for the age-matched control group in both studies. These studies demonstrate that AD and PD patients are twice as likely to be infected with *Toxoplasma* than age-matched individuals without the disease. Although this does not by any means prove causation, it raises an interesting question as to whether *Toxoplasma* infection could act as a trigger for certain neurodegenerative disorders. Furthermore, extensive work has demonstrated another correlation between infection with *Toxoplasma* and the development of Schizophrenia. Reviewed in (Torrey and Yolken, 2003), a number of studies between 1953 and 1979 have consistently shown increased seropositivity for *Toxoplasma* in Schizophrenia and other severe psychiatric disorders using a variety of immunological assays. Although some of these early studies were flawed in lacking to describe the clinical parameters used to define Schizophrenia, or the origin and composition of their control groups; the consistency in their findings is striking. Since that time, Yolken and Torrey have replicated and expanded these studies and confirmed *Toxoplasma* infection as a significant risk factor in Schizophrenia and that Schizophrenics had significantly higher antibodies to *Toxoplasma* than age-matched controls (Yolken et al., 2001; Torrey and Yolken, 2003; Leweke et al., 2004; Torrey et al., 2007; Torrey et al., 2012). Furthermore, higher IgM antibodies to *Toxoplasma* are

also associated with mania (Dickerson et al., 2014), suggesting that infection isn't specific to one disease but rather may act as a trigger for a variety of disorders.

In line with *Toxoplasma* infection correlating to neurodegenerative and psychiatric disorders, it appears to be associated with a variety of behavioral and mood abnormalities as well. For the past 2 decades, studies of human behavior in *Toxoplasma* infected individuals have largely been led by Professor Flegr by using a combination of retrospective studies and administration of psychological exams reviewed in (Flegr, 2013a), (Flegr, 2013b) and (Flegr, 2007). Dr. Flegr has shown that individuals infected with *Toxoplasma* exhibit behavioral changes which increase with time since onset of infection (Flegr et al., 2000; Flegr et al., 2003; Flegr et al., 2011), display increase reaction time resulting in more automobile accidents (Flegr et al., 2009) and that sex-differences were present in psychological alterations as measured by Catell's questionnaire (Flegr et al., 1996).

While Dr. Jaroslav Flegr is the leading researcher in *Toxoplasma* induced behavioral changes in humans, many studies have investigated the effects of this infection on behavior in rodents. Analogous to the behavior changes observed in humans, rodents also display dramatic changes in behavior following infection with *Toxoplasma* (Gonzalez et al., 2007; Vyas et al., 2007; Hermes et al., 2008; Afonso et al., 2012; Vyas, 2013; Hari Dass and Vyas, 2014). Indeed, mice chronically infected with *Toxoplasma*, have a reduction in innate fear as evidenced by an increased amount of time spent in the open arms of an elevated plus maze (Gonzalez et al., 2007; Afonso et al., 2012). Strikingly, and in contrast to the human data, infection with *Toxoplasma* in rodents

causes very specific changes in behavior; most interesting is a study conducted by Vyas in 2007 demonstrating specific loss of aversion to cat odors following infection with *Toxoplasma* (Vyas et al., 2007). A follow up study proposed that loss of innate fear was occurring through epigenetic modulation in the amygdala (Hari Dass and Vyas, 2014). To attempt to tease out a mechanism for these prominent behavioral changes, other groups have looked extensively in the CNS, measuring subtle changes in anatomy, neurons complexity and general inflammation (Hermes et al., 2008; Cekanaviciute et al., 2014; Parlog et al., 2014). These neurological defects might contribute to the behavioral changes observed in infected animals. This is explored in greater detail in Chapter 4 of this dissertation.

1.7 The Regulation of Glutamate by Astrocytes:

As glutamate is the major excitatory neurotransmitter in the CNS, the implications of glutamate excitotoxicity are broad. Traditionally, elevated extracellular glutamate concentrations have been observed under acute CNS insults such as ischemia (Zhang et al., 2008) and traumatic brain injury (Obrenovitch and Urenjak, 1997; Werner and Engelhard, 2007). However, many studies have associated elevated ECS glutamate concentrations with neurodegenerative disorders such as amyotrophic lateral sclerosis (Foran and Trotti, 2009), multiple sclerosis (MS) (Gonsette, 2008), Alzheimer's disease (AD) (Schallier et al., 2011) and with CNS infections such as cerebral malaria (Miranda et al., 2010). Understanding the mechanisms that underlie elevated ECS concentrations of glutamate following CNS insults is critical in developing preventative measures to avoid

neuronal death. Any changes in extracellular glutamate concentrations could lead to major changes in neuronal biology in the brain. As discussed previously, this may support correlative studies suggesting *Toxoplasma* infection as a causative agent in a number of behavioral and psychological changes (Flegr et al., 1996; Flegr et al., 2000; Yolken et al., 2001; Torrey and Yolken, 2003; Webster et al., 2006; Flegr, 2007; Torrey et al., 2007; Flegr et al., 2009; Miranda et al., 2010; Flegr et al.; Torrey et al., 2012; Flegr, 2013a). These studies, coupled with behavioral studies done on mice which demonstrate increased risk seeking behavior and marked behavioral changes (Conejero-Goldberg et al., 2003; Vyas et al., 2007; Vyas, 2013), suggest that infection with *Toxoplasma gondii* alters brain chemistry, a focus of Chapter 4 of this thesis.

Although glutamate is readily available in the periphery, it does not cross the BBB and is thus virtually completely synthesized within the CNS, primarily by astrocytes. Astrocytes have the important job of regulating CNS glutamate levels by adjusting uptake, release, synthesis into glutamine and synthesis from α-ketoglutarate or lactate/alanine (Hertz et al., 1999; Danbolt, 2001; Hertz and Zielke, 2004). Although neurons can synthesize glutamate from glutamine through the enzymatic actions of glutaminase, they are unable to sustain glutamate production in the CNS without exhausting their carbon skeleton supply. Indeed, two key enzymes (pyruvate carboxylase and cytosolic malic enzyme) are restricted to astrocytes and are involved in: 1) *de-novo* synthesis (from glucose and pyruvate) of the carbon skeleton of glutamate, and 2) the return of the carbon skeleton of excess glutamate to the metabolic pathway for glucose oxidation, respectively. As a consequence, neurons constantly require new carbon

skeletons from glial cells to sustain their TCA cycle. When these supplies are withdrawn or slow down, neurons are unable to generate amino acid transmitters such as glutamate and their rate of oxidative metabolism is impaired. These processes are reviewed extensively here: (Hertz et al., 1999; Danbolt, 2001).

Following neuronal activity, the astrocytic glutamate transporters GLT-1 and GLAST are responsible for the large majority of the uptake of glutamate into astrocytes (Danbolt, 2001; Hertz and Zielke, 2004). Although both are expressed throughout the CNS, glutamate uptake is mediated predominantly by GLAST in the cerebellum and by GLT-1 in the cerebrum (Gegelashvili et al., 2000; Danbolt, 2001). Both transporters utilize ionic gradient to transport glutamate inside astrocytes: co-transporting three Na+ and one H+ cations and exporting one K+ ion (Owe et al., 2006); consequently, this process is very energy demanding as the Na+/K+ ATP pump must constantly work to restore ionic gradients (Rothstein et al., 1996; Gegelashvili et al., 2000; Danbolt, 2001). These transporters are extremely efficient as extracellular levels of glutamate would reach levels near 2nM in the absence of glutamate release (Levy et al., 1998). A decrease in GLT-1/GLAST transporters would cause a rapid rise in extracellular concentrations of glutamate. Furthermore, about 75% of glutamate taken up by astrocytes is converted to glutamine by glutamine synthetase (Hertz et al., 1999; Gegelashvili et al., 2000; Danbolt, 2001; Hertz and Zielke, 2004). This process allows transport of the amino acid back to neurons where it will be converted into glutamate by neuronal glutaminase for excitatory signaling. Glutamine synthetase activity along with glutamate transporters keeps astrocytic intracellular concentrations of glutamate between 500 and 3000μM; however,

during astrocyte activation, published data has demonstrated a reduction in glutamine synthetase and thus an increase in intracellular glutamate concentrations (Bristot Silvestrin et al., 2012).

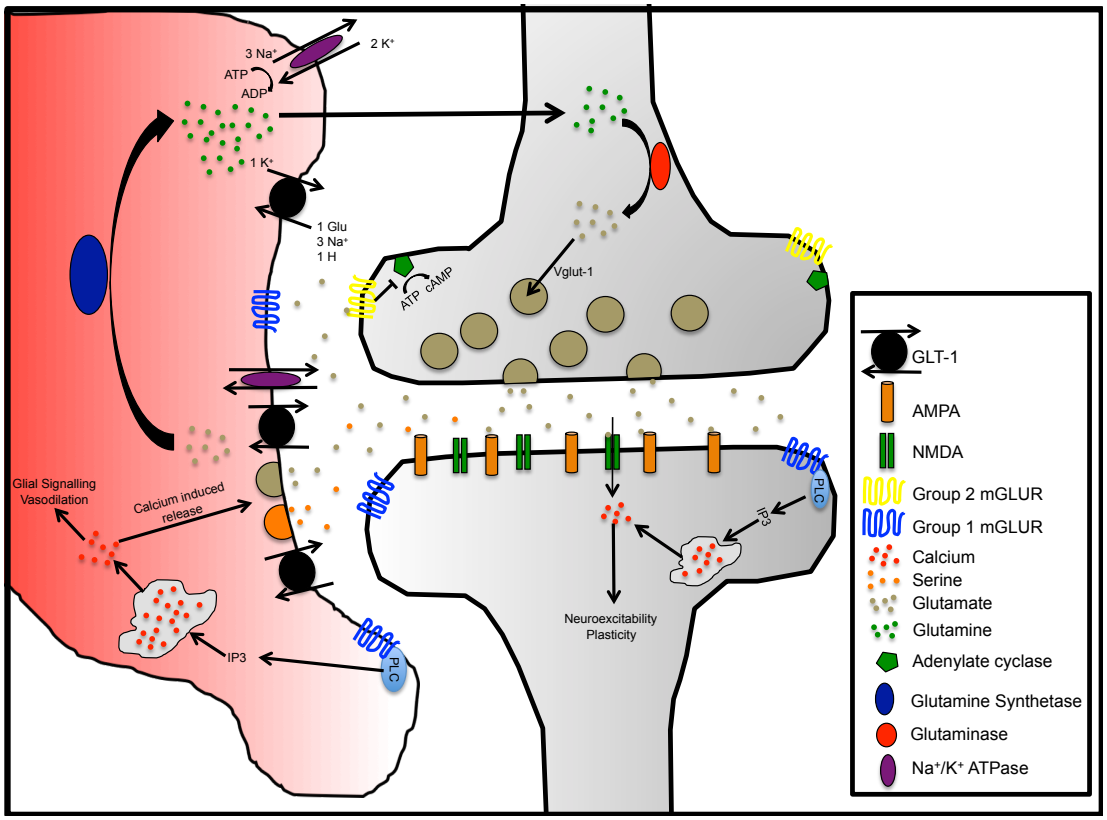

Fig 1. Regulation of Glutamate:
Glutamate uptake by GLT-1 on synaptic astrocytic processes (red) is dependent on Na^+/K^+ ATPase. Binding of extracellular glutamate to Group 1 and Group 2 mGLURs induce Ca^{2+} dependent intracellular signaling. Chronic stimulation of mGlurs can lead to excitotoxicity.

Astrocytes are undeniably the main regulators of extracellular levels of glutamate in the CNS. To prevent neuroexcitotoxicity related pathology, astrocytes must maintain healthy expression of glutamate transporters and glutamine synthetase. Chapter 4 discusses in detail our latest unpublished findings highlighting the loss of GLT-1 during infection with *Toxoplasma gondii* and the resulting neurophatology.

1.8 References:

1 Afonso C, Paixao VB, Costa RM (2012) Chronic Toxoplasma infection modifies the structure and the risk of host behavior. PLoS One 7:e32489.

2 Ajaz M, Jefferies S, Brazil L, Watts C, Chalmers A (2014) Current and investigational drug strategies for glioblastoma. Clin Oncol (R Coll Radiol) 26:419-430.

3 Amiry-Moghaddam M, Williamson A, Palomba M, Eid T, de Lanerolle NC, Nagelhus EA, Adams ME, Froehner SC, Agre P, Ottersen OP (2003) Delayed K+ clearance associated with aquaporin-4 mislocalization: phenotypic defects in brains of alpha-syntrophin-null mice. Proc Natl Acad Sci U S A 100:13615-13620.

4 Antinori A, Ammassari A, De Luca A, Cingolani A, Murri R, Scoppettuolo G, Fortini M, Tartaglione T, Larocca LM, Zannoni G, Cattani P, Grillo R, Roselli R, Iacoangeli M, Scerrati M, Ortona L (1997) Diagnosis of AIDS-related focal brain lesions: a decision-making analysis based on clinical and neuroradiologic characteristics combined with polymerase chain reaction assays in CSF. Neurology 48:687-694.

5 Attwell D, Buchan AM, Charpak S, Lauritzen M, Macvicar BA, Newman EA (2010) Glial and neuronal control of brain blood flow. Nature 468:232-243.

6 Ball KK, Gandhi GK, Thrash J, Cruz NF, Dienel GA (2007) Astrocytic connexin distributions and rapid, extensive dye transfer via gap junctions in the inferior colliculus: implications for [(14)C]glucose metabolite trafficking. J Neurosci Res 85:3267-3283.

7 Baxter AG (2007) The origin and application of experimental autoimmune encephalomyelitis. Nat Rev Immunol 7:904-912.

8 Bergles DE, Diamond JS, Jahr CE (1999) Clearance of glutamate inside the synapse and beyond. Curr Opin Neurobiol 9:293-298.

9 Biasoli D, Sobrinho MF, da Fonseca AC, de Matos DG, Romao L, de Moraes Maciel R, Rehen SK, Moura-Neto V, Borges HL, Lima FR (2014) Glioblastoma cells inhibit astrocytic p53-expression favoring cancer malignancy. Oncogenesis 3:e123.

10 Bilbo SD, Smith SH, Schwarz JM (2012) A lifespan approach to neuroinflammatory and cognitive disorders: a critical role for glia. J Neuroimmune Pharmacol 7:24-41.

11 Binder DK, Nagelhus EA, Ottersen OP (2012) Aquaporin-4 and epilepsy. Glia 60:1203-1214.

12 Binder DK, Yao X, Zador Z, Sick TJ, Verkman AS, Manley GT (2006) Increased seizure duration and slowed potassium kinetics in mice lacking aquaporin-4 water channels. Glia 53:631-636.

13 Bingle L, Brown NJ, Lewis CE (2002) The role of tumour-associated macrophages in tumour progression: implications for new anticancer therapies. The Journal of pathology 196:254-265.

14 Bowens NH, Dohare P, Kuo YH, Mongin AA (2013) DCPIB, the proposed selective blocker of volume-regulated anion channels, inhibits several glutamate transport pathways in glial cells. Mol Pharmacol 83:22-32.

15 Bradshaw AD (2009) The role of SPARC in extracellular matrix assembly. J Cell Commun Signal 3:239-246.

16 Bradshaw AD, Francki A, Motamed K, Howe C, Sage EH (1999) Primary mesenchymal cells isolated from SPARC-null mice exhibit altered morphology and rates of proliferation. Mol Biol Cell 10:1569-1579.

17 Brekken RA, Sage EH (2001) SPARC, a matricellular protein: at the crossroads of cell-matrix communication. Matrix Biol 19:816-827.

18 Bristot Silvestrin R, Bambini-Junior V, Galland F, Daniele Bobermim L, Quincozes-Santos A, Torres Abib R, Zanotto C, Batassini C, Brolese G, Goncalves CA, Riesgo R, Gottfried C (2012) Animal model of autism induced by prenatal exposure to valproate: altered glutamate metabolism in the hippocampus. Brain Res 1495:52-60.

19 Bushong EA, Martone ME, Jones YZ, Ellisman MH (2002) Protoplasmic astrocytes in CA1 stratum radiatum occupy separate anatomical domains. J Neurosci 22:183-192.

20 Carson MJ, Reilly CR, Sutcliffe JG, Lo D (1998) Mature microglia resemble immature antigen-presenting cells. Glia 22:72-85.

21 Carson MJ, Doose JM, Melchior B, Schmid CD, Ploix CC (2006) CNS immune privilege: hiding in plain sight. Immunol Rev 213:48-65.

22 Carson MJ, Bilousova TV, Puntambekar SS, Melchior B, Doose JM, Ethell IM (2007) A rose by any other name? The potential consequences of microglial heterogeneity during CNS health and disease. Neurotherapeutics 4:571-579.

23 Cekanaviciute E, Dietrich HK, Axtell RC, Williams AM, Egusquiza R, Wai KM, Koshy AA, Buckwalter MS (2014) Astrocytic TGF-beta Signaling Limits Inflammation and Reduces Neuronal Damage during Central Nervous System Toxoplasma Infection. J Immunol 193.

24 Charles NA, Holland EC, Gilbertson R, Glass R, Kettenmann H (2011) The brain tumor microenvironment. Glia 59:1169-1180.

25 Conejero-Goldberg C, Torrey EF, Yolken RH (2003) Herpesviruses and Toxoplasma gondii in orbital frontal cortex of psychiatric patients. Schizophr Res 60:65-69.

26 Contini C (2008) Clinical and diagnostic management of toxoplasmosis in the immunocompromised patient. Parassitologia 50:45-50.

27 Dabritz HA, Miller MA, Atwill ER, Gardner IA, Leutenegger CM, Melli AC, Conrad PA (2007) Detection of Toxoplasma gondii-like oocysts in cat feces and estimates of the environmental oocyst burden. J Am Vet Med Assoc 231:1676-1684.

28 Daikhin Y, Yudkoff M (2000) Compartmentation of brain glutamate metabolism in neurons and glia. J Nutr 130:1026S-1031S.

29 Danbolt NC (2001) Glutamate uptake. Prog Neurobiol 65:1-105.

30 David C, Nance JP, Hubbard J, Hsu M, Binder D, Wilson EH (2012) Stabilin-1 expression in tumor associated macrophages. Brain Res 1481:71-78.

31 Denkers EY, Gazzinelli RT (1998) Regulation and function of T-cell-mediated immunity during Toxoplasma gondii infection. Clin Microbiol Rev 11:569-588.

32 Dickerson F, Stallings C, Origoni A, Vaughan C, Katsafanas E, Khushalani S, Yolken R (2014) Antibodies to Toxoplasma gondii in individuals with mania. Bipolar Disord 16:129-136.

33 Djukic B, Casper KB, Philpot BD, Chin LS, McCarthy KD (2007) Conditional knock-out of Kir4.1 leads to glial membrane depolarization, inhibition of potassium and glutamate uptake, and enhanced short-term synaptic potentiation. J Neurosci 27:11354-11365.

34 Drogemuller K, Helmuth U, Brunn A, Sakowicz-Burkiewicz M, Gutmann DH, Mueller W, Deckert M, Schluter D (2008) Astrocyte gp130 expression is critical for the control of Toxoplasma encephalitis. J Immunol 181:2683-2693.

35 Dubey JP (1986a) A review of toxoplasmosis in cattle. Vet Parasitol 22:177-202.

36 Dubey JP (1986b) Toxoplasmosis. J Am Vet Med Assoc 189:166-170.

37 Dubey JP, Fayer R (1986) Sarcocystosis, toxoplasmosis, and cryptosporidiosis in cattle. Vet Clin North Am Food Anim Pract 2:293-298.

38 Eid T, Lee TS, Thomas MJ, Amiry-Moghaddam M, Bjornsen LP, Spencer DD, Agre P, Ottersen OP, de Lanerolle NC (2005) Loss of perivascular aquaporin 4 may underlie deficient water and K+ homeostasis in the human epileptogenic hippocampus. Proc Natl Acad Sci U S A 102:1193-1198.

39 Ferguson DJ, Hutchison WM (1987) An ultrastructural study of the early development and tissue cyst formation of Toxoplasma gondii in the brains of mice. Parasitol Res 73:483-491.

40 Fischer HG, Nitzgen B, Reichmann G, Hadding U (1997) Cytokine responses induced by Toxoplasma gondii in astrocytes and microglial cells. Eur J Immunol 27:1539-1548.

41 Fitzgerald J, Fawcett J (2007) Repair in the central nervous system. J Bone Joint Surg Br 89:1413-1420.

42 Flegr J (2007) Effects of toxoplasma on human behavior. Schizophr Bull 33:757-760.

43 Flegr J (2013a) How and why Toxoplasma makes us crazy. Trends Parasitol 29:156-163.

44 Flegr J (2013b) Influence of latent Toxoplasma infection on human personality, physiology and morphology: pros and cons of the Toxoplasma-human model in studying the manipulation hypothesis. J Exp Biol 216:127-133.

45 Flegr J, Kodym P, Tolarova V (2000) Correlation of duration of latent Toxoplasma gondii infection with personality changes in women. Biol Psychol 53:57-68.

46 Flegr J, Zitkova S, Kodym P, Frynta D (1996) Induction of changes in human behaviour by the parasitic protozoan Toxoplasma gondii. Parasitology 113 (Pt 1):49-54.

47 Flegr J, Lenochova P, Hodny Z, Vondrova M (2011) Fatal attraction phenomenon in humans: cat odour attractiveness increased for toxoplasma-infected men while decreased for infected women. PLoS Negl Trop Dis 5:e1389.

48 Flegr J, Klose J, Novotna M, Berenreitterova M, Havlicek J (2009) Increased incidence of traffic accidents in Toxoplasma-infected military drivers and protective effect RhD molecule revealed by a large-scale prospective cohort study. BMC Infect Dis 9:72.

49 Flegr J, Preiss M, Klose J, Havlicek J, Vitakova M, Kodym P (2003) Decreased level of psychobiological factor novelty seeking and lower intelligence in men latently infected with the protozoan parasite Toxoplasma gondii Dopamine, a missing link between schizophrenia and toxoplasmosis? Biol Psychol 63:253-268.

50 Foran E, Trotti D (2009) Glutamate transporters and the excitotoxic path to motor neuron degeneration in amyotrophic lateral sclerosis. Antioxid Redox Signal 11:1587-1602.

51 Friedman HS, Kerby T, Calvert H (2000) Temozolomide and treatment of malignant glioma. Clin Cancer Res 6:2585-2597.

52 Furman CS, Gorelick-Feldman DA, Davidson KG, Yasumura T, Neely JD, Agre P, Rash JE (2003) Aquaporin-4 square array assembly: opposing actions of M1 and M23 isoforms. Proc Natl Acad Sci U S A 100:13609-13614.

53 Furnari FB, Fenton T, Bachoo RM, Mukasa A, Stommel JM, Stegh A, Hahn WC, Ligon KL, Louis DN, Brennan C, Chin L, DePinho RA, Cavenee WK (2007) Malignant astrocytic glioma: genetics, biology, and paths to treatment. Genes Dev 21:2683-2710.

54 Gagliano N, Costa F, Cossetti C, Pettinari L, Bassi R, Chiriva-Internati M, Cobos E, Gioia M, Pluchino S (2009) Glioma-astrocyte interaction modifies the astrocyte phenotype in a co-culture experimental model. Oncol Rep 22:1349-1356.

55 Gazzinelli R, Xu Y, Hieny S, Cheever a, Sher a (1992) Simultaneous depletion of CD4+ and CD8+ T lymphocytes is required to reactivate chronic infection with Toxoplasma gondii. Journal of immunology (Baltimore, Md : 1950) 149:175-180.

56 Gazzinelli RT, Eltoum I, Wynn TA, Sher A (1993) Acute cerebral toxoplasmosis is induced by in vivo neutralization of TNF-alpha and correlates with the down-regulated expression of inducible nitric oxide synthase and other markers of macrophage activation. J Immunol 151:3672-3681.

57 Gegelashvili G, Dehnes Y, Danbolt NC, Schousboe A (2000) The high-affinity glutamate transporters GLT1, GLAST, and EAAT4 are regulated via different signalling mechanisms. Neurochem Int 37:163-170.

58 Giraudon P, Bernard A (2009) Chronic viral infections of the central nervous system: Aspects specific to multiple sclerosis. Rev Neurol (Paris) 165:789-795.

59 Golembieski Wa, Ge S, Nelson K, Mikkelsen T, Rempel Sa (1999) Increased SPARC expression promotes U87 glioblastoma invasion in vitro. International journal of developmental neuroscience : the official journal of the International Society for Developmental Neuroscience 17:463-472.

60 Golembieski Wa, Thomas SL, Schultz CR, Yunker CK, McClung HM, Lemke N, Cazacu S, Barker T, Sage EH, Brodie C, Rempel Sa (2008) HSP27 mediates SPARC-induced changes in glioma morphology, migration, and invasion. Glia 56:1061-1075.

61 Gonsette RE (2008) Neurodegeneration in multiple sclerosis: the role of oxidative stress and excitotoxicity. J Neurol Sci 274:48-53.

62 Gonzalez LE, Rojnik B, Urrea F, Urdaneta H, Petrosino P, Colasante C, Pino S, Hernandez L (2007) Toxoplasma gondii infection lower anxiety as measured in the plus-maze and social interaction tests in rats A behavioral analysis. Behav Brain Res 177:70-79.

63 Halassa MM, Fellin T, Takano H, Dong JH, Haydon PG (2007) Synaptic islands defined by the territory of a single astrocyte. J Neurosci 27:6473-6477.

64 Halonen SK, Weiss LM (2000) Investigation into the mechanism of gamma interferon-mediated inhibition of Toxoplasma gondii in murine astrocytes. Infection and immunity 68:3426-3430.

65 Halonen SK, Taylor GA (2001) Gamma Interferon-Induced Inhibition of Toxoplasma gondii in Astrocytes Is Mediated by IGTP. Society 69:5573-5576.

66 Halonen SK, Chiu F, Weiss LM (1998) Effect of cytokines on growth of Toxoplasma gondii in murine astrocytes. Infection and immunity 66:4989-4993.

67 Hari Dass SA, Vyas A (2014) Toxoplasma gondii infection reduces predator aversion in rats through epigenetic modulation in the host medial amygdala. Mol Ecol.

68 Hatton GI (2002) Glial-neuronal interactions in the mammalian brain. Adv Physiol Educ 26:225-237.

69 Hermes G, Ajioka JW, Kelly KA, Mui E, Roberts F, Kasza K, Mayr T, Kirisits MJ, Wollmann R, Ferguson DJ, Roberts CW, Hwang JH, Trendler T, Kennan RP, Suzuki Y, Reardon C, Hickey WF, Chen L, McLeod R (2008) Neurological and behavioral abnormalities, ventricular dilatation, altered cellular functions, inflammation, and neuronal injury in brains of mice due to common, persistent, parasitic infection. J Neuroinflammation 5:48.

70 Hertz L, Zielke HR (2004) Astrocytic control of glutamatergic activity: astrocytes as stars of the show. Trends Neurosci 27:735-743.

71 Hertz L, Dringen R, Schousboe A, Robinson SR (1999) Astrocytes: glutamate producers for neurons. J Neurosci Res 57:417-428.

72 Hsu MS, Lee DJ, Binder DK (2007) Potential role of the glial water channel aquaporin-4 in epilepsy. Neuron glia biology 3:287-297.

73 Hyzinski-Garcia MC, Vincent MY, Haskew-Layton RE, Dohare P, Keller RW, Jr., Mongin AA (2011) Hypo-osmotic swelling modifies glutamate-glutamine cycle in the cerebral cortex and in astrocyte cultures. J Neurochem 118:140-152.

74 Jin BJ, Zhang H, Binder DK, Verkman AS (2013) Aquaporin-4-dependent K(+) and water transport modeled in brain extracellular space following neuroexcitation. J Gen Physiol 141:119-132.

75 Khan IA, MacLean JA, Lee FS, Casciotti L, DeHaan E, Schwartzman JD, Luster AD (2000) IP-10 is critical for effector T cell trafficking and host survival in Toxoplasma gondii infection. Immunity 12:483-494.

76 Khwaja FW, Svoboda P, Reed M, Pohl J, Pyrzynska B, Van Meir EG (2006) Proteomic identification of the wt-p53-regulated tumor cell secretome. Oncogene 25:7650-7661.

77 Kusbeci OY, Miman O, Yaman M, Aktepe OC, Yazar S (2011) Could Toxoplasma gondii have any role in Alzheimer disease? Alzheimer Dis Assoc Disord 25:1-3.

78 Kzhyshkowska J (2006) Stabilin-1, a homeostatic scavenger receptor with multiple functions. Journal of Cellular and Molecular Medicine 10.

79 Kzhyshkowska J, Krusell L (2009) Cross-talk between endocytic clearance and secretion in macrophages. Immunobiology 214:576-593.

80 Kzhyshkowska J, Mamidi S, Gratchev A, Kremmer E, Schmuttermaier C, Krusell L, Haus G, Utikal J, Schledzewski K, Scholtze J, Goerdt S (2006) Novel stabilin-

1 interacting chitinase-like protein (SI-CLP) is up-regulated in alternatively activated macrophages and secreted via lysosomal pathway. Blood 107:3221-3228.

81 Kzhyshkowska J, Gratchev A, Martens J-h, Pervushina O, Mamidi S, Johansson S, Schledzewski K, Hansen B, He X, Tang J, Nakayama K, Goerdt S (2004) Stabilin-1 localizes to endosomes and the trans-Golgi network in human macrophages and interacts with GGA adaptors. Journal of Leukocyte Biology 76:1151-1161.

82 Lambert H, Barragan A (2010) Modelling parasite dissemination: host cell subversion and immune evasion by Toxoplasma gondii. Cell Microbiol 12:292-300.

83 Lane TF, Sage EH (1990) Functional mapping of SPARC: peptides from two distinct Ca+(+)-binding sites modulate cell shape. J Cell Biol 111:3065-3076.

84 Lau A, Tymianski M (2010) Glutamate receptors, neurotoxicity and neurodegeneration. Pflugers Arch 460:525-542.

85 Le DM, Besson A, Fogg DK, Choi KS, Waisman DM, Goodyer CG, Rewcastle B, Yong VW (2003) Exploitation of astrocytes by glioma cells to facilitate invasiveness: a mechanism involving matrix metalloproteinase-2 and the urokinase-type plasminogen activator-plasmin cascade. J Neurosci 23:4034-4043.

86 Lee DJ, Hsu MS, Seldin MM, Arellano JL, Binder DK (2012) Decreased expression of the glial water channel aquaporin-4 in the intrahippocampal kainic acid model of epileptogenesis. Experimental Neurology 235:246-255.

87 Lee M, McGeer E, McGeer PL (2013) Neurotoxins released from interferon-gamma-stimulated human astrocytes. Neuroscience 229:164-175.

88 Levy LM, Attwell D, Hoover F, Ash JF, Bjoras M, Danbolt NC (1998) Inducible expression of the GLT-1 glutamate transporter in a CHO cell line selected for low endogenous glutamate uptake. FEBS Lett 422:339-342.

89 Leweke FM, Gerth CW, Koethe D, Klosterkotter J, Ruslanova I, Krivogorsky B, Torrey EF, Yolken RH (2004) Antibodies to infectious agents in individuals with recent onset schizophrenia. Eur Arch Psychiatry Clin Neurosci 254:4-8.

90 Lin SC, Bergles DE (2004) Synaptic signaling between neurons and glia. Glia 47:290-298.

91 Louis DN, Ohgaki H, Wiestler OD, Cavenee WK, Burger PC, Jouvet A, Scheithauer BW, Kleihues P (2007) The 2007 WHO classification of tumours of the central nervous system. Acta Neuropathol 114:97-109.

92 Mantovani A, Germano G, Marchesi F, Locatelli M, Biswas SK (2011) Cancer-promoting tumor-associated macrophages: New vistas and open questions. European journal of immunology 41:2522-2525.

93 Metea MR, Newman EA (2006) Glial cells dilate and constrict blood vessels: a mechanism of neurovascular coupling. J Neurosci 26:2862-2870.

94 Miman O, Kusbeci OY, Aktepe OC, Cetinkaya Z (2010) The probable relation between Toxoplasma gondii and Parkinson's disease. Neurosci Lett 475:129-131.

95 Miranda AS, Vieira LB, Lacerda-Queiroz N, Souza AH, Rodrigues DH, Vilela MC, Gomez MV, Machado FS, Rachid MA, Teixeira AL (2010) Increased levels of glutamate in the central nervous system are associated with behavioral symptoms in experimental malaria. Braz J Med Biol Res 43:1173-1177.

96 Motamed K, Sage EH (1998) SPARC inhibits endothelial cell adhesion but not proliferation through a tyrosine phosphorylation-dependent pathway. J Cell Biochem 70:543-552.

97 Murphy-Ullrich JE, Lane TF, Pallero MA, Sage EH (1995) SPARC mediates focal adhesion disassembly in endothelial cells through a follistatin-like region and the Ca(2+)-binding EF-hand. J Cell Biochem 57:341-350.

98 Mutter N, Stupp R (2006) Temozolomide: a milestone in neuro-oncology and beyond? Expert Rev Anticancer Ther 6:1187-1204.

99 Myer DJ, Gurkoff GG, Lee SM, Hovda DA, Sofroniew MV (2006) Essential protective roles of reactive astrocytes in traumatic brain injury. Brain 129:2761-2772.

100 Nagelhus EA, Mathiisen TM, Ottersen OP (2004) Aquaporin-4 in the central nervous system: cellular and subcellular distribution and coexpression with KIR4.1. Neuroscience 129:905-913.

101 Nagy JI, Dudek FE, Rash JE (2004) Update on connexins and gap junctions in neurons and glia in the mammalian nervous system. Brain Res Brain Res Rev 47:191-215.

102 Nance JP, Vannella KM, Worth D, David C, Carter D, Noor S, Hubeau C, Fitz L, Lane TE, Wynn TA, Wilson EH (2012) Chitinase dependent control of protozoan cyst burden in the brain. PLoS Pathog 8:e1002990.

103 Nedergaard M, Ransom B, Goldman SA (2003) New roles for astrocytes: redefining the functional architecture of the brain. Trends Neurosci 26:523-530.

104 Neely JD, Amiry-Moghaddam M, Ottersen OP, Froehner SC, Agre P, Adams ME (2001) Syntrophin-dependent expression and localization of Aquaporin-4 water channel protein. Proc Natl Acad Sci U S A 98:14108-14113.

105 Nicchia GP, Srinivas M, Li W, Brosnan CF, Frigeri A, Spray DC (2005) New possible roles for aquaporin-4 in astrocytes: cell cytoskeleton and functional relationship with connexin43. FASEB J 19:1674-1676.

106 Nicchia GP, Rossi A, Mola MG, Pisani F, Stigliano C, Basco D, Mastrototaro M, Svelto M, Frigeri A (2010) Higher order structure of aquaporin-4. Neuroscience 168:903-914.

107 Nimmerjahn A, Kirchhoff F, Helmchen F (2005) Resting microglial cells are highly dynamic surveillants of brain parenchyma in vivo. Science 308:1314-1318.

108 Noell S, Fallier-Becker P, Beyer C, Kroger S, Mack AF, Wolburg H (2007) Effects of agrin on the expression and distribution of the water channel protein aquaporin-4 and volume regulation in cultured astrocytes. Eur J Neurosci 26:2109-2118.

109 Obrenovitch TP, Urenjak J (1997) Is high extracellular glutamate the key to excitotoxicity in traumatic brain injury? J Neurotrauma 14:677-698.

110 Ogata K, Kosaka T (2002) Structural and quantitative analysis of astrocytes in the mouse hippocampus. Neuroscience 113:221-233.

111 Owe SG, Marcaggi P, Attwell D (2006) The ionic stoichiometry of the GLAST glutamate transporter in salamander retinal glia. J Physiol 577:591-599.

112 Palani S, Maksimow M, Miiluniemi M, Auvinen K, Jalkanen S, Salmi M (2011) Stabilin-1/CLEVER-1, a type 2 macrophage marker, is an adhesion and scavenging molecule on human placental macrophages. European journal of immunology 41:2052-2063.

113 Pappas G, Roussos N, Falagas ME (2009) Toxoplasmosis snapshots: global status of Toxoplasma gondii seroprevalence and implications for pregnancy and congenital toxoplasmosis. Int J Parasitol 39:1385-1394.

114 Park S-Y, Jung M-Y, Lee S-J, Kang K-B, Gratchev A, Riabov V, Kzhyshkowska J, Kim I-S (2009) Stabilin-1 mediates phosphatidylserine-dependent clearance of cell corpses in alternatively activated macrophages. Journal of cell science 122:3365-3373.

115 Parlog A, Harsan LA, Zagrebelsky M, Weller M, von Elverfeldt D, Mawrin C, Korte M, Dunay IR (2014) Chronic murine toxoplasmosis is defined by subtle changes in neuronal connectivity. Dis Model Mech 7:459-469.

116 Ploix CC, Noor S, Crane J, Masek K, Carter W, Lo DD, Wilson EH, Carson MJ (2011) CNS-derived CCL21 is both sufficient to drive homeostatic CD4+ T cell proliferation and necessary for efficient CD4+ T cell migration into the CNS parenchyma following Toxoplasma gondii infection. Brain Behav Immun 25:883-896.

117 Promeneur D, Lunde LK, Amiry-Moghaddam M, Agre P (2013) Protective role of brain water channel AQP4 in murine cerebral malaria. Proc Natl Acad Sci U S A 110:1035-1040.

118 Rangel LP, Costa DC, Vieira TC, Silva JL (2014) The aggregation of mutant p53 produces prion-like properties in cancer. Prion 8:75-84.

119 Ransohoff RM, Kivisakk P, Kidd G (2003) Three or more routes for leukocyte migration into the central nervous system. Nat Rev Immunol 3:569-581.

120 Rath BH, Fair JM, Jamal M, Camphausen K, Tofilon PJ (2013) Astrocytes enhance the invasion potential of glioblastoma stem-like cells. PLoS One 8:e54752.

121 Rothstein JD, Dykes-Hoberg M, Pardo CA, Bristol LA, Jin L, Kuncl RW, Kanai Y, Hediger MA, Wang Y, Schielke JP, Welty DF (1996) Knockout of glutamate transporters reveals a major role for astroglial transport in excitotoxicity and clearance of glutamate. Neuron 16:675-686.

122 Rozanski GM, Li Q, Stanley EF (2013a) Transglial transmission at the dorsal root ganglion sandwich synapse: glial cell to postsynaptic neuron communication. Eur J Neurosci 37:1221-1228.

123 Rozanski GM, Nath AR, Adams ME, Stanley EF (2013b) Low voltage-activated calcium channels gate transmitter release at the dorsal root ganglion sandwich synapse. J Physiol 591:5575-5583.

124 Schallier A, Smolders I, Van Dam D, Loyens E, De Deyn PP, Michotte A, Michotte Y, Massie A (2011) Region and age-specific changes in glutamate

transport in the AbetaPP23 mouse model for Alzheimer's disease. J Alzheimers Dis 24:287-300.

125 Schlüter D, Kwok L-Y, Lütjen S, Soltek S, Hoffmann S, Körner H, Deckert M (2003) Both lymphotoxin-alpha and TNF are crucial for control of Toxoplasma gondii in the central nervous system. Journal of immunology (Baltimore, Md : 1950) 170:6172-6182.

126 Sofroniew MV, Vinters HV (2010) Astrocytes: biology and pathology. Acta Neuropathol 119:7-35.

127 Solinas G, Germano G, Mantovani a, Allavena P (2009) Tumor-associated macrophages (TAM) as major players of the cancer-related inflammation. Journal of leukocyte biology 86:1065-1073.

128 Stenzel W, Soltek S, Schlüter D, Deckert M (2004) The intermediate filament GFAP is important for the control of experimental murine Staphylococcus aureus-induced brain abscess and Toxoplasma encephalitis. Journal of neuropathology and experimental neurology 63:631-640.

129 Strack A, Asensio VC, Campbell IL, Schluter D, Deckert M (2002) Chemokines are differentially expressed by astrocytes, microglia and inflammatory leukocytes in Toxoplasma encephalitis and critically regulated by interferon-gamma. Acta Neuropathol 103:458-468.

130 Strohschein S, Huttmann K, Gabriel S, Binder DK, Heinemann U, Steinhauser C (2011) Impact of aquaporin-4 channels on K+ buffering and gap junction coupling in the hippocampus. Glia 59:973-980.

131 Stupp R, Dietrich PY, Ostermann Kraljevic S, Pica A, Maillard I, Maeder P, Meuli R, Janzer R, Pizzolato G, Miralbell R, Porchet F, Regli L, de Tribolet N, Mirimanoff RO, Leyvraz S (2002) Promising survival for patients with newly diagnosed glioblastoma multiforme treated with concomitant radiation plus temozolomide followed by adjuvant temozolomide. J Clin Oncol 20:1375-1382.

132 Stupp R, Mason WP, van den Bent MJ, Weller M, Fisher B, Taphoorn MJ, Belanger K, Brandes AA, Marosi C, Bogdahn U, Curschmann J, Janzer RC, Ludwin SK, Gorlia T, Allgeier A, Lacombe D, Cairncross JG, Eisenhauer E, Mirimanoff RO (2005) Radiotherapy plus concomitant and adjuvant temozolomide for glioblastoma. N Engl J Med 352:987-996.

133 Suzuki Y, Conley FK, Remington JS (1989) Importance of endogenous IFN-gamma for prevention of toxoplasmic encephalitis in mice. Journal of immunology (Baltimore, Md : 1950) 143:2045-2050.

134 Suzuki Y, Rani S, Liesenfeld O, Kojima T, Lim S, Nguyen TA, Dalrymple SA, Murray R, Remington JS (1997) Impaired resistance to the development of toxoplasmic encephalitis in interleukin-6-deficient mice. Infect Immun 65:2339-2345.

135 Swanson RA, Ying W, Kauppinen TM (2004) Astrocyte influences on ischemic neuronal death. Curr Mol Med 4:193-205.

136 Takano T, Kang J, Jaiswal JK, Simon SM, Lin JH, Yu Y, Li Y, Yang J, Dienel G, Zielke HR, Nedergaard M (2005) Receptor-mediated glutamate release from volume sensitive channels in astrocytes. Proc Natl Acad Sci U S A 102:16466-16471.

137 Talmadge JE, Donkor M, Scholar E (2007) Inflammatory cell infiltration of tumors: Jekyll or Hyde. Cancer metastasis reviews 26:373-400.

138 Torrey EF, Yolken RH (2003) Toxoplasma gondii and schizophrenia. Emerg Infect Dis 9:1375-1380.

139 Torrey EF, Bartko JJ, Yolken RH (2012) Toxoplasma gondii and other risk factors for schizophrenia: an update. Schizophr Bull 38:642-647.

140 Torrey EF, Bartko JJ, Lun ZR, Yolken RH (2007) Antibodies to Toxoplasma gondii in patients with schizophrenia: a meta-analysis. Schizophr Bull 33:729-736.

141 Vasievich Ea, Huang L (2011) The suppressive tumor microenvironment: a challenge in cancer immunotherapy. Molecular pharmaceutics 8:635-641.

142 Vyas A (2013) Parasite-augmented mate choice and reduction in innate fear in rats infected by Toxoplasma gondii. J Exp Biol 216:120-126.

143 Vyas A, Kim SK, Giacomini N, Boothroyd JC, Sapolsky RM (2007) Behavioral changes induced by Toxoplasma infection of rodents are highly specific to aversion of cat odors. Proc Natl Acad Sci U S A 104:6442-6447.

144 Webster JP, Lamberton PH, Donnelly CA, Torrey EF (2006) Parasites as causative agents of human affective disorders? The impact of anti-psychotic, mood-stabilizer and anti-parasite medication on Toxoplasma gondii's ability to alter host behaviour. Proc Biol Sci 273:1023-1030.

145 Werner C, Engelhard K (2007) Pathophysiology of traumatic brain injury. Br J Anaesth 99:4-9.

146 Wetherington J, Serrano G, Dingledine R (2008) Astrocytes in the epileptic brain. Neuron 58:168-178.

147 Wilson EH, Hunter Ca (2004) The role of astrocytes in the immunopathogenesis of toxoplasmic encephalitis. International journal for parasitology 34:543-548.

148 Wilson EH, Weninger W, Hunter CA (2010) Trafficking of immune cells in the central nervous system. J Clin Invest 120:1368-1379.

149 Wilson EH, Harris TH, Mrass P, John B, Tait ED, Wu GF, Pepper M, Wherry EJ, Dzierzinski F, Roos D, Haydon PG, Laufer TM, Weninger W, Hunter Ca (2009) Behavior of parasite-specific effector CD8+ T cells in the brain and visualization of a kinesis-associated system of reticular fibers. Immunity 30:300-311.

150 Wolburg H, Noell S, Wolburg-Buchholz K, Mack A, Fallier-Becker P (2009) Agrin, aquaporin-4, and astrocyte polarity as an important feature of the blood-brain barrier. Neuroscientist 15:180-193.

151 Workman G, Sage EH (2011) Identification of a sequence in the matricellular protein SPARC that interacts with the scavenger receptor stabilin-1. Journal of cellular biochemistry 112:1003-1008.

152 Yi JH, Hazell AS (2006) Excitotoxic mechanisms and the role of astrocytic glutamate transporters in traumatic brain injury. Neurochem Int 48:394-403.

153 Yolken RH, Bachmann S, Ruslanova I, Lillehoj E, Ford G, Torrey EF, Schroeder J (2001) Antibodies to Toxoplasma gondii in individuals with first-episode schizophrenia. Clin Infect Dis 32:842-844.

154 Yunker CK, Golembieski W, Lemke N, Schultz CR, Cazacu S, Brodie C, Rempel Sa (2008) SPARC-induced increase in glioma matrix and decrease in vascularity are associated with reduced VEGF expression and secretion. International journal of cancer Journal international du cancer 122:2735-2743.

155 Zhang B, Yao G, Zhang Y, Gao J, Yang B, Rao Z, Gao J (2011) M2-Polarized tumor-associated macrophages are associated with poor prognoses resulting from accelerated lymphangiogenesis in lung adenocarcinoma. Clinics 66:1879-1886.

156 Zhang Y, Zhang H, Feustel PJ, Kimelberg HK (2008) DCPIB, a specific inhibitor of volume regulated anion channels (VRACs), reduces infarct size in MCAo and the release of glutamate in the ischemic cortical penumbra. Exp Neurol 210:514-520.

CHAPTER TWO

Stabilin-1 Expression in Tumor Associated Macrophages

2.1 Abstract:

Glioblastoma multiforme is a very aggressive and common form of brain tumor. Current therapies consist of a combination of surgical removal, chemotherapy and radiation therapy. These drastic treatments still leave a current prognosis of median survival of less than 1 year. Lack of effectiveness of these treatments has left researchers looking for alternative forms of treatment. A significant alternative currently being investigated is the use of the immune system to potentially target and eliminate tumor cells directly. Stabilin-1, a scavenger receptor expressed by macrophages, has the potential in inhibiting tumor growth by binding and internalizing secreted protein acidic and rich in cysteine (SPARC). SPARC is known to be upregulated in the tumor microenvironment and is involved in extracellular matrix remodeling, cell proliferation and migration. Decreasing SPARC expression using siRNA has been shown to decrease tumor invasiveness and survival. We investigated the phenotype of stabilin-1 expressing immune cells in the tumor environment and demonstrated a transient population of alternatively activated macrophages expressing stabilin-1 in the tumor environment and the disappearance of that population as the tumor progresses.

2.2 Introduction:

Glioblastoma multiforme is the most common and aggressive form of CNS tumors. Though current therapies including surgical removal, chemotherapy and radiation seem to extend the survival of the affected patients, the current prognosis still has a median survival of less than 1 year. Surgical removal and radiation therapy crudely target large regions of the brain while chemotherapy targets all dividing cells of the body, thus these methods tend to leave the patient with considerable side effects (Sughrue et al., 2009). Moreover, the lack of effectiveness of these treatments has left researchers looking for alternative forms of treatment. One significant alternative is the use of the immune system, with its high specificity, it has the potential to target and eliminate the tumor cells directly; though knowledge of the immune environment within and around gliomas is lacking. Furthermore, the markers unique to glioma cells and the extent of immunosuppression in the glioma milieu remain largely unknown.

Matricellular proteins are secreted into the extracellular space and interact with cell surface receptors, proteases and structural proteins such as collagen (Bornstein and Sage, 2002). SPARC (secreted protein acidic and rich in cysteine, osteonectin) is a matricellular protein which promotes cell migration as it facilitates an intermediate stage of adhesion as opposed to the strong adhesion of most matricellular proteins (Bornstein and Sage, 2002). The role of SPARC in cell migration makes it an important factor during normal development, wound healing and tissue remodeling (Brekken and Sage, 2001; Framson and Sage, 2004; Workman and Sage, 2011). SPARC is upregulated by glioma cells, and is associated with increased tumor metastasis and proliferation

(Golembieski et al., 1999; Schultz et al., 2002; Rich et al., 2003; Schittenhelm et al., 2006). This may be partially due to the increase of several proteases, which leads to tissue degradation and allows room for infiltrative tumor cells to migrate (Golembieski et al., 2008). Targeting and decreasing SPARC expression with siRNA has proven to decrease tumor invasiveness and tumor cell survival (Shi et al., 2007; Seno et al., 2009).

Recently, the scavenger receptor stabilin-1 was identified as the first known receptor for SPARC. When bound, SPARC is internalized by stabilin-1 and rendered to the endosomal pathway where it is subsequently degraded (Kzhyshkowska, 2006; Kzhyshkowska et al., 2006). Stabilin-1 is expressed on the surface of alternatively activated macrophages (AAMø) which participate in wound healing and in the anti-inflammatory process (Kzhyshkowska et al., 2004; Mosser and Edwards, 2009; Park et al., 2009; Palani et al., 2011). Although SPARC is known to exist in the tumor environment, the presence or location of its receptors are not yet known. The capacity of stabilin-1 expressing macrophages to clear SPARC has the potential to be significant in the control of glioma growth and proliferation.

Macrophages display a wide spectrum of activation states which are generalized as either classically activated (M1) or alternatively activated (M2) (Mosser and Edwards, 2009). In contrast to the microbicidal, inflammatory classically activated macrophages; M2 macrophages are anti-inflammatory and are involved in tissue repair through upregulation of CXCR3, IL-10, arginase-1, the mannose receptor MMR and the scavenger receptor stabilin-1 (Kzhyshkowska et al., 2006; Mosser and Edwards, 2009). During glioblastomas, a population of macrophages associates with the tumor: tumor

associated macrophages (TAMs). This population of macrophages comprises a significant proportion of the tumor, accounting for up to 50% of the tumor mass (Solinas et al., 2009). The phenotype of TAMs is not yet well defined, though it is generally accepted that TAMs are primarily M2 activated. Furthermore, TAMs display pro-tumor functions: promoting tumor cell survival, proliferation and metastasis (Mantovani et al., 2002; Luo et al., 2006; Talmadge et al., 2007; Solinas et al., 2009; Gordon and Martinez, 2010; Zhang et al., 2011). Indeed, high levels of TAMs are often associated with a worse prognosis (Bingle et al., 2002; Zhang et al., 2011).

In this study, we investigated the phenotype of tumor associated macrophages in an attempt to clarify their activation status and whether or not they expressed stabilin-1. Here we demonstrate a significant increase of total lymphocyte and macrophage infiltration in the glioma injected hemisphere (GL) two weeks post injection, a two fold increase in stabilin-1 and MMR expression compared to the naïve hemisphere at day 7 post injection and reduction of stabilin-1 expression in the glioma hemisphere by day 14 post injection.

These data demonstrate the presence of stabilin-1 at the site of initial glioma growth but then a downregulation of stabilin-1 as the tumor progresses. It is well known that tumors can cause phenotypic changes in infiltrating immune cells and thus may be responsible for the change in stabilin-1 expression. Increasing this receptor expression on infiltrating macrophages may help in the control of glioma growth.

2.3 Materials and Methods:

Mice and Injections: Female C57BL/6 were obtained from Jackson Laboratories and maintained in a pathogen free environment under IACUC established protocols at the University of California Riverside. The murine (C57BL/6) glioma cell line, GL-26, which is highly tumorigenic in the C57BL/6 mice, was obtained as a generous gift from Dr. Pedro Lowenstein. GL26 cells were cultured in DMEM/F12 supplemented with 10% FCS, 1% penicillin/ streptomycin, 1% L-glutamine and 1% non-essential amino acids. Cultured GL-26 cells were then harvested by trypsinization and 90,000 GL-26 cells in 3μL of sterile PBS was injected intracranially 1mm anterior and 2 mm lateral to the junction of the coronal and sagittal sutures (bregma) at a depth of 2mm using a stereotactic mouse frame. Mice were anesthetized with ketamine (1:5) and xylazine (1:50) in sterile PBS with volume injected determined by individual mouse weight.

Histology: Mice were perfused intracardially with 4% paraforlmaldehyde (PFA) in PBS and brains were extracted, incubated in 4% PFA overnight and then 30% sucrose in PBS until brains equalized. Next, brains were flash frozen in isopentane, embedded in OCT and cryosectioned in coronal sections (12 μm). Sections were stained with eosin and haematoxylin.

Real Time PCR: Stabilin-1 specific primers (forward 5′-GCTTTGAACCTCAGCCACTC-3′ and reverse 5′-GGCAATTACACTGCCCACTT-3′) and macrophage mannose receptor specific primers (forward5′-CTCTGTTCAGCTATTGGACGC-3′ and reverse 5′- TGGCACTCCCAAACATAATTT-3′) for Real Time PCR were purchased from IDT's primer Quest

(http://www.idtdna.com/Scitools/ Applications/Primerquest/). cDNA synthesis and Real-time PCR was performed using the Bioline One-step Kit with the CFX-96 real-time PCR Detection System (Bio-Rad). The reaction total was a 20µl mixture with 10µl SYBR Green/SensiFAST qPCR Master Mix (2x) and 400nM primer. The reaction conditions were as follows: 10 min at 45°C, followed by 2 min at 95°C and then 40 cycles of 5s at 95°C and 20s at 60°C. The HPRT (Hypoxine Phosphoribosyl- Transferase) forward primer (5′-CCCTCTGGTAGATTGTCGCTTA-3′) and reverse primer (5′AGATGCTGTTACTGATAGGAAATTGA -3′) were used as an endogenous control. Quantified results represent the fold induction of target gene expression using the differential CT method. NTC, no-template control (reagent alone without template) was included in each assay to detect any possible contamination of the PCR reagents.

Preparation of Brain Mononuclear Cells (BMNCs) suspension: For BMNCs, harvested brain tissues were minced with a razor blade and passed multiple times through an 18-gauge needle. The suspension was then incubated with 100µl of collagenase/dispase (1mg/ml) (Roche Diagnostics, Indianapolis, IN) for 45 min at 37°C and then a further 45 min at 37°C with 300µl DNAse (10 mg/ml) (Sigma). Following enzymatic digestion, the cell suspension was passed through a 70µm cell strainer, resuspended in 40 ml of RPMI complete and centrifuged at 1200rpm for 10 min at 4°C. The pellet was resuspended in 60% isotonic Percoll (GE Healthcare Bioscience, Uppsala, Sweden) solution (in RPMI complete) and overlaid with 30% percoll solution made in 1x sterile PBS. The Percoll gradient was centrifuged at 2000rpm for 25 min at 25°C without brakes. After centrifugation, the myelin layer on top of the gradient was removed.

BMNCs (lymphocytes, macrophages, dendritic cells and microglia) were harvested from the 30%-60% percoll interphase and washed twice in complete RPMI medium for further analysis.

Immunofluorescent staining: Brains from C57BL/6 mice injected with gliomas were extracted 7 days post injection and frozen in OCT. Serial section (18 microns) were cut and incubated with primary antibodies for stabilin-1 (Santa Cruz antibodies) and biotinylated tomato lectin for 3 hours at room temperature. Secondary antibodies (streptavidin 488 and donkey anti goat 568) were incubated for 2 hours in room temperature. Slides were then mounted with ProLong Gold anti fade reagent with DAPI (Life Technologies).

Flow Cytometry: 1x10^6 BMNCs were placed in FACS tubes (BD Falcon™, MA, USA), centrifuged at 1200 rpm for 5 minutes at 4°C and resuspended in FACS buffer (1X PBS containing 4%BSA, 0.01%EDTA). After a further round of centrifugation the cells were pre-incubated with a saturating solution of FC block (eBioscience, San Diego, USA) for 5 minutes on ice and stained with various conjugated antibodies against CD11b, CD45, and CD40 (purchased from eBioscience), MMR (biolegend, San Diego, CA) as well as a non-conjugated antibody against rabbit anti Stabilin-1 (Santa Cruz antibodies, Santa Cruz, CA) for 30min on ice. Samples stained with Stabilin-1 went through a secondary incubation with anti-rabbit Alexa Fluor 647 for 30 minutes on ice. Cells were washed with FACS buffer and analyzed using the BD FACSCantoTM II flow cytometer and FlowJo analysis software v.8.7.3.

2.4 Results:

2.4.1 Scavenger receptor stabilin-1 is expressed in early glioma:

A model of glioma was used in this study where GL-26 cells were injected intra-cranially and allowed to grow for either 7, 14 or 21 days **(Fig. 2-1A, B)**. Injection of 90,000 GL-26 cells in the caudate putamen (CPu) leads to a stable tumor which initially grows in the needle tract before expanding in the border between the striatum and the external capsule (ec). By day 14, the needle tract is mostly closed and the tumor expands from the dorsal portion of the caudate putamen to the exterior of the cortex **(Fig. 2-1A)** and by day 21, the tumor has expanded to both hemispheres **(Fig. 2-1B).**

To determine if stabilin-1 is present in the tumor environment, expression of stabilin-1 was measured using RT-qPCR at day 7 post injection in the right striatum. Furthermore, as stabilin-1 has been shown to be predominantly expressed on AAMø, expression of MMR was also measured to test if AAMø were present in our tumor model. Both stabilin-1 and MMR transcripts are up-regulated 1.912 ± 0.6391 and 1.881 ± 0.5023 times **(Fig. 2-1C)** respectively in the injected hemisphere (GL) when compared to the non-injected hemisphere (NI).

At day 14, although high levels of MMR are maintained on the injected hemisphere, the expression of stabilin-1 was reduced **(Fig. 2-1C)**. Indeed, at day 14 post glioma injection, MMR expression increased 3.265 ± 1.423 fold higher in the injected hemisphere whereas stabilin-1 expression was reduced to equal levels in both hemispheres (1.031 ± 0.4456 fold higher in the injected hemisphere compared to non-injected hemisphere).

Immunofluorescent staining at day 7 post injection for stabilin-1 and tomato lectin at the site of the tumor reveals both membrane and cytoplasmic stabilin-1 within the tumor tissue **(Fig. 2-1D)**. Tomato lectin is known to stain for macrophages, blood vessels and microglia. These images suggest a small population of infiltrating macrophages which express stabilin-1 within gliomas.

These data demonstrate the presence of a growing glioma at day 7 and 14 post injection which is associated with increased MMR expression and early (day 7) stabilin-1 upregulation in the injected hemisphere.

2.4.2 Stabilin-1 expression on macrophages decreases with tumor growth:

To determine the cell types which express stabilin-1 in the tumor environment, infiltrating macrophages, lymphocytes and local microglial populations were analyzed at day 7 and 14 post glioma injection by flow cytometry. At day 7 post injection, there were no differences in total mononuclear cell numbers between the non-injected and injected hemisphere (**Fig. 2-2A)**. Furthermore, no differences in macrophage, lymphocyte or microglial populations either in composition or cell numbers between the non-injected hemisphere and the injected hemisphere were apparent **(Fig. 2-2A)**. Of the cells analyzed, stabilin-1 expression was detected on macrophages and microglia but not lymphocytes **(Fig. 2-2B)**. The proportion of stabilin-1 expressing macrophages **(Fig. 2-2C)** and the levels of expression **(Fig. 2-2D)** were not significantly different between the injected and the non-injected hemisphere at day 7 post injection.

By day 14, although there were no significant differences observed in the total

number of mononuclear cells recovered from the injected and non-injected hemisphere, the increase in glioma size was accompanied by an increase in infiltrating macrophage ($p= 0.0371$) and lymphocyte ($p= 0.0056$) numbers in the injected hemisphere **(Fig. 2-2A)**. This indicates a growing adaptive T-cell associated response. The proportion of stabilin-1 expressing macrophages were significantly lower ($p= 0.0322$) in the injected compared to the non-injected hemisphere **(Fig. 2-2C)**. Experiments were conducted on separate days and thus a direct comparison cannot be made between expression levels (MFI) between day 7 and day 14. However, the level of stabilin-1 expression on infiltrating macrophages at day 14 was significantly lower ($p=0.0329$) in the tumor associated hemisphere when compared to the non-injected hemisphere **(Fig. 2-2D)**.

These data suggest that stabilin-1 is expressed on AAMø and that this expression is less likely to be associated with the tumor environment as the glioma progresses.

2.4.3 Stabilin-1 expressing macrophages also express CD40, MMR:

In order to define the phenotype of stabilin-1 expressing macrophages, CD40 and MMR expression was measured as representation of classical and alternative activation respectively. At day 7, stabilin-1 was present on both alternative and CD40+ macrophages **(Fig. 2-3A)**. As the tumor progresses, there is a loss of stabilin-1 expression on AAMø in the injected compared to the non-injected hemisphere by day 14 ($p=0.0443$) **(Fig. 2-3B)**. Proportions of CD40 expressing macrophages also expressing stabilin-1 are not significantly different between hemispheres.

A group analysis at day 7 post injection reveals no differences in stabilin-1

expression on AAMø population and MMR- macrophages. As the tumor progresses, stabilin-1 is preferentially expressed on AAMø by day 14 (**Fig. 2-3C)** (two-way ANOVA p=0.0192). Furthermore, there is a significantly larger population of CD40+ macrophages expressing stabilin-1 at day 7 (two-way ANOVA p=0.0312) compared to CD40- macrophages. This expression dramatically shifts at day 14 resulting in preferential stabilin-1 expression on CD40- macrophage populations as opposed to M1 **(Fig. 2-3D)** (two-way ANOVA p=0.0279).

These data suggest a shift in the cell phenotype which expresses stabilin-1 between day 7 and 14 post injection. Initially, stabilin-1 is expressed on both CD40+ and MMR+ macrophage phenotypes. However, as the tumor progresses and stabilin-1 is downregulated, it is mostly expressed on the MMR+ macrophages and is dramatically reduced on CD40+ macrophages.

2.5 Discussion:

In this report, we stereotactically injected GL-26 tumor cells in the right hemisphere of mice brains to determine the phenotype and progression of the macrophage response during the first two weeks of tumor growth. GL-26 cells are very invasive, proliferate fast and form a glioblastoma in the mouse with similar properties to the glioblastomas seen in humans.

The role of SPARC in tumor proliferation and metastasis has been described since the late 1990's, but besides recent siRNA gene silencing of SPARC, no study has addressed a mechanism for blocking or degrading SPARC as a potentially therapeutic target in the control of gliomas (Golembieski et al., 1999; Schultz et al., 2002; Rich et al., 2003; Shi et al., 2007; Seno et al., 2009). stabilin-1 is the only known receptor of SPARC and works as a scavenger receptor, internalizing and degrading bound SPARC (Kzhyshkowska, 2006; Kzhyshkowska et al., 2006; Kzhyshkowska et al., 2012). Being expressed on macrophages, stabilin-1 has the potential of being expressed in the tumor microenvironment and slow the tumor proliferation by decreasing local SPARC levels.

It is well known, however, that TAMs change phenotypes with the progression of the tumor (Mantovani et al., 2002; Luo et al., 2006; Talmadge et al., 2007; Solinas et al., 2009; Gordon and Martinez, 2010; Zhang et al., 2011; Ruffell et al., 2012). Indeed, as the tumor progresses, factors that promote the pro-tumorigenic polarization of TAMs can be divided into those derived from the immune system, from the tumor cells or from tissue stress. TAMs receive IL-10, IL-4 and IL-13 signaling from T-regs and Th2 cells, IL-10 and CCL2 signals from the tumor cells and sense hypoxia and ECM degradation in the

tumor microenvironment. These signals cause the TAMs to in turn suppress the immune system with CCL22 and ROS secretion, promote tumor invasion through ECM remodeling and EGF secretion and finally, promote angiogenesis at the tumor site via VEGFA secretion (Mantovani et al., 2011; Ruffell et al., 2012). Though macrophages have the potential of expressing the SPARC scavenger receptor stabilin-1, it is unknown whether TAMs express stabilin-1 and whether this expression is maintained when TAMs become pro-tumorigenic. It should be noted that TAMS are known to also secrete SPARC. Whether SPARC expressing TAMS are also expressing stabilin-1 in a self-regulatory process or whether these are two distinct macrophage populations is not known and warrants further investigation. Our studies show a time dependent shift in the stabilin-1 expressing population. The disappearance of this phenotype as the tumor progresses may be due to tumor derived signals or intrinsic to the function of these macrophages leading to the dominant presence of SPARC.

In this report, we examined the macrophages in the tumor microenvironment for stabilin-1 expression during the initial progression of the tumor. We show an initial upregulation of stabilin-1 transcripts in the hemisphere injected with GL-26 cells which is not maintained two weeks post injection. Furthermore, we show an initial population of stabilin-1 expressing macrophages which is significantly reduced at day 14 post injection. At day 7, the stabilin-1 expressing macrophages are activated as demonstrated by their high co-expression of CD40. At day 14 however, the macrophages still expressing stabilin-1 are more polarized towards the M2 phenotype, as seen by the co-expression of MMR. These results suggest an initial anti-tumor attempt by the activated macrophage to

express stabilin-1 in the tumor environment. Possibly due to signals from the tumor cells and tissue disruption, TAMs stop expressing stabilin-1 as they switch phenotypes to one that promotes tissue remodeling and angiogenesis.

The question that remains is obviously whether or not stabilin-1 expressing TAMs could possibly slow tumor progression or change the tumor microenvironment. Though we have not conducted these studies, overexpressing stabilin-1 in macrophages in glioma bearing mice would be a crucial next step in characterizing the role of this subset of macrophages in the tumor environment. In addition, although our model uses the GL-26 line due to its similarity in aggressiveness and proliferative capabilities to human glioblastomas, the tumor in human glioblastomas differs from the mouse GL-26 line. Indeed, human glioblastomas arise from several diverse cell types which can arise from neural, myeloid and glial origins (Seyfried, 2001; Yuan et al., 2004; Huysentruyt et al., 2011). What role stabilin-1 could play in this situation remains to be investigated.

It has been shown through siRNA targeting of SPARC that depletion of SPARC slows tumor progression and metastasis (Shi et al., 2007; Seno et al., 2009). Though these results are exciting, they are not therapeutically relevant to humans. However, degradation of SPARC through stabilin-1 in our own macrophages deserves more attention as a potential target for glioblastoma therapy.

2.6 Figures and Legends:

Figure 2-1. Stabilin-1 expression in the tumor environment.

12 μm brain coronal sections of day 7 or 14 post injection with GL-26 were stained with haematoxylin followed by eosin to confirm tumor presence and growth (A). Naïve, day 7, 14 and 21 post GL-26 injected brains are photographed prior to sectioning (B). Brains were taken at day 7 or 14 post injection with GL-26 and separated by hemisphere (GL-26 injected and non-injected). RNA was extracted for real time PCR analysis and the differential CT method was used to plot stabilin-1 (STB1) and MMR expression in the injected hemisphere relative to the naïve hemisphere (NI) (C). Immunofluorescent staining for tomato lectin (green) and stabilin-1 (red) was performed on 18 μm thick section from brains extracted 7 days post glioma injection (D). Scale bar is 170 μm

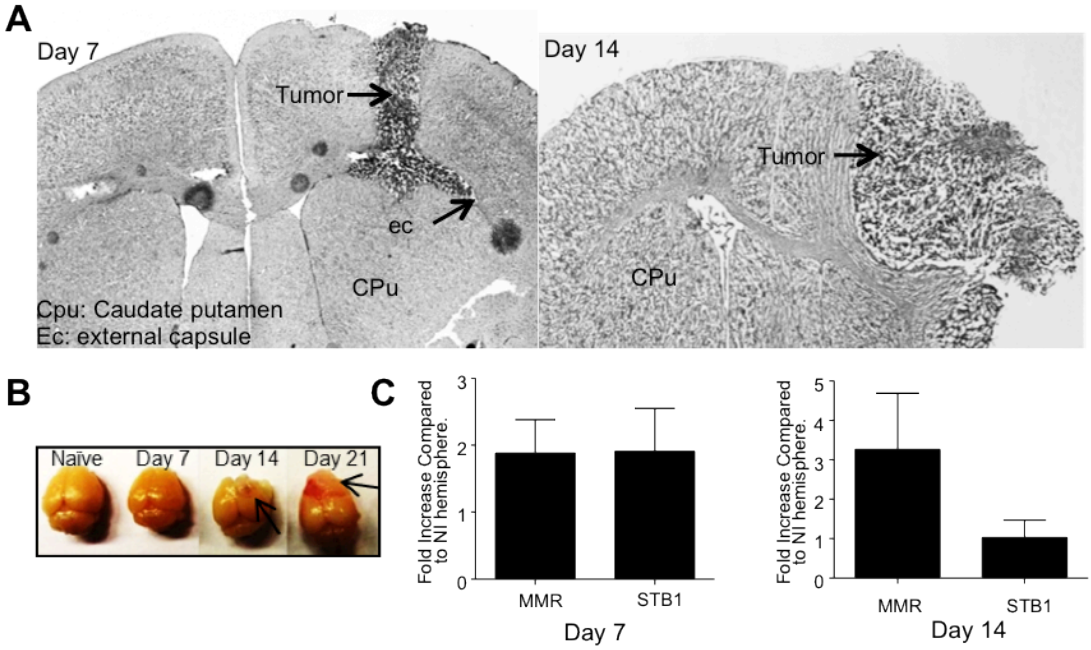
A
Day 7
Tumor
ec
CPu
Cpu: Caudate putamen
Ec: external capsule
Day 14
Tumor
CPu
B
Naïve
Day 7
Day 14
Day 21
C
Fold Increase Compared to NI hemisphere.
MMR
STB1
Day 7
Fold Increase Compared to NI hemisphere.
MMR
STB1
Day 14
D
Tissue
Stabilin-1
Tomato Lectin
Tumor

Figure 2-2. Stabilin-1 expression on macrophages.

Brain mononuclear cells were extracted, counted and stained for CD45 and CD11b allowing for differentiation of lymphocyte, macrophage and microglial populations (A). Cells were also stained for stabilin-1, and cells expressing stabilin-1 were identified (B). Proportion of total macrophages at day 7 and 14 post injection which are positive for stabilin-1(C), and expression levels measured with mean fluorescent intensity for stabilin-1 at day 7 and day 14 post injection (D) were determined. *NI: Non-injected hemisphere, GL: glioma injected hemisphere.*

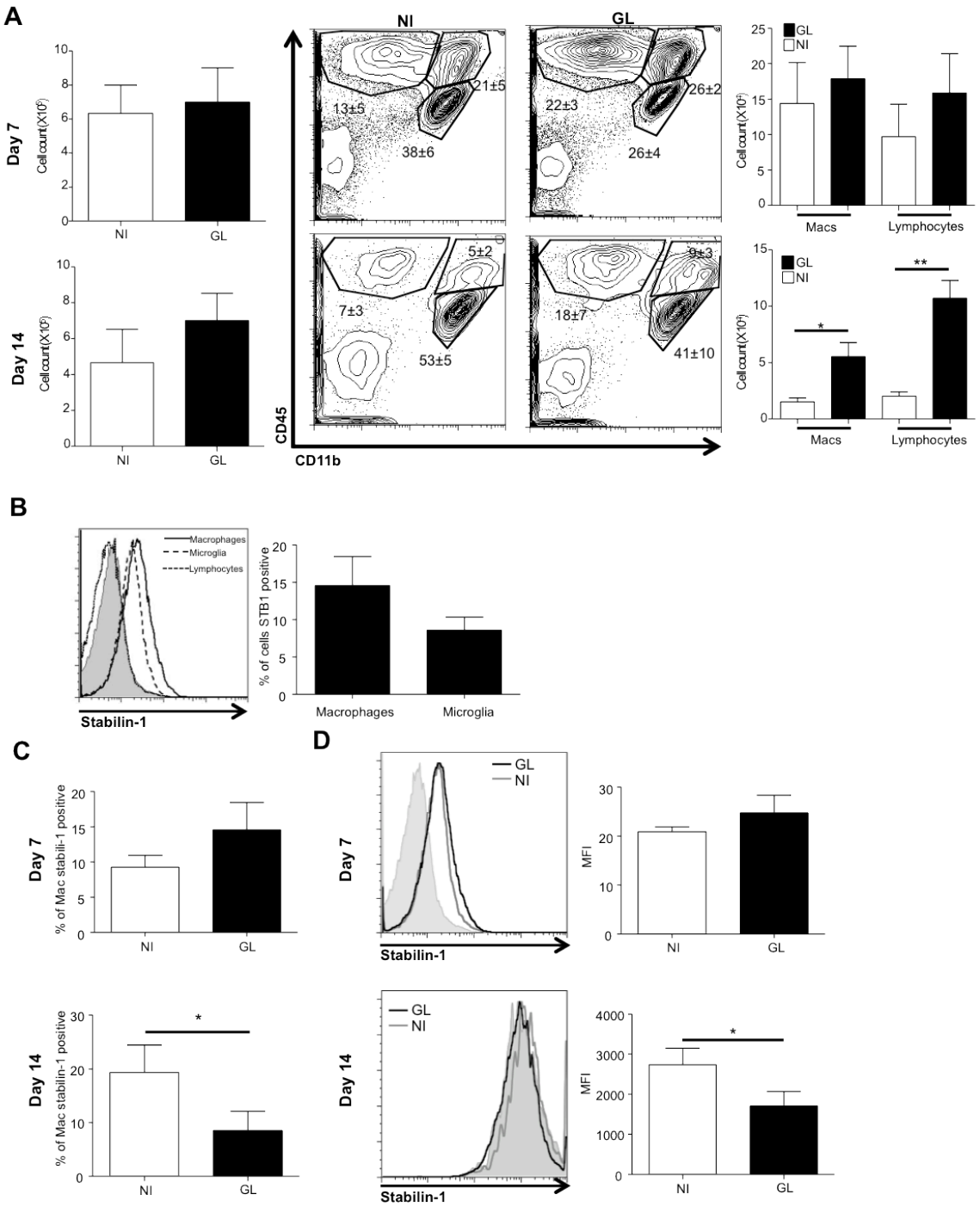
A
Day 7
Cell count(X10⁶)
NI
GL
Day 14
NI
GL
NI
GL
13±5
21±5
38±6
22±3
26±2
26±4
7±3
5±2
53±5
18±7
9±3
41±10
CD45
CD11b
GL
NI
Macs
Lymphocytes
*
**
B
Macrophages
Microglia
Lymphocytes
Stabilin-1
% of cells STB1 positive
Macrophages
Microglia
C
Day 7
% of Mac stabili-1 positive
NI
GL
Day 14
% of Mac stabilin-1 positive
*
D
Day 7
GL
NI
Stabilin-1
MFI
Day 14
GL
NI
Stabilin-1
MFI
*

Figure 2-3. Stabilin-1 expressing macrophages change as the tumor progresses.

Stabilin-1 expressing macrophage populations were analyzed for co-expression of MMR and CD40 at day 7 post injection (A). Analysis of proportions of stabilin-1 (STB1+) macrophages for co-expression of MMR at day 14 (B). Macrophage populations in glioma brains at day 7 and 14 post injection were analyzed for M1 and M2 phenotypes using MMR+/STB1+ or MMR-/STB1+ (C) and CD40+/STB1+ or CD40-/STB1+ (D).

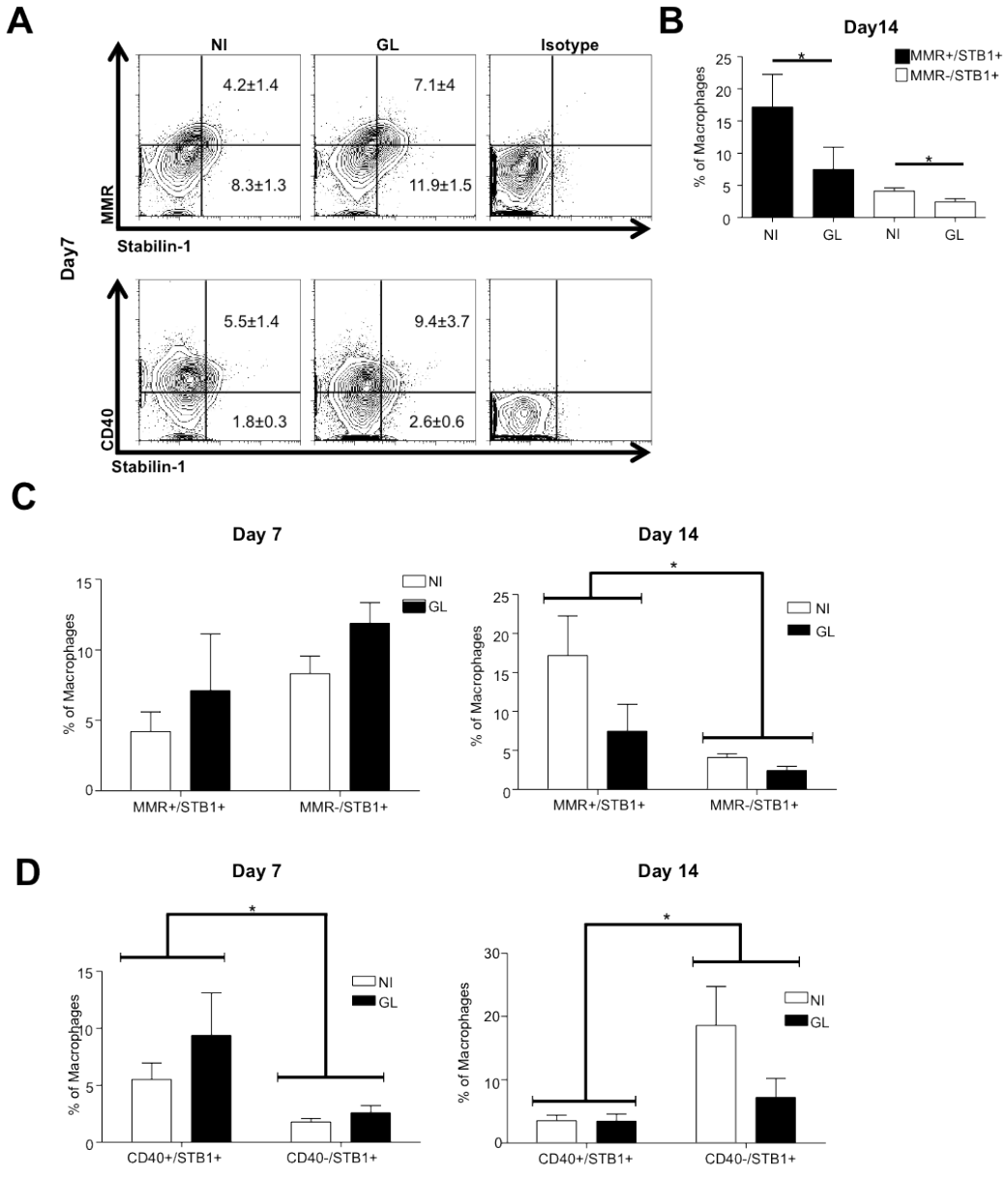
A
NI
GL
Isotype
4.2±1.4
7.1±4
8.3±1.3
11.9±1.5
MMR
Stabilin-1
Day7
5.5±1.4
9.4±3.7
1.8±0.3
2.6±0.6
CD40
Stabilin-1
B
Day14
MMR+/STB1+
MMR-/STB1+
% of Macrophages
NI
GL
NI
GL
C
Day 7
Day 14
NI
GL
% of Macrophages
MMR+/STB1+
MMR-/STB1+
D
Day 7
Day 14
CD40+/STB1+
CD40-/STB1+

2.7 References:

1 Bingle L, Brown NJ, Lewis CE (2002) The role of tumour-associated macrophages in tumour progression: implications for new anticancer therapies. The Journal of pathology 196:254-265.

2 Bornstein P, Sage EH (2002) Matricellular proteins: extracellular modulators of cell function. Current opinion in cell biology 14:608-616.

3 Brekken RA, Sage EH (2001) SPARC, a matricellular protein: at the crossroads of cell-matrix communication. Matrix Biol 19:816-827.

4 Framson PE, Sage EH (2004) SPARC and tumor growth: where the seed meets the soil? Journal of cellular biochemistry 92:679-690.

5 Golembieski Wa, Ge S, Nelson K, Mikkelsen T, Rempel Sa (1999) Increased SPARC expression promotes U87 glioblastoma invasion in vitro. International journal of developmental neuroscience : the official journal of the International Society for Developmental Neuroscience 17:463-472.

6 Golembieski Wa, Thomas SL, Schultz CR, Yunker CK, McClung HM, Lemke N, Cazacu S, Barker T, Sage EH, Brodie C, Rempel Sa (2008) HSP27 mediates SPARC-induced changes in glioma morphology, migration, and invasion. Glia 56:1061-1075.

7 Gordon S, Martinez FO (2010) Alternative Activation of Macrophages: Mechanism and Functions. Immunity 32:593-604.

8 Huysentruyt LC, Akgoc Z, Seyfried TN (2011) Hypothesis: are neoplastic macrophages/microglia present in glioblastoma multiforme? ASN neuro 3:183-193.

9 Kzhyshkowska J (2006) Stabilin-1, a homeostatic scavenger receptor with multiple functions. Journal of Cellular and Molecular Medicine 10.

10 Kzhyshkowska J, Workman G, Cardó-vila M, Arap W, Pasqualini R, Gratchev A, Goerdt S, Sage EH, Cardo M, Krusell L (2012) Novel Function of Alternatively Activated Macrophages : Stabilin-1-Mediated Clearance of SPARC 1. The Journal of Immunology.

11 Kzhyshkowska J, Mamidi S, Gratchev A, Kremmer E, Schmuttermaier C, Krusell L, Haus G, Utikal J, Schledzewski K, Scholtze J, Goerdt S (2006) Novel stabilin-1 interacting chitinase-like protein (SI-CLP) is up-regulated in alternatively

activated macrophages and secreted via lysosomal pathway. Blood 107:3221-3228.

12 Kzhyshkowska J, Gratchev A, Martens J-h, Pervushina O, Mamidi S, Johansson S, Schledzewski K, Hansen B, He X, Tang J, Nakayama K, Goerdt S (2004) Stabilin-1 localizes to endosomes and the trans-Golgi network in human macrophages and interacts with GGA adaptors. Journal of Leukocyte Biology 76:1151-1161.

13 Luo Y, Zhou H, Krueger J, Kaplan C, Lee S-h, Dolman C, Markowitz D, Wu W, Liu C, Reisfeld RA, Xiang R (2006) Targeting tumor-associated macrophages as a novel strategy against breast cancer. The journal of clinical investigation 116.

14 Mantovani A, Sozzani S, Locati M, Allavena P, Sica A (2002) Macrophage polarization: tumor-associated macrophages as a paradigm for polarized M2 mononuclear phagocytes. Trends in immunology 23:549-555.

15 Mantovani A, Germano G, Marchesi F, Locatelli M, Biswas SK (2011) Cancer-promoting tumor-associated macrophages: New vistas and open questions. European journal of immunology 41:2522-2525.

16 Mosser DM, Edwards JP (2009) Exploring the full spectrum of macrophage activation. Genetics 8:958-969.

17 Palani S, Maksimow M, Miiluniemi M, Auvinen K, Jalkanen S, Salmi M (2011) Stabilin-1/CLEVER-1, a type 2 macrophage marker, is an adhesion and scavenging molecule on human placental macrophages. European journal of immunology 41:2052-2063.

18 Park S-Y, Jung M-Y, Lee S-J, Kang K-B, Gratchev A, Riabov V, Kzhyshkowska J, Kim I-S (2009) Stabilin-1 mediates phosphatidylserine-dependent clearance of cell corpses in alternatively activated macrophages. Journal of cell science 122:3365-3373.

19 Rich JN, Shi Q, Hjelmeland M, Cummings TJ, Kuan C-T, Bigner DD, Counter CM, Wang X-F (2003) Bone-related genes expressed in advanced malignancies induce invasion and metastasis in a genetically defined human cancer model. The Journal of biological chemistry 278:15951-15957.

20 Ruffell B, Affara NI, Coussens LM (2012) Differential macrophage programming in the tumor microenvironment. Trends in immunology 33:119-126.

21 Schittenhelm J, Mittelbronn M, Roser F, Tatagiba M, Mawrin C, Bornemann a (2006) Patterns of SPARC expression and basement membrane intactness at the

tumour-brain border of invasive meningiomas. Neuropathology and applied neurobiology 32:525-531.

22 Schultz C, Lemke N, Ge S, Golembieski WA, Rempel SA (2002) Secreted Protein Acidic and Rich in Cysteine Promotes Glioma Invasion and Delays Tumor Growth in Vivo Secreted Protein Acidic and Rich in Cysteine Promotes Glioma Invasion and Delays Tumor Growth in Vivo 1. Animals:6270-6277.

23 Seno T, Harada H, Kohno S, Teraoka M, Inoue A, Ohnishi T (2009) Downregulation of SPARC expression inhibits cell migration and invasion in malignant gliomas. International Journal of Oncology:707-715.

24 Seyfried TN (2001) Perspectives on Brain Tumor Formation Involving Macrophages, Glia, and Neural Stem. Perspectives in Biology and Medicine 44:263-282.

25 Shi Q, Bao S, Song L, Wu Q, Bigner DD, Hjelmeland aB, Rich JN (2007) Targeting SPARC expression decreases glioma cellular survival and invasion associated with reduced activities of FAK and ILK kinases. Oncogene 26:4084-4094.

26 Solinas G, Germano G, Mantovani a, Allavena P (2009) Tumor-associated macrophages (TAM) as major players of the cancer-related inflammation. Journal of leukocyte biology 86:1065-1073.

27 Sughrue ME, Yang I, Kane AJ, Rutkowski MJ, Fang S, James CD, Parsa AT (2009) Immunological considerations of modern animal models of malignant primary brain tumors. Journal of translational medicine 7:84.

28 Talmadge JE, Donkor M, Scholar E (2007) Inflammatory cell infiltration of tumors: Jekyll or Hyde. Cancer metastasis reviews 26:373-400.

29 Workman G, Sage EH (2011) Identification of a sequence in the matricellular protein SPARC that interacts with the scavenger receptor stabilin-1. Journal of cellular biochemistry 112:1003-1008.

30 Yuan X, Curtin J, Xiong Y, Liu G, Waschsmann-Hogiu S, Farkas DL, Black KL, Yu JS (2004) Isolation of cancer stem cells from adult glioblastoma multiforme. Oncogene 23:9392-9400.

31 Zhang B, Yao G, Zhang Y, Gao J, Yang B, Rao Z, Gao J (2011) M2-Polarized tumor-associated macrophages are associated with poor prognoses resulting from accelerated lymphangiogenesis in lung adenocarcinoma. Clinics 66:1879-1886.

CHAPTER THREE

Antitumor activity of a polypyridyl chelating ligand: *in-vitro* and *in-vivo* inhibition of glioma

3.1 Abstract:

Glioblastoma multiforme is an extremely aggressive and invasive form of central nervous system (CNS) tumor commonly treated with the chemotherapeutic drug Temozolomide (TMZ). Unfortunately, even with treatment the median survival time is less than 12 months. SBP, a phenanthroline-based ligand originally developed to deliver gold based anti-cancer drugs, has recently been shown to have significant anti-tumor activity in its own right. SBP is hypothesized to initiate tumor cell death via interaction with non-DNA targets, and considering most glioblastoma drugs kill tumors through DNA damage processes, SBP was tested as a potential novel drug candidate against glial based tumors. *In-vitro* studies demonstrated that SBP significantly inhibited the growth of rodent GL-26 and C6 glioma cells, as well as human U-87, and SW1088 glioblastomas/astrocytomas. Furthermore, using a syngeneic glioma model in mice, *in-vivo* administration of SBP significantly reduced tumor volume and increased survival time. There was no significant toxicity towards non-tumorigenic primary murine and human astrocytes *in vitro*, and limited toxicity was observed in *ex-vivo* tissues obtained from non-cancerous mice. TUNEL staining and recovery assays suggest that SBP induces apoptosis in gliomas. This exploratory study suggests SBP is effective in slowing the growth of tumorigenic cells in the brain while exhibiting limited toxicity to normal cells and tissues, and should therefore be further investigated for its potential in glioblastoma treatment.

3.2 Introduction:

Glioblastoma multiforme is an extremely aggressive and invasive form of central nervous system (CNS) tumor with a survival prognosis of less than one year (Stupp et al., 2002; Hegi et al., 2004; Safdie et al., 2012; Poteet et al., 2013). Current therapies employ surgical removal in combination with radiation therapy and chemotherapy (Stupp et al., 2005). Though this removes a large part of the tumor, it often does not eliminate all tumor cells and relapses generally occur quickly. Furthermore, current chemotherapy and radiation therapy can leave patients with substantial deleterious side effects (Sughrue et al., 2009). Temozolomide (TMZ; see Scheme 3-1) is a chemotherapeutic drug that has been in use since 1999 to treat advanced glioblastomas and melanomas. Its anti-tumor effects stem from its capability to methylate DNA at the N-7 or O-6 position of guanine, thereby damaging the DNA and causing cell death (Srivastava et al., 1998; Hegi et al., 2004; Mutter and Stupp, 2006; Kim et al., 2010; Poteet et al., 2013). Unfortunately, virtually all patients relapse with TMZ-resistant disease and many patients do not respond to TMZ (Hegi et al., 2005). The resistance to current chemotherapies, limited success of treatment, and poor long term prognosis warrants the search for and creation of new drugs, which alone or in combination with other forms of therapy could target and eradicate tumor cells more efficiently (Hegi et al., 2004; Chamberlain et al., 2007).

Gold compounds have been long thought to possess strong anti-tumor activity, stemming from the fact that initial studies found some gold compounds were able to inhibit HeLa cell growth (Thang et al., 1976). Unfortunately, gold-based drugs were found to be unstable *in-vivo* and had no therapeutic advantage over established

chemotherapeutics (Thang et al., 1976; Wein et al., 2011). However, the subsequent development of coordinating ligands designed to stabilize gold complexes resulted in the discovery of the anticancer activities of gold(III) polypyridyl complexes, prompting a renewed interest in this area of drug design (Messori et al., 2000; Shi et al., 2006; Wein et al., 2011; Palanichamy et al., 2012). While the development of gold(III) drugs possessing polypyridyl ligand architectures has been progressing, some reports have indicated the polypyridyl ligands themselves exhibit antitumor activity similar to that of the parent gold complex, suggesting that the free ligand may play a role in the activity of this class of gold therapeutics. In a recent study of a gold(III) complex bearing the 2,9-di-*sec*-butyl-1,10-phenanthroline (SBP; see Scheme 3-1) polypyridyl ligand, control experiments found that the free SBP ligand exhibited remarkable *in-vitro* activity against a variety of head-neck and lung (A549 and H1703 lung, and 886LN, Tu212, and Tu686 head/neck) cancer lines. In particular, the study revealed that SBP had *in-vitro* IC_{50} values in the nanomolar concentration range, which were 20-100 times lower than the commonly used chemotherapy cisplatin (See Scheme 3-1) and 4-14 times lower than the parent gold(III) complex (Sanghvi et al., 2013). Thus although metals complexed to phenanthroline-based ligands continue to be investigated for their anti-tumor properties (Narla et al., 2001; Scharwitz et al., 2008; Bieda et al., 2009a; Bieda et al., 2009b; Dobroschke et al., 2009; Tan et al., 2010; Komor and Barton, 2013), our understanding of the properties and potential chemotherapeutic action of the ligands themselves remains an unexplored area of research.

One important finding in regards to the antitumor efficacy of SBP was that it had

significant activity against the cisplatin-resistant H1703 lung tumor cell line, suggesting that SBP likely initiates tumor cell death via a mechanism involving a non-DNA target (Sanghvi et al., 2013). To date, the most successful drugs for treatment of glioblastoma, including TMZ, have been lipophilic alkylating agents that disrupt tumor cell growth through processes that initiate DNA damage (Ajaz et al., 2014). Cisplatin and other platinum-based drugs, which initiate tumor cell death by forming intrastrand crosslinks with DNA guanine base pairs, have also been found to demonstrate *in-vitr*o activity against glioblastoma tumors (Wolff et al., 1999). Though platinum-based drugs have had more limited success *in-vivo*, novel drug delivery approaches for glioblastoma treatment are being pursued (Charest et al., 2013; Miura et al., 2013). Given the aforementioned activity of SBP against cisplatin-resistant tumor cells, and the fact SBP is hypothesized to have non-DNA intracellular targets (Sanghvi et al., 2013), it was of interest to determine if this drug might have potential as a new lead compound for glioblastoma treatment. In particular, it was desired to determine if a compound with a potentially different mechanism of antitumor activity might show promise as a therapeutic against glioblastoma tumors. Prior to carrying out detailed mechanistic studies on the antitumor activity of SBP, it was first desired to characterize the general *in-vitro* efficacy of this drug against a panel of glioblastoma tumor cell lines and to determine if SBP has *in-vivo* activity on an implanted murine glioma brain tumor model.

In the current study, a panel of rodent and human glioma cell lines was used for *in-vitro* efficacy and toxicity assays. In addition, a syngeneic mouse model that recapitulates several aspects of human glioblastoma was used to investigate the anti-tumor capabilities

of SBP *in vivo*. We report that SBP has significant *in-vitro* activity against rodent (GL-26, C6) and human (U-87 and SW1088) glioblastoma/astrocytoma tumor cells, and *in-vivo* activity against implanted murine brain tumors. Finally, we provide preliminary studies on whether SBP limits tumor cell growth via cell cycle arrest or apoptosis.

3.3 Materials and Methods:

Compound Synthesis: 2,9-di-*sec*-butyl-1,10-phenanthroline (SBP) was synthesized and purified according to previously reported protocols (Pallenberg et al., 1995; Jakobsen and Tilset, 2011).

Cell Lines: The murine (C57BL/6) glioma cell line, GL-26, which is highly tumorigenic in C57BL/6 mice, was obtained as a generous gift from Dr. Pedro Lowenstein, University of Michigan, Ann Arbor (Candolfi et al., 2007; David et al., 2012). GL-26 cells were cultured in DMEM/F12 supplemented with 10% FCS, 1% penicillin/ streptomycin, 1% L-glutamine, and 1% non-essential amino acids. Primary murine astrocytes were purified from C57BL/6 neonate brains and cultured in DMEM/F12 supplemented with 10% FCS, 1% non-essential amino acids, 1% L-glutamine, 50IU/ml penicillin, 50mg/ml streptomycin, and 10mM Hepes buffer. U-87 (human glioblastoma), SW1088 (human astrocytoma) and C6 (rat glioma) were purchased from ATCC (cat# HTB-14, HTB-12 and CCL-107) and cultured following the ATCC's guidelines. Primary human astrocytes were purchased from Sciencell (cat# HA-1800) and cultured following Sciencell's recommendations. Human foreskin fibroblasts (HFFs) were cultured in DMEM/F12 supplemented with 10% FCS and 1% penicillin/ streptomycin.

Growth Assay: The sulforhodamine B (SRB) cytotoxicity assays were adapted from Skehan et al (Skehan et al., 1990). Briefly, cells were plated at a density of 4,000 cells/well of a 96 well plate in a volume of 100μL overnight at 37°C and cultured in a humidified atmosphere of 5% CO_2. Cells were exposed to SBP or TMZ at 0–25 μM for

48 hr before the culture supernatant was discarded and the cells fixed for 1 hr with 10% cold trichloroacetic acid (100 μL per well). Cells used in recovery assay received fresh media for 48hrs following the 48hr drug incubation before fixation. Fixed cells were then washed 5 times with de-ionized water, air dried, and stained with 0.4% SRB for 10 min (50 μL per well). After washing 5 times in 1% acetic acid and air-drying, bound SRB was dissolved in 10 mM unbuffered Tris base (pH 10.5; 100 μL per well). Bound SRB was then quantified by absorbance at 492 nm on a SpectraMax plate reader (Molecular Devices). The percent survival was then calculated based upon the absorbance values relative to control wells (0 μM SBP in 0.1% DMSO). All cell growth assays were done such that each drug concentration was tested in triplicate, and each of these independent experiments was done three times.

Propidium Iodide: GL-26 cells were plated at 4000 cells/well in a 96 well plate in GL-26 media. The cells were treated 1 day post-plating with 0-25μM SBP for 48 hours. The cells were then detached with Trypsin/EDTA (Cellgro), washed and resuspended at 500,000 cells/ml in ice cold Na^+/K^+ balanced PBS and fixed by gently adding 70% ethanol and incubating for 2hrs at 4°C. GL-26 cells were then resuspended in 300 – 500 μl PI/Triton X-100 staining solution: 10 ml of 0. 1 % (v/v) Triton X-100 (Sigma) in Na^+/K^+ balanced PBS with 2 mg DNAse-free RNAse A (Sigma) and 0.40 ml of 500 μg/ml PI (Roche). The stain was allowed to incubate at 37°C for 15 minutes before data acquisition on a BD FacsCanto II flow cytometer. Independent experiments were carried out where only adherent cells were tested, as well as a combination of both adherent and detached cells were tested. Each of these experiments was repeated three times.

***In-Vivo Experiments**:* All animal research was performed in accordance with the Animal Welfare Act. All protocols were approved by the Institutional Animal Care and Use Committee (IACUC) of the University of California, Riverside. Female C57BL/6 mice were obtained from Jackson Laboratories and maintained in a specific pathogen free environment. Mice were anesthetized with continuous administration of 2.5% isofluorane. Cultured GL-26 cells were harvested by trypsinization and 90,000 GL-26 cells in 3μL of sterile Na^+/K^+ balanced PBS were injected intracranially. A stereotactic mouse frame was used to carry out the injection 1.0 mm anterior and 2.0 mm lateral to the junction of the coronal and sagittal sutures (bregma), and at a depth of 2.0 mm. Care was taken to alternate injection order and group assignment (treated vs. non-treated) to assure equal GL-26 cell viability between the two treatment groups. SBP was administered intravenously through the retro-orbital route at a concentration of 10 mg/kg in 200 μL sterile Na^+/K^+ balanced PBS. Drug was administered one, seven, and 13 days after tumor implantation and sacrificed at day 19 post implantation for tumor size analysis. A separate cohort was treated with 5mg/kg SBP every 6 days and allowed to progress until moribund for a survival analysis (Untreated, N=5; SBP-Treated, N=5).

Histology: For brain tumor histology, mice were perfused intracardially with 4% formaldehyde in Na^+/K^+ balanced PBS and brains were incubated in 4% formaldehyde overnight followed by 30% sucrose in Na^+/K^+ balanced PBS. Brains were flash frozen in isopentane, embedded in optimal cutting temperature compound (OCT), coronally cryosectioned (12 μm) and stained with hematoxylin and eosin. Another cohort of equivalently drug-treated mice without tumors was used for liver, lung and gut histology.

In this instance, mice were sacrificed on day 19, and the liver, lung and gut tissues collected and placed in 4% formaldehyde in Na^+/K^+ balanced PBS overnight. The organs were then placed for 48hrs in 70% EtOH before further dehydrating, paraffin embedding and sectioning at 6 μm. Sections were then stained with hematoxylin and eosin and pathology was assessed blindly and independently by a trained pathologist. A TUNEL staining kit was obtained from TREVIGEN (NeuroTACS II *In Situ* Apoptosis Detection Kit, Cat#4823-30-K) and used for both *ex-vivo* slices and *in-vitro* staining according to manufacturers instructions.

Liver Toxicity: Intra-cardial blood was collected from the non-tumor bearing mice, allowed to clot and then subjected to centrifugation for 10 minutes to collect serum. Aspartate transaminase and Alanine transaminase levels were measured in the serum using Bio Scientific (3913 Todd Lane Suite 312 Austin, TX) colorimetric kits (Cat#5605-01 and 3460-08 respectively).

Statistical Analysis: All statistical analyses were done using GraphPad Prism software. Statistics on growth assays, tumor area and AST/ALT concentrations were done using an unpaired two-tailed Student's T-Test. A best-fit line was applied to the weights of tumor-bearing treated and not-treated mice. If the line deviates from a slope of 0, it indicates a change in the mouse weight over the recorded time. The survival curve was analyzed using a Mantel-Cox and a Gehan-Breslow-Wilcoxon Test using GraphPad Prism software.

3.4 Results:

3.4.1 SBP inhibits glioma cell growth *in-vitro*:

To determine if SBP had the capacity to inhibit the growth of glioma cell lines, GL-26 and C6 cells were cultured in-vitro and incubated with concentrations of SBP and TMZ from 0.1 μM to 25 μM for 48 hours. The drug was then removed and the effect of SBP on cell growth was assessed. A dose-related decrease in cell growth between 0.8 and 6 μM was observed in cells treated with SBP, whereas TMZ did not affect cell viability at any tested concentrations. At the IC50 value observed for SBP (1.63 μM)**(Fig. 3-1A, E)**, GL-26 growth was significantly reduced when compared to GL-26 treated with TMZ (no IC50 observed; p=0.03) **(Fig. 3-1A)**. Similarly, at the IC50 for SBP (0.19 μM) **(Fig. 3-1E)**, C6 cell growth was significantly lower than in C6 cells treated with TMZ (no IC50 observed; p=0.0112) **(Fig. 3-1A)**.

In order to assess the toxicity of the drug on normal cells, murine primary astrocytes were treated with SBP (0.1-25 μM) for 48 hours and toxicity was quantified using an SRB assay. At the observed SBP IC50 of GL-26 cells (1.63 μM), primary murine astrocyte growth was inhibited by only 14% and no cell growth inhibition was observed at the IC50 of C6 cells (0.19 μM) treated with SBP **(Fig. 3-1B)**. This suggests that SBP has a therapeutic window of between 0.19 μM and 1.63 μM for the murine cells tested.

In an effort to assess the translational efficacy of SBP, the drug was tested against two human glioma lines. U-87 (human glioblastoma) and SW1088 (human astrocytoma) cells were incubated with the same concentration regime of SBP described above. At the

IC50 of U-87 treated with SBP (3.04 μM) **(Fig. 3-1E)**, glioma growth is significantly reduced when compared to U-87 treated with TMZ (no IC50 observed; p=0.0102) **(Fig. 3-1C)**. At the IC50 of SW1088 cells treated with SBP (0.33 μM) **(Fig. 3-1E)**, cell growth is significantly lower than in SW1088 cells treated with TMZ (no IC50 observed; p=0.0005) **(Fig. 3-1C)**. To determine whether there was any toxicity of SBP on non-cancerous human cells, primary human astrocytes and human foreskin fibroblasts (HFF) were treated with SBP. At the IC50 of SW1088 cells (0.33 μM)**(Fig. 3-1E)**, HFF cell growth and primary human astrocyte growth were unaffected **(Fig. 3-1D)**. This suggests the therapeutic window for SBP in human cells is between 0.33 μM and 3.04 μM.

In total, these results suggest SBP is significantly more effective at inhibiting the growth of these specific mouse and human tumor cells than the currently used glioma chemotherapy, TMZ. The concentration of SBP with the greatest efficacy against tumor cells and least toxicity in normal astrocytes was 3.2 μM for rodent cells and 0.4 μM for human cells **(Fig. 3-1F)** in vitro.

3.4.2 SBP induces GL-26 apoptosis:

An important consideration is whether chemotherapeutics kill off and remove cancer cells or simply inhibit their growth. If cell growth is inhibited by the drug, continuous treatment is required to prevent regrowth. Therefore, preliminary studies were carried out in an effort to determine if SBP induces tumor cell death or if the drug simply disrupts cell growth. First, to test if constant SBP administration is necessary to maintain growth inhibition, an SRB recovery assay was performed. Allowing the glioma cells to

recover for 48hrs in fresh medium did not rescue cell growth. Instead significantly greater cell death was observed in the 'recovered' versus acutely treated cells (p=0.002) **(Fig. 3-2A)**. These data demonstrate that GL-26 cells continue dying after the removal of SBP and suggested that SBP targeted and disrupted cell survival rather than cell proliferation mechanisms.

To assess the effects of SBP on cell proliferation versus apoptosis, cell cycle analysis was performed using propidium iodide. Figure 2B demonstrates that SBP-treated cells were still capable of advancing to the S, G2 and mitotic phases, and were thus not arrested in the G1 phase. However, the proportion of cells in these phases was reduced and treated cells had a significantly larger population of dead cells compared to untreated controls. To confirm if cell death was the result of apoptosis, cultured GL-26 cells treated with SBP were subjected to TUNEL staining **(Fig. 3-2C)**. No positive staining was detected in the untreated sample, suggesting that no apoptosis occurred during the culturing of GL-26 cells in media alone **(Fig. 3-2C)**. The nuclease-treated positive control was uniformly TUNEL positive and the dark staining in the SBP-treated GL-26 cells indicates that these cells are also undergoing apoptosis. These results demonstrate that SBP does not affect cell cycle progression, but rather kills GL-26 cells by inducing apoptosis.

3.4.3 SBP inhibits *in-vivo* glioma growth:

Although no mouse model accurately mimics the generation of human glioblastoma multiforme (GBM), intracranial injection of the GL-26 cell line leads to a

morphologically similar and syngeneic tumor. It is also highly aggressive and invasive making it a valuable test for potential therapeutics. The tumors are extremely proliferative and mice routinely die within 30 days following intracranial injection. This type of tumor implantation has been shown to lead to a robust tumor within a week (Candolfi et al., 2007; David et al., 2012; Safdie et al., 2012). After implanting the tumors, treatment mice were treated intravenously with SBP and control mice were treated intravenously with saline solution on 1, 7 and 13 days post GL-26 cell injection.

All treatment and control mice were sacrificed at day 19, and serial brain sections were stained with hematoxylin and eosin to reveal general morphology. In untreated mice, tumors were extensive. Glioma growth expanded from the striatum to most of the cortex of the injected hemisphere **(Fig. 3-3A)**. In contrast, mice treated with SBP had markedly smaller tumors **(Fig. 3-3B)**. Indeed, tumors in the SBP group were largely restricted to areas directly adjacent to the needle tract, and constrained to small areas of the striatum, although sometimes they expanded minimally to the cortex. In some cases, the untreated tumors expanded to the contralateral hemisphere, whereas the treated tumors never penetrated this region **(Fig. 3-3A)**. For each animal, tumor size was quantified by pixel area starting at the largest tumor cross-section (position 0) and measuring the tumor area in 100 μm intervals (rostral and caudal). Untreated animals were found to possess significantly larger tumors than the SBP treated group (Not treated: 48187 ± 7736, SBP treated: 5489 ± 1369, p=0.0056, measured at the largest tumor cross-section) **(Fig. 3-3B)**.

Body weights were recorded for 19 days after tumor implantation, and as expected, a decrease in weight was observed in both treated and non-treated groups

during the first week post tumor implantation **(Fig. 3-3C**) (Safdie et al., 2012). However, whereas mice treated with SBP regained nearly all their initial weight (>98%), mice left untreated exhibited continued weight loss **(Fig. 3-3C)**. A best-fit line (not shown) revealed that the non-treated group significantly deviated from zero (p=0.0261) whereas the SBP treated mice weights did not (p=0.8792).

The *in-vitro* assays demonstrated that SBP inhibited GL-26 cell growth via the induction of apoptosis. To determine if apoptosis of GL-26 cells was a potential cause of the reduced tumor size *in-vivo*, *in situ* TUNEL staining was conducted on serial brain sections from treated and untreated mice (**Fig. 3-3D**). The untreated tumor displays faint positive TUNEL stain consistent with tumor growth and destruction of normal tissue (Kim et al., 2010). In contrast, SBP treated tumors revealed dark brown cytoplasmic and nuclear staining indicative of cell necrosis and increased DNA fragmentation, respectively **(Fig. 3-3D)**. This data is consistent with SBP causing cell death via apoptosis as seen *in vitro*.

To test if decreased tumor size and increased tumor cell apoptosis translates to an increase in survival time, mice were allowed to progress to moribund state and survival monitored. Mice treated with SBP survived significantly longer than untreated mice (Mantel-Cox test p=0.0384; and Gehan-Breslow-Wilcoxon test p=0.0472) with untreated mice living a median of 35 days and SBP treated mice living a median of 46 days **(Fig. 3-3E)**. In combination with the *ex-vivo* TUNEL, this data suggests that SBP treatment slows tumor growth, likely via apoptosis, and leads to improved survival.

3.4.4 SBP does not cause overt peripheral pathology:

Even though minimal inhibition of primary astrocytes was observed in both murine and human cells, *in vivo* administration can cause accumulation and breakdown products not observed *in vitro*. To determine the *in-vivo* toxicity of SBP, non-tumor bearing mice were treated with either saline or 10 mg/kg SBP. After administering these treatments on days 1, 7, and 13, the same regime for tumor inhibition, both the untreated control mice and SBP-treated mice were euthanized on day 19. The liver, lungs, and proximal small intestines were subsequently collected for histopathological analysis. In the duodenum, no general pathology that might have resulted from inhibition of cell division was detected, as there were no differences in crypt or villus architecture, or goblet cell density between treated and untreated mice. Analysis of lung tissue also revealed no overt pathology. Treated liver sections revealed minor endothelial damage, but no overt hepatocyte damage **(Fig. 3-4A)**. Serum concentrations of liver enzymes were also measured to provide an indication of potential toxicity (Danan and Benichou, 1993; Amacher, 1998). Neither aspartate transaminase (AST) nor alanine transaminase (ALT) concentrations, early indicators of toxicity caused by an intravenously administrated drug (Danan and Benichou, 1993; Scheig, 1996; Amacher, 1998), were significantly different between treated and non-treated mice **(Fig. 3-4B)**. These results reveal that SBP results in negligible *in-vivo* toxicity when 10 mg/kg SBP is administered to mice over a 19 day period.

3.5 Discussion:

With current combination therapies extending the survival rate of patients with gliomas by a mean of 8-18 months (Chamberlain et al., 2007; Poteet et al., 2013), more potent compounds are desperately needed to control tumor growth. In this study, we used the GL-26 cell line as a model for glioblastoma. The GL-26 cells exhibit similar aggressive, proliferative and tumorigenic properties as gliomas seen in humans and express the mouse version of CD133, associated with tumor stem cells (Candolfi et al., 2007; Golebiewska et al., 2013). Although implantation of GL-26 cells has limitations compared to a xenotransplant that enables *in-vivo* testing on human tumor cells or a genetic model that enables the evaluation of cancer-initiating events (Chen et al., 2012), these cells, when injected into the mouse striatum establish a large and rapidly growing tumor that is morphologically similar to GBM (Stupp et al., 2002; Candolfi et al., 2007; Smith et al., 2009; Sughrue et al., 2009; David et al., 2012; Golebiewska et al., 2013). It also allows analysis in an immunologically intact animal where the tumor is tolerated in the murine brain. The resulting highly invasive tumor makes it a strong and therefore valuable test for potential therapies (Candolfi et al., 2007; Smith et al., 2009; Safdie et al., 2012).

Previously, SBP was found to have remarkable *in-vitro* activity against a panel of three head-neck and two lung tumor lines, and when tested against a cisplatin-resistant tumor was found to have an IC_{50} value approximately 100 times lower than cisplatin (Sanghvi et al., 2013). The prime mechanism of cisplatin is thought to be intercalation of DNA (Komor and Barton, 2013). Such a significant reduction in IC_{50} by SBP could

therefore point to a novel mechanism not dependent on DNA interactions. Glioma treatment is notoriously difficult and the limitations are often due to tumor resistance to typical DNA targeting antiglioma drugs. Thus, we sought to test the *in-vitro* anticancer activity of SBP against the rodent C6 and GL-26, and the human U-87 and SW1088 cell lines and compare it to the clinically used glioblastoma drug TMZ. Even though previous reports have shown the *in-vitro* activity of polypyridyl ligands (Thang et al., 1976; Chamberlain et al., 2007; Roy et al., 2008; Wesselinova et al., 2009; Wein et al., 2011; Palanichamy et al., 2012), this report is to our knowledge the first study on the *in-vitro* and *in-vivo* anticancer activity of this class of compounds against glioblastoma tumors. The data reported here demonstrate strong *in-vitro* toxicity of SBP against glioma cell lines at low micromolar concentrations, with significantly diminished toxicity to both non-cancerous human fibroblasts and non-cancerous primary human and murine astrocytes. In addition, we demonstrate that intravenously administered SBP can significantly reduce the growth of an intracranially implanted murine brain tumor resulting in an increase in survival similar to the TMZ murine glioma model (Kim et al., 2010).

A major concern in new drug development is the side effects associated with the drug. We have demonstrated high levels of cytotoxicity against GL-26, C6 and SW1088 at low micromolar concentrations, with minimal toxicity towards primary murine and human astrocytes and the non-cancerous HFF cell line. AST and ALT are often used as markers for liver health during chemotherapy, where elevated levels indicate liver damage and the AST/ALT ratio can further be used to differentiate between the causes of

liver damage (Danan and Benichou, 1993; Scheig, 1996; Amacher, 1998). Following treatment with SBP, AST and ALT levels were similar to untreated mice and fell well within their respective normal physiological ranges. Furthermore, histopathalogical analysis of the proximal gut, lung and liver only revealed minor damage to liver endothelial cells. These results mirror the low toxicity observed in TMZ-treated patients (Friedman et al., 2000; Su et al., 2004; Pouratian et al., 2007; Niewald et al., 2011). Perhaps more importantly, SBP treatment resulted in smaller, more contained tumors. This is especially relevant, as contained tumors are easier to remove surgically (Duffau, 2009). Thus, the route of administration, the strong anti-tumor properties and the low toxicity to normal cells suggest SBP has potential for future anti-cancer development.

Even though *in-vivo* experiments corroborated the *in-vitro* data that demonstrated increased apoptosis in SBP treated groups compared to non-treated controls, the obvious question remains: what is the mechanism by which SBP induces apoptosis? More specifically, is SBP-induced apoptosis a result of a similar mechanism as TMZ, which is thought to methylate guanine residues in the DNA (Srivastava et al., 1998; Hegi et al., 2004; Mutter and Stupp, 2006; Chamberlain et al., 2007; Kim et al., 2010; Poteet et al., 2013). At first glance, it might be expected that SBP acts as a DNA intercalator, as the compound has significant aromatic character. This class of compounds is known to have significant interactions with DNA, which can result in disruption of DNA replication and induction of cell death in a similar fashion to the commonly used chemotherapy cisplatin (Kelland, 2006). However, as previously stated, SBP has enhanced anti-proliferative effects on cisplatin-resistant cell lines. This suggests that the drug likely initiates tumor

cell death via a mechanism not related to DNA interactions (Sanghvi et al., 2013). Additionally, the fact that TMZ exhibits no inhibition of tumor cell growth at any of the concentrations tested for SBP further corroborates the notion that SBP likely has a distinct DNA-independent mechanism. All of the tumor cell lines used in this study were desensitized to TMZ, a known DNA methylating agent, whereas all of the tumor cell lines were sensitive to SBP further suggesting that SBP acts differently than TMZ to inhibit growth. Finally, SBP has significantly reduced cytotoxicity toward non-cancerous cells. Since DNA repair mechanisms are more vital to tumor cell proliferation compared to normal cell division, the observation that SBP has significantly stronger anti-proliferative activity against tumor cell lines versus normal cells could point to SBP targeting enzymes involved in DNA repair. A report from Mendes, *et al.* describes the PARP-1 inhibition of gold(III) complexes possessing phenanthroline ligands that are in the same family as SBP (Mendes et al., 2011). The gold(III) complex bearing the unsubstituted 1,10-phenanthroline was found in particular to be a potent PARP-1 inhibitor, involved in DNA repair mechanisms, and the authors attribute the gold complex's activity to binding with the zinc finger motif in the enzyme. Given that SBP can act as a potent metal chelator, inhibition of DNA repair via binding to the zinc finger domain of PARP-1 is a plausible antitumor mechanism for this drug. Future research efforts in our lab will focus on testing this hypothesis.

In this report, the anti-tumor activity of SBP on glioblastomas was tested both *in-vitro* and *in-vivo.* The data demonstrate the potent anti-tumor activity of SBP *in-vitro* with minimal toxicity to normal cells. The anti-tumor activity of SBP does not appear to

be mediated by cell cycle disruption, but rather by inducing cell death as demonstrated by propidium iodide and TUNEL staining. SBP also reduced tumor size in an intracranial murine brain tumor without causing apparent pathology to normal tissues. Finally, SBP significantly increased survival time of mice intracranially injected with the GL-26 cell lines. Though further research should focus on the capability of SBP to stop or eradicate well-established tumors and the mechanism of action, the results described here clearly demonstrate that SBP has significant anti-glioma activity, making it an important chemotherapy candidate for this aggressive, invasive and difficult to treat class of tumor.

3.6 Figures and Legends:

Scheme 3-1. Molecular structure of 2,9-di-*sec*-butyl-1,10-phenanthroline (SBP).

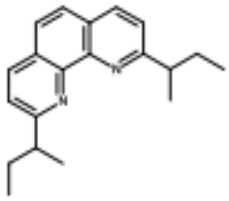

2,9-di-sec-butyl-1,10-phenanthroline (SBP)

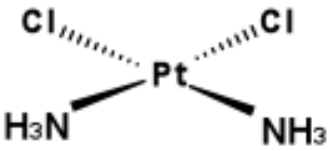

Cisplatin

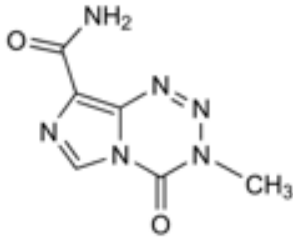

Temozolomide (TMZ)

Figure 3-1. *In-vitro* GL-26 inhibition with SBP.

GL-26 and C6 cells were grown in a 96 well plate and treated with SBP or TMZ at 0.1 to 25μM (A). To test SBP toxicity on non-tumor cells, primary murine astrocytes were plated and treated as above (B). U-87 and SW1088 cells were grown in a 96 well plate and treated with SBP or TMZ at 0.1 to 25μM (C). To test SBP toxicity on non-tumor cells, primary human astrocytes and human foreskin fibroblasts (HFF) were plated and treated as above (D). IC_{50} (μM) displayed for each cell line tested (F). The largest toxicity window between normal and glioma cells plotted for both murine and human cells. (Student's T-test, primary murine astrocytes vs GL-26 and C6 $p<0.0001$; primary human astrocytes and HFF vs SW1088 $p=0.0006$ and $p=0.0007$ respectively) (F). The Sulforhodamine B colorimetric assay (SRB) was used to measure and plot fraction of growth of treated wells compared to a non-treated controls. All cell growth assays were done in a minimum of triplicates and repeated a minimum of 9 times.

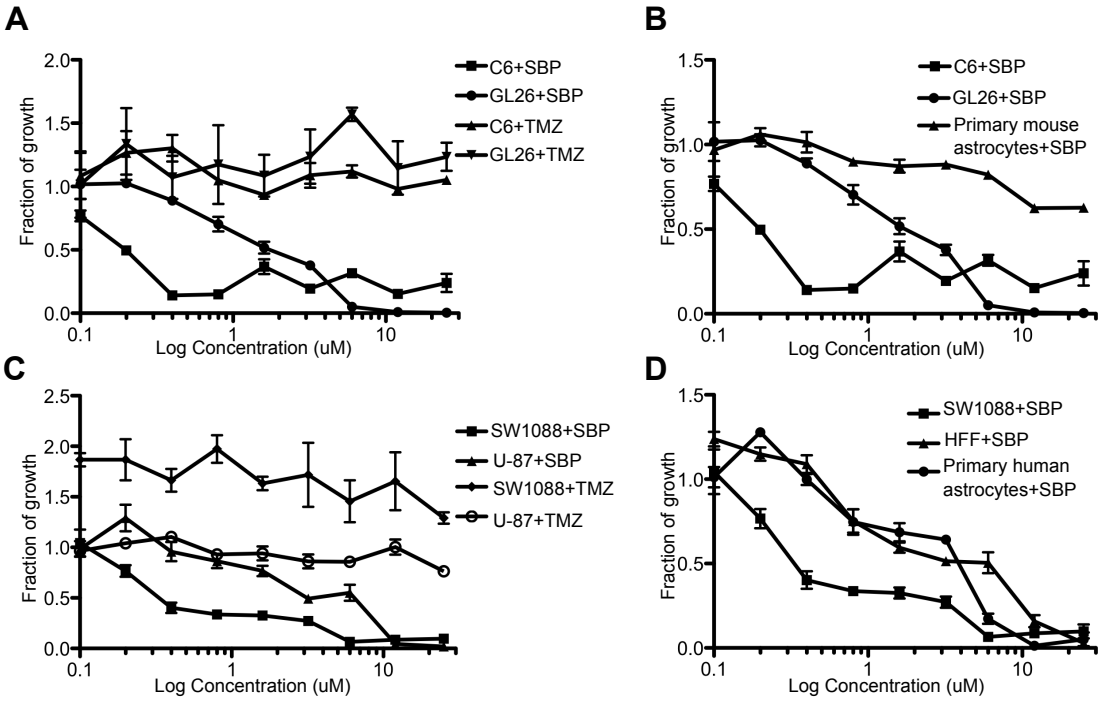

E

Cell Line	Primary human astrocytes	SW1088	U-87	C6	GL-26
IC $_{50}$ (μM)	3.93	0.33	3.04	0.19	1.63

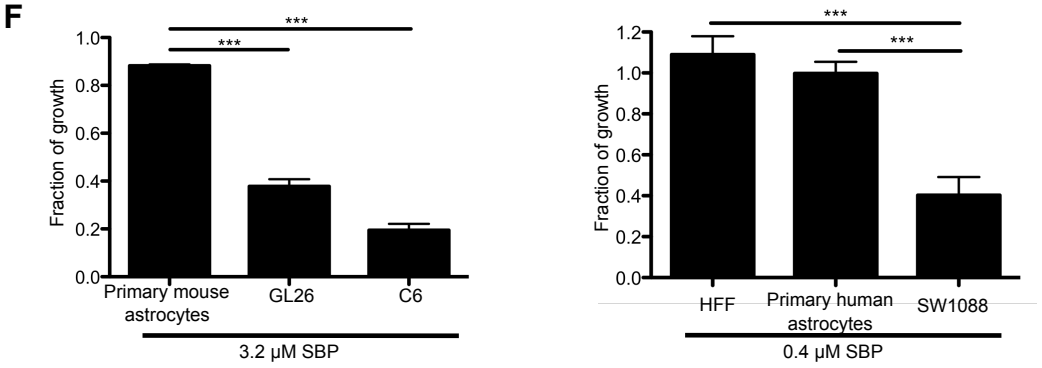

Figure 3-2. The compound SBP induces apoptosis.

GL-26 cells were grown in a 96 well plate and treated with 0.4 to 25μM SBP. After 48hr incubation, the drug was removed and cells cultured for an additional 48hrs in fresh media. SRB was used to measure and plot fraction of growth of treated wells compared to a non-treated control. Non-recovered GL-26 cells are plotted for reference (A). Propidium iodide staining intensity was measured by flow cytometry and plotted vs. cell number to identify cell cycle stages (S: Synthesis, M: Mitotic) (B). SBP treated and untreated cultured GL-26 cells were stained for apoptosis (TUNEL). The positive control was treated with the kit's nuclease to generate DNA breaks in every cell (C). Both recovery and propidium iodide experiments were independently repeated a minimum of 3 times.

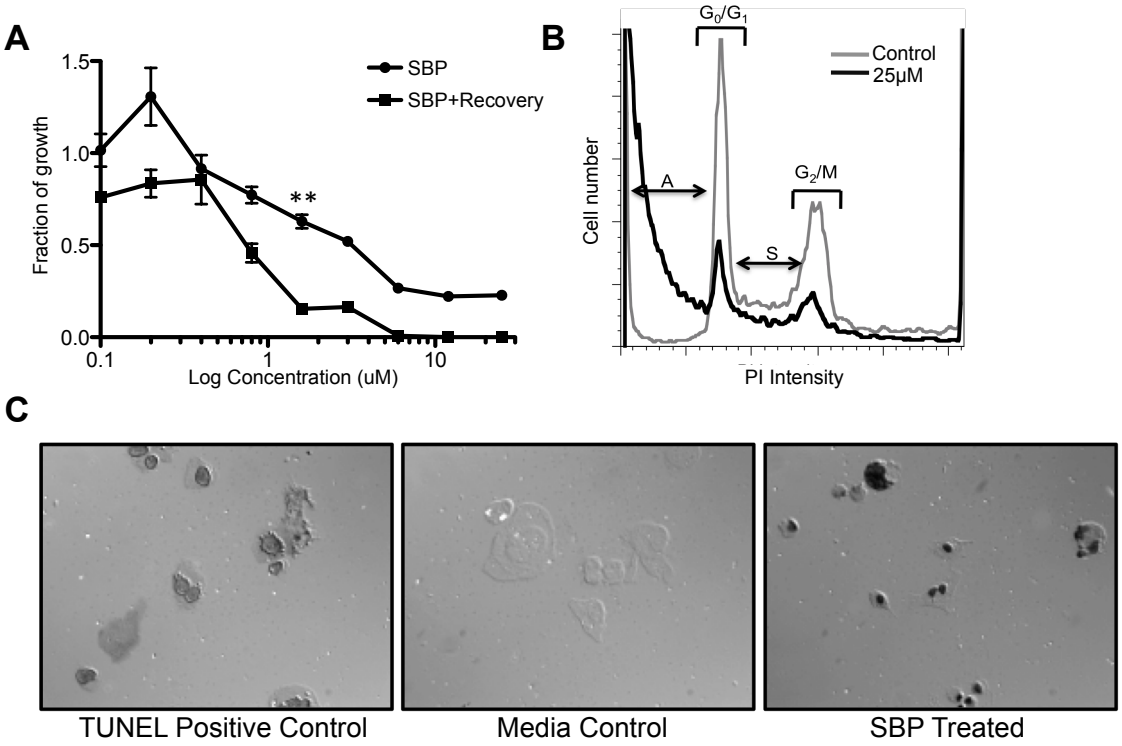
A
1.5
1.0
0.5
0.0
Fraction of growth
SBP
SBP+Recovery
**
0.1
1
10
Log Concentration (uM)
B
G0/G1
Control
25μM
A
G2/M
S
Cell number
PI Intensity
C
TUNEL Positive Control
Media Control
SBP Treated

Figure 3-3. SBP inhibits *in-vivo* glioma growth.

Hematoxylin and eosin stained ex-vivo coronal slices were taken from SBP treated mice and non-treated mice (N=3 for each group) (A) and tumor section areas quantified (Student's T-test, not-treated: 48187 ± 7736, SBP treated: 5489 ± 1369 p=0.0056). T=tumor (B). Tumor bearing mice were treated on day 1, 7 and 13 post injection and sacrificed on day 19. Mouse weights were recorded during the 19-day trial. A best-fit line (not shown) reveals a significant weight decrease in not-treated animals (p=0.0261) but not in SBP treated animals (p=0.8792) (C). Ex-vivo slices were stained for apoptosis (TUNEL) in SBP treated (middle panel) and non-treated mice (right panel). Positive control was treated with the kit's nuclease to generate DNA breaks in every cell (left panel) (D). For all experiments above, N=4 for both treated and non-treated mice. GL-26 implanted mice were either left untreated (N=5) or treated every 6 days with 10mg/kg SBP (N=5) and allowed to progress to moribund. Both a Mantel-Cox test p=0.0384; and Gehan-Breslow-Wilcoxon test p=0.0472 reveal a significant increase in survival time in SBP treated animals (E).

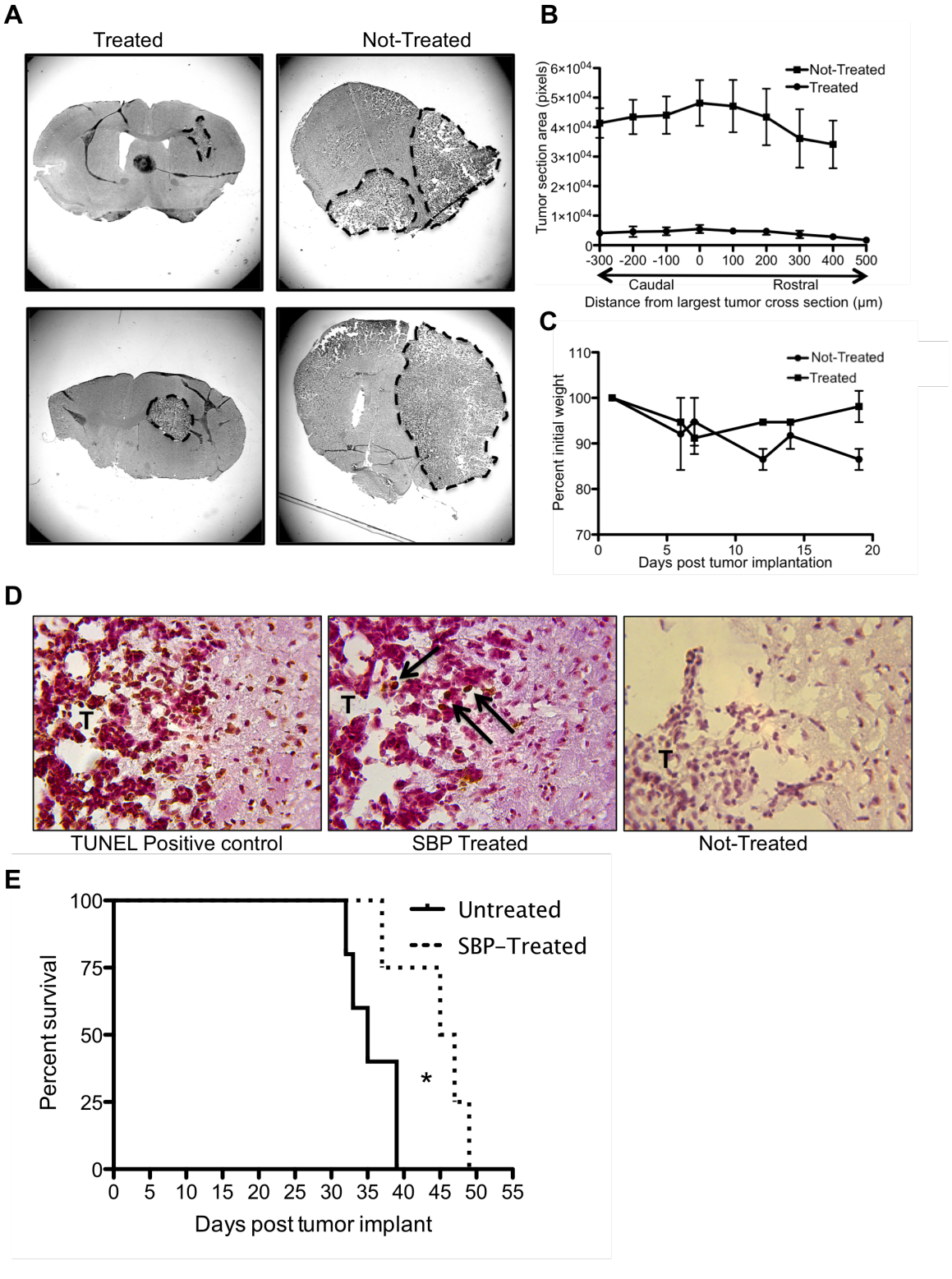
A
Treated
Not-Treated
B
Tumor section area (pixels)
6×10^04
5×10^04
4×10^04
3×10^04
2×10^04
1×10^04
0
Not-Treated
Treated
-300 -200 -100 0 100 200 300 400 500
Caudal
Rostral
Distance from largest tumor cross section (μm)
C
Percent initial weight
110
100
90
80
70
Not-Treated
Treated
0 5 10 15 20
Days post tumor implantation
D
T
T
T
TUNEL Positive control
SBP Treated
Not-Treated
E
Percent survival
100
75
50
25
0
Untreated
SBP-Treated
*
0 5 10 15 20 25 30 35 40 45 50 55
Days post tumor implant

Figure 3-4. SBP does not cause peripheral pathology.

6μm sections from the liver, lung and gut were obtained from SBP treated and non-treated mice, stained with hematoxylin and eosin and assessed blindly by a trained pathologist (A) (N=4 for both treated and non-treated mice). Blood samples from both treated and untreated mice were tested for levels of alanine aminotransferase and aspartate aminotransferase (Student's T-test, ALT: p=0.2596 and AST p=0.3982) (B) (N=4 for both treated and non-treated mice).

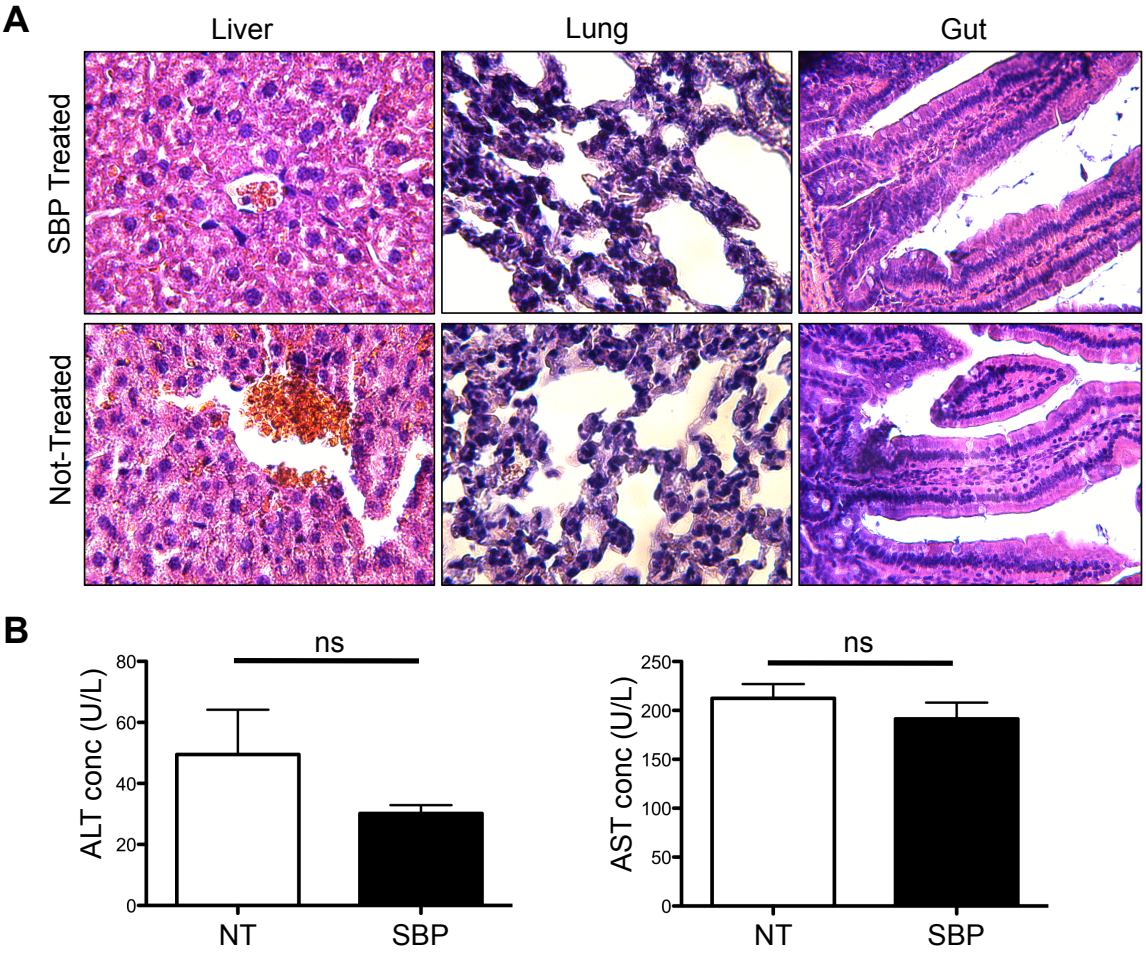
A
Liver
Lung
Gut
SBP Treated
Not-Treated
B
ns
ALT conc (U/L)
0
20
40
60
80
NT
SBP
ns
AST conc (U/L)
0
50
100
150
200
250
NT
SBP

3.7 References:

1 Ajaz M, Jefferies S, Brazil L, Watts C, Chalmers A (2014) Current and investigational drug strategies for glioblastoma. Clin Oncol (R Coll Radiol) 26:419-430.

2 Amacher DE (1998) Serum transaminase elevations as indicators of hepatic injury following the administration of drugs. Regul Toxicol Pharmacol 27:119-130.

3 Bieda R, Ott I, Gust R, Sheldrick WS (2009a) Cytotoxic Rhodium(III) Polypyridyl Complexes Containing the Tris(pyrazolyl)methane Coligand: Synthesis, DNA Binding Properties and Structure–Activity Relationships. European Journal of Inorganic Chemistry 2009:3821-3831.

4 Bieda R, Ott I, Dobroschke M, Prokop A, Gust R, Sheldrick WS (2009b) Structure-activity relationships and DNA binding properties of apoptosis inducing cytotoxic rhodium(III) polypyridyl complexes containing the cyclic thioether [9]aneS(3). J Inorg Biochem 103:698-708.

5 Candolfi M, Curtin JF, Nichols WS, Muhammad AG, King GD, Pluhar GE, McNiel EA, Ohlfest JR, Freese AB, Moore PF, Lerner J, Lowenstein PR, Castro MG (2007) Intracranial glioblastoma models in preclinical neuro-oncology: neuropathological characterization and tumor progression. J Neurooncol 85:133-148.

6 Chamberlain MC, Glantz MJ, Chalmers L, Van Horn A, Sloan AE (2007) Early necrosis following concurrent Temodar and radiotherapy in patients with glioblastoma. J Neurooncol 82:81-83.

7 Charest G, Sanche L, Fortin D, Mathieu D, Paquette B (2013) Optimization of the route of platinum drugs administration to optimize the concomitant treatment with radiotherapy for glioblastoma implanted in the Fischer rat brain. J Neurooncol 115:365-373.

8 Chen J, McKay RM, Parada LF (2012) Malignant glioma: lessons from genomics, mouse models, and stem cells. Cell 149:36-47.

9 Danan G, Benichou C (1993) Causality assessment of adverse reactions to drugs--I. A novel method based on the conclusions of international consensus meetings: application to drug-induced liver injuries. J Clin Epidemiol 46:1323-1330.

10 David C, Nance JP, Hubbard J, Hsu M, Binder D, Wilson EH (2012) Stabilin-1 expression in tumor associated macrophages. Brain Res 1481:71-78.

11 Dobroschke M, Geldmacher Y, Ott I, Harlos M, Kater L, Wagner L, Gust R, Sheldrick WS, Prokop A (2009) Cytotoxic rhodium(III) and iridium(III) polypyridyl complexes: structure-activity relationships, antileukemic activity, and apoptosis induction. ChemMedChem 4:177-187.

12 Duffau H (2009) A personal consecutive series of surgically treated 51 cases of insular WHO Grade II glioma: advances and limitations. J Neurosurg 110:696-708.

13 Friedman HS, Kerby T, Calvert H (2000) Temozolomide and treatment of malignant glioma. Clin Cancer Res 6:2585-2597.

14 Golebiewska A, Bougnaud S, Stieber D, Brons NH, Vallar L, Hertel F, Klink B, Schrock E, Bjerkvig R, Niclou SP (2013) Side population in human glioblastoma is non-tumorigenic and characterizes brain endothelial cells. Brain 136:1462-1475.

15 Hegi ME, Diserens AC, Godard S, Dietrich PY, Regli L, Ostermann S, Otten P, Van Melle G, de Tribolet N, Stupp R (2004) Clinical trial substantiates the predictive value of O-6-methylguanine-DNA methyltransferase promoter methylation in glioblastoma patients treated with temozolomide. Clin Cancer Res 10:1871-1874.

16 Hegi ME, Diserens AC, Gorlia T, Hamou MF, de Tribolet N, Weller M, Kros JM, Hainfellner JA, Mason W, Mariani L, Bromberg JE, Hau P, Mirimanoff RO, Cairncross JG, Janzer RC, Stupp R (2005) MGMT gene silencing and benefit from temozolomide in glioblastoma. N Engl J Med 352:997-1003.

17 Jakobsen S, Tilset M (2011) A rapid synthesis of asymmetric alkyl- and aryl-2,9-disubstituted 1,10-phenanthrolines. Tetrahedron Letters 52:3072-3074.

18 Kelland LR (2006) The Development of Orally Active Platinum Drugs. In: Cisplatin, pp 497-521: Verlag Helvetica Chimica Acta.

19 Kim TG, Kim CH, Park JS, Park SD, Kim CK, Chung DS, Hong YK (2010) Immunological factors relating to the antitumor effect of temozolomide chemoimmunotherapy in a murine glioma model. Clin Vaccine Immunol 17:143-153.

20 Komor AC, Barton JK (2013) The path for metal complexes to a DNA target. Chem Commun (Camb) 49:3617-3630.

21 Mendes F, Groessl M, Nazarov AA, Tsybin YO, Sava G, Santos I, Dyson PJ, Casini A (2011) Metal-based inhibition of poly(ADP-ribose) polymerase--the guardian angel of DNA. J Med Chem 54:2196-2206.

22 Messori L, Abbate F, Marcon G, Orioli P, Fontani M, Mini E, Mazzei T, Carotti S, O'Connell T, Zanello P (2000) Gold(III) complexes as potential antitumor agents: solution chemistry and cytotoxic properties of some selected gold(III) compounds. J Med Chem 43:3541-3548.

23 Miura Y, Takenaka T, Toh K, Wu S, Nishihara H, Kano MR, Ino Y, Nomoto T, Matsumoto Y, Koyama H, Cabral H, Nishiyama N, Kataoka K (2013) Cyclic RGD-linked polymeric micelles for targeted delivery of platinum anticancer drugs to glioblastoma through the blood-brain tumor barrier. ACS Nano 7:8583-8592.

24 Mutter N, Stupp R (2006) Temozolomide: a milestone in neuro-oncology and beyond? Expert Rev Anticancer Ther 6:1187-1204.

25 Narla RK, Chen CL, Dong Y, Uckun FM (2001) In vivo antitumor activity of bis(4,7-dimethyl-1,10-phenanthroline) sulfatooxovanadium(IV) (METVAN [VO(SO4)(Me2-Phen)2]). Clin Cancer Res 7:2124-2133.

26 Niewald M, Berdel C, Fleckenstein J, Licht N, Ketter R, Rube C (2011) Toxicity after radiochemotherapy for glioblastoma using temozolomide--a retrospective evaluation. Radiat Oncol 6:141.

27 Palanichamy K, Sreejayan N, Ontko AC (2012) Overcoming cisplatin resistance using gold(III) mimics: anticancer activity of novel gold(III) polypyridyl complexes. J Inorg Biochem 106:32-42.

28 Pallenberg AJ, Koenig KS, Barnhart DM (1995) Synthesis and Characterization of Some Copper(I) Phenanthroline Complexes. Inorganic Chemistry 34:2833-2840.

29 Poteet E, Choudhury GR, Winters A, Li W, Ryou MG, Liu R, Tang L, Ghorpade A, Wen Y, Yuan F, Keir ST, Yan H, Bigner DD, Simpkins JW, Yang SH (2013) Reversing the Warburg Effect as a Treatment for Glioblastoma. J Biol Chem 288:9153-9164.

30 Pouratian N, Gasco J, Sherman JH, Shaffrey ME, Schiff D (2007) Toxicity and efficacy of protracted low dose temozolomide for the treatment of low grade gliomas. J Neurooncol 82:281-288.

31 Roy S, Hagen KD, Maheswari PU, Lutz M, Spek AL, Reedijk J, van Wezel GP (2008) Phenanthroline derivatives with improved selectivity as DNA-targeting anticancer or antimicrobial drugs. ChemMedChem 3:1427-1434.

32 Safdie F, Brandhorst S, Wei M, Wang W, Lee C, Hwang S, Conti PS, Chen TC, Longo VD (2012) Fasting enhances the response of glioma to chemo- and radiotherapy. PLoS One 7:e44603.

33 Sanghvi CD, Olsen PM, Elix C, Peng S, Wang D, Chen Z, Shin DM, Hardcastle KI, Eichler F J, MacBetha E C (2013) Antitumor Properties of Five-Coordinate Gold(III) Complexes Bearing Substituted Polypyridyl Ligands. Journal of Inorganic Biochemistry 128:68-76.

34 Scharwitz MA, Ott I, Geldmacher Y, Gust R, Sheldrick WS (2008) Cytotoxic half-sandwich rhodium(III) complexes: Polypyridyl ligand influence on their DNA binding properties and cellular uptake. Journal of Organometallic Chemistry 693:2299-2309.

35 Scheig R (1996) Evaluation of tests used to screen patients with liver disorders. Prim Care 23:551-560.

36 Shi P, Jiang Q, Zhao Y, Zhang Y, Lin J, Lin L, Ding J, Guo Z (2006) DNA binding properties of novel cytotoxic gold(III) complexes of terpyridine ligands: the impact of steric and electrostatic effects. J Biol Inorg Chem 11:745-752.

37 Skehan P, Storeng R, Scudiero D, Monks A, McMahon J, Vistica D, Warren JT, Bokesch H, Kenney S, Boyd MR (1990) New colorimetric cytotoxicity assay for anticancer-drug screening. J Natl Cancer Inst 82:1107-1112.

38 Smith KE, Fritzell S, Badn W, Eberstal S, Janelidze S, Visse E, Darabi A, Siesjo P (2009) Cure of established GL261 mouse gliomas after combined immunotherapy with GM-CSF and IFNgamma is mediated by both CD8+ and CD4+ T-cells. Int J Cancer 124:630-637.

39 Srivastava DK, Berg BJ, Prasad R, Molina JT, Beard WA, Tomkinson AE, Wilson SH (1998) Mammalian abasic site base excision repair. Identification of the reaction sequence and rate-determining steps. J Biol Chem 273:21203-21209.

40 Stupp R, Dietrich PY, Ostermann Kraljevic S, Pica A, Maillard I, Maeder P, Meuli R, Janzer R, Pizzolato G, Miralbell R, Porchet F, Regli L, de Tribolet N, Mirimanoff RO, Leyvraz S (2002) Promising survival for patients with newly diagnosed glioblastoma multiforme treated with concomitant radiation plus temozolomide followed by adjuvant temozolomide. J Clin Oncol 20:1375-1382.

41 Stupp R, Mason WP, van den Bent MJ, Weller M, Fisher B, Taphoorn MJ, Belanger K, Brandes AA, Marosi C, Bogdahn U, Curschmann J, Janzer RC, Ludwin SK, Gorlia T, Allgeier A, Lacombe D, Cairncross JG, Eisenhauer E, Mirimanoff RO (2005) Radiotherapy plus concomitant and adjuvant temozolomide for glioblastoma. N Engl J Med 352:987-996.

42 Su YB, Sohn S, Krown SE, Livingston PO, Wolchok JD, Quinn C, Williams L, Foster T, Sepkowitz KA, Chapman PB (2004) Selective CD4+ lymphopenia in melanoma patients treated with temozolomide: a toxicity with therapeutic implications. J Clin Oncol 22:610-616.

43 Sughrue ME, Yang I, Kane AJ, Rutkowski MJ, Fang S, James CD, Parsa AT (2009) Immunological considerations of modern animal models of malignant primary brain tumors. Journal of translational medicine 7:84.

44 Tan C, Lai S, Wu S, Hu S, Zhou L, Chen Y, Wang M, Zhu Y, Lian W, Peng W, Ji L, Xu A (2010) Nuclear permeable ruthenium(II) beta-carboline complexes induce autophagy to antagonize mitochondrial-mediated apoptosis. J Med Chem 53:7613-7624.

45 Thang DC, Jacquignon P, Dufour M (1976) Synthèse d'amines hétérocycliques, cancérostatiques potentiels. Journal of Heterocyclic Chemistry 13:641-644.

46 Wein AN, Stockhausen AT, Hardcastle KI, Saadein MR, Peng SB, Wang D, Shin DM, Chen ZG, Eichler JF (2011) Tumor cytotoxicity of 5,6-dimethyl-1,10-phenanthroline and its corresponding gold(III) complex. J Inorg Biochem 105:663-668.

47 Wesselinova D, Kaloyanov N, Dimitrov G (2009) Cytotoxicity and effects of 1,10-phenanthroline and 5-amino-1,10-phenanthroline derivatives on some immunocompetent cells. Eur J Med Chem 44:5099-5102.

48 Wolff JE, Trilling T, Molenkamp G, Egeler RM, Jurgens H (1999) Chemosensitivity of glioma cells in vitro: a meta analysis. J Cancer Res Clin Oncol 125:481-486.

CHAPTER FOUR

Toxoplasma gondii infection disrupts CNS glutamate homeostasis and neuronal connectivity: implications for behavioral abnormality

4.1 Abstract:

Chronic immune responses are often necessary to control infection but can be highly problematic especially in neurologically sensitive areas like the brain. *Toxoplasma gondii* is a protozoan parasite which can infect any mammalian nucleated cell. It is an extremely successful parasite, infecting about 10-15% of Americans and as much as 80% of people in parts of South America and Europe. Infection by *Toxoplasma* is characterized by the lifelong presence of parasitic cysts in the brain, requiring a competent immune system to prevent parasite reactivation and massive neuronal death. In the immunocompetent individual, *Toxoplasma* infection is largely asymptomatic, though many recent studies suggest that *Toxoplasma* infection strongly correlates to certain neurodegenerative and psychiatric disorders. Little is known about the effects of lifelong brain infections, and thus inflammation, on the psychological health of the host. During *Toxoplasma* infection CNS resident astrocytes become reactive. Astrocytes are critical in regulating levels of the neurotransmitter glutamate. Here we present data demonstrating a significant reduction of the primary glutamate transporter GLT-1 and the enzyme glutamine synthetase following infection. Using microdialysis, we demonstrate a significant increase in glutamate extracellular concentrations, rising over the course of infection. Consistent with this dysregulation of glutamate, analysis of neurons in chronically infected mice reveal fewer dendritic spines in the frontal cortex and areas with decreased NeuN immunoreactivity. EEG recordings and behavioral testing suggest specific changes in brain activity and behavior following infection. Finally, this profound defect in neuronal pathology and host behavior can be rescued by treatment with the ß-

lactam antibiotic Ceftriaxone which specifically induces the expression of GLT-1. Altogether, these data demonstrate that following an infection with *T. gondii*, the delicate regulation of glutamate by astrocytes is disrupted and accounts for a range of deficits observed in chronic infection.

4.2 Introduction:

The balancing act required to fight infection while maintaining tissue homeostasis is perhaps no more critical than in the CNS. Here, the physical restraints imposed by the skull and blood brain barrier alongside low MHC expression and a lack of circulating lymphocytes can delay and limit the immune response. However, perhaps due to these properties, many infectious agents target or localize to the brain (Lafferty and Shaw, 2013). These include bacterial, viral and parasitic pathogens. In many cases, such infections including Herpes virus and *Toxoplasma* are chronic and require immune competency to remain latent (Fagard et al., 1999; Giraudon and Bernard, 2009; Honjo et al., 2009). Our understanding of the effects of continuous immune reactivity, in a tissue that is designed to keep such responses to a minimum, is perfunctory.

Recently, the concept that infections can have a profound and lasting effect on brain function and even host behavior has gained momentum (Giraudon and Bernard, 2009; Honjo et al., 2009; Lafferty and Shaw, 2013). In the case of the protozoan parasite *Toxoplasma gondii,* this lifelong infection resides predominantly as latent cysts inside neurons and requires continuous infiltration of lymphocytes to the brain to prevent parasite reactivation and fatal encephalitis (Fagard et al., 1999). Furthermore, this is not a selective parasite. *Toxoplasma* is one of the most successful pathogens on the planet infecting approximately a third of the world's population with prevalence rates in Europe and the USA between 15-80% (Pappas et al., 2009). Although infection is common, disease induced by *Toxoplasma* is rare and with few exceptions has only been associated with individuals that have profound defects in their immune system. However, in recent

years, interest has focused on the potential relationship of infection with *Toxoplasma* on neurodegenerative and psychiatric disorders. Infection with *Toxoplasma* is a significant risk factor in Parkinson's (Miman et al., 2010), Alzheimer's (AD) (Kusbeci et al., 2011), mania (Dickerson et al., 2014) and Schizophrenia (Yolken et al., 2001; Conejero-Goldberg et al., 2003; Torrey and Yolken, 2003; Webster et al., 2006; Torrey et al., 2007; Torrey et al., 2012) and is correlated with specific changes in murine (Gonzalez et al., 2007; Afonso et al., 2012) and human behavior (Flegr et al., 2000; Flegr, 2007; Flegr et al., 2009; Flegr, 2013b, a). The range of severity and the variety of disease associated with *Toxoplasma* infection suggest the potential for global, as well as specific, alterations in neuronal networks and signaling.

Glutamate is arguably the most important excitatory neurotransmitter in the brain and unregulated levels can cause neuroexcitotoxicity; therefore, CNS glutamate is strictly controlled. Although glutamate is readily available in the periphery, it does not cross the BBB and is thus virtually completely synthesized *de-novo* within the CNS, primarily by astrocytes (Hertz et al., 1999; Danbolt, 2001; Hertz and Zielke, 2004), with neurons able to catalyze glutamine to glutamate through glutaminase. Astrocytes have the important job of regulating CNS glutamate levels by adjusting uptake, release, synthesis into glutamine, and synthesis from α-ketoglutarate or lactate/alanine (Rothstein et al., 1996; Hertz et al., 1999; Danbolt, 2001; Hertz and Zielke, 2004). These cells play an active role in controlling *Toxoplasma* infection with the ability to up-regulate pro-inflammatory cytokines, secrete chemoattractants and internally kill parasites via IGTP (Halonen and Taylor, 2001; Strack et al., 2002; Wilson and Hunter, 2004). However, observations of

astrocytic swelling during infection (Wilson et al., 2009) may point to significant changes in astrocyte physiology. Astrocytic swelling has been linked to the trans-membrane water permeable channel aquaporin-4 (AQP-4) which is highly polarized to astrocytic endfeet surrounding blood vessels (Neely et al., 2001; Amiry-Moghaddam et al., 2004; Nagelhus et al., 2004). Such changes in astrocyte activation and morphology have been linked to dysregulation in glutamate metabolism either via slowing glutamate clearance or dumping of glutamate into the extracellular space (Kimelberg et al., 1995; Feustel et al., 2004; Parpura et al., 2004; Kimelberg et al., 2006; Hyzinski-Garcia et al., 2011; Takaki et al., 2012; Lee et al., 2013).

As glutamate is the major excitatory neurotransmitter in the CNS, the implications of glutamate excitotoxicity are broad. Traditionally, elevated extracellular glutamate concentrations have been observed under acute CNS insults such as ischemia (Zhang et al., 2008) and traumatic brain injury (Obrenovitch and Urenjak, 1997; Werner and Engelhard, 2007). However, many studies have associated elevated ECS glutamate concentrations with neurodegenerative disorders such as amyotrophic lateral sclerosis (ALS) (Foran and Trotti, 2009), multiple sclerosis (MS) (Gonsette, 2008), Alzheimer's disease (Lau and Tymianski, 2010; Schallier et al., 2011) and with CNS infections such as cerebral malaria (CM) (Miranda et al., 2010). Understanding the mechanisms that underlie elevated ECS concentrations of glutamate following CNS insults is critical in developing preventative measures to avoid neuronal death. If there are changes in glutamate concentrations then this could lead to major changes in neuronal biology in the brain.

In these studies we demonstrate that during infection with *Toxoplasma,* astrocyte glutamate regulation is disrupted and CNS extracellular levels of glutamate reach non-homeostatic ranges. Consistent with a dysregulation of glutamate we demonstrate a pattern of neurological damage including decreases in ß-III tubulin, V-Glut1 expression, numbers of dendritic spines and functional output as measured by EEG analysis. Thus, this infection, and the resulting inflammation, leads to dysregulation of glutamate control by astrocytes resulting in neuronal pathology and previously undocumented loss of electroencephalogram power. Finally, damage to neuronal health can be rescued by upregulation of the glutamate transporter GLT-1. The significance of these results suggest that in contrast to treating chronic *Toxoplasma* infection as quiescent and benign, we should be aware of the significant risk to normal neurological pathways and changes in brain chemistry, supported by many correlative studies suggesting *Toxoplasma* infection as a causative agent in a broad range of neurological disease (Flegr et al.; Flegr et al., 1996; Flegr et al., 2000; Yolken et al., 2001; Conejero-Goldberg et al., 2003; Flegr et al., 2003; Torrey and Yolken, 2003; Webster et al., 2006; Flegr, 2007; Torrey et al., 2007; Flegr et al., 2009; Torrey et al., 2012; Flegr, 2013b, a) (Vyas et al., 2007; Hermes et al., 2008; Vyas, 2013). These studies have potential implications for the etiology of a vast range of neuronal disorders in a significant proportion of the world's population. Further, we show that although the source of such dysregulation, namely the parasite, cannot yet be removed pharmaceutically, we may be able to treat many of the resulting symptoms with an approved antibiotic.

4.3 Materials and Methods:

Animals: All animal research has been done in accordance to the Animal Welfare Act. All protocols were approved by the Institutional Animal Care and Use Committee (IACUC) of the University of California, Riverside. All surgery was performed under isofluorane anesthesia, and all efforts were made to minimize suffering. Female C57BL/6 mice were obtained from Jackson Laboratories and maintained in a pathogen free environment under IACUC established protocols at the University of California Riverside.

Infections and treatments: Female C57BL/6 or BALB/c mice were infected intraperitoneally with 20 cysts of the Me49 strain in 200µl of sterile Na+/K+ balanced PBS. Ceftriaxone (TCI, cat# C2226) was administered at 200mg/kg intraperitoneally for 7 days starting at day 35-post infection (day 21-post infection for EEG/microdialysis experiments). Care was taken in alternating sides each day to administer drug. Untreated animals received saline injections.

Anesthesia and Surgery: Mice were anesthetized in an induction box with 3.5% isofluorane and maintained with continuous administration of 2.5% isofluorane through a nose cone.

Microdialysis: For microdialysis experiments, mice were placed in a stereotaxic frame and a 1.5 cm incision was made in order to expose the junction of the coronal and sagittal sutures (bregma). A burr hole was made with a 1mm drill bit 2.58mm rostral and 1.5mm lateral from bregma using a stereotaxic mouse atlas (Franklin and Paxinos, 2008). A CMA 7 guide cannula (CMA P000137) was then lowered 0.5mm ventrally and held in

place with glass ionomer cement (CMA-72-9168). Two additional holes were made on each lateral side of bregma using an anchor screw drill bit (CMA 8003264) to place 2 anchor screws (CMA 7431021) into the skull. The skull was then roughened to allow optimal ionomer bonding by using a 1mm drill bit and gently scraping the entire skull surface around the anchor screws and the guide cannula. Finally, a tether bolt (CMA 61-0037) was held in place while the ionomer cement was applied over the anchor screws, tether bolt and guide cannula. The skin was then gently lifted over the cement and the mouse was allowed to recover on a 38ºC mat.

Electroencephalography: For electroencephalography (EEG) experiments, a burr hole was made as described above at the same stereotaxic coordinates. A twisted bipolar stainless steel bipolar electrode (Plastics One) was inserted 1mm under the dura mater and grounded to the dura. The EEG implant was held in place with glass ionomer cement.

Electron Microscopy: Female C57BL/6 mice infected with Me49 were sacrificed at 3, 6 and 12 weeks post infection and perfused intra-cardiacally with 2.5% gluteraldehyde (Alta Aesar, Cat# 111-30-8), 4% paraformaldehyde (PFA) (Electron Microscopy Sciences, Cat# 19208) in 0.1M sodium cacodylate buffer (Pfaltz & Bauer, Cat# 124-65-2). Brains were removed and post-fixed in the same buffer. Electron microscopy of the frontal cortex of the brain was performed by Renovo Neural inc, 10000 Cedar Avenue, Cleveland, Ohio, 44106. 6-10 Z stacks containing blood vessels 5-6µm wide were selected per group and average astrocyte endfeet width was quantified by measuring perivascular astrocyte area and dividing by the blood vessel circumference.

Real Time PCR: Female C57BL/6 mice infected with Me49 were sacrificed at day 7, 14, 21, 28, 35, 42 and 56 post infection (N=3 per timepoint), and perfused intra-cardically with sterile PBS. Brains were removed and homogenized in TRIzol (Ambion, Cat# 15596026). RNA was extracted using the TRIzol/ chloroform method and concentrations of nucleic acids were determined on a nanodrop 2000. GLT-1 specific primers (forward 5′-ACCTTGCAATCCCTCTTCGG-3′ and reverse 5′-AGACCGGTACCAGGAGTGG-3′), GLAST specific primers (forward 5′-CTGGTAACCCGGAAGAACCC-3′ and reverse 5′-GGGGAGCACAAATCTGGTGA-3′), and Glutamine synthetase specific primers (forward 5′ -ACCCCTATGCGGTGACAGAA-3′ and reverse 5′-CGTCGCCTGTTTCGTTGAG-3′) for Real Time PCR were purchased from IDT's primer Quest (http://www.idtdna.com/Scitools/ Applications/Primerquest/). cDNA synthesis and Real-time PCR were performed using the Bioline One-step Kit with the CFX-96 real-time PCR Detection System (Bio-Rad). The reaction total was a 20µl mixture with 10µl SYBR Green/SensiFAST qPCR Master Mix (2x) and 400nM primer. The reaction conditions were as follows: 10 min at 45°C, followed by 2 min at 95°C and then 40 cycles of 5s at 95°C and 20s at 60°C. The GAPDH (Glyceraldehyde 3-phosphate dehydrogenase) forward primer (5′-AGGCCGGTGCTGAGTATGTC-3′) and reverse primer (5′-TGCCTGCTTCACCACCTTCT-3′) were used as an endogenous control. Quantified results represent the fold induction of target gene expression using the differential CT method. NTC, no-template control (reagent alone without template) was included in each assay to detect any possible contamination of the PCR reagents.

Western Blots: Brains from naïve and 6-week infected C57BL/6 mice were homogenized in protein lysis buffer with DTT and protease inhibitors using the Bullet Blender (Next Advance). Protein concentrations were determined using a BCA protein assay kit from Thermo Scientific (Cat# 23252). 2µg (for GLT-1) or 5µg (for GS) was denatured at 95ºC for 5 minutes in 2µl 10% SDS, 5µl loading buffer, and topped off to 20µl with RIPA buffer. A 10% Tris-HCL gel (BIO-RAD, Cat# 161-1101), was loaded and run at 50-100V in running buffer. The gel was transferred to a nitrocellulose membrane using the semi-dry method in blotting buffer. The membrane was blocked for 1 hour in blocking buffer (5%w/vol BSA, 1X TBST), washed in TBST and incubated with primary antibodies (Rabbit anti Glutamine Synthetase, Sigma Cat# G2781; Rabbit anti GLT-1, Thermo Scientific Cat# PA5-17099) overnight at 4ºC. The membrane was then washed in TBST and incubated in secondary antibodies and imaged on a fluorescent imager (Odyssey, LI-COR Biosciences).

Immunohistochemistry: 6 week infected mice were sacrificed and perfused intra-cardically with PBS followed by 4% PFA. Brains were extracted, post-fixed overnight in 4% PFA followed by a 3 day 30% sucrose equilibration. Brains were frozen at -80ºC in optimal cutting temperature compound (OCT). 10-15µm cryostat sections were then blocked with 10% donkey serum in PBS for 1 hour at room temperature. Primary antibodies against GLT-1, Glutamine synthetase, GFAP, ß-III-Tubulin, Iba-1, NeuN and Vglut-1 (Rat anti GFAP, Invitrogen Cat#130300; Rabbit anti Glutamine Synthetase, Sigma Cat# G2781; Rabbit anti GLT-1, Thermo Scientific Cat# PA5-17099; Rabbit anti Vglut-1, Invitrogen Cat# 48-2400; Chicke anti ß-III-Tubulin, Chemicon Cat# AB9354;

Anti NeuN, Abcam Cat# ab177487; Anti Iba-1, Abcam Cat# ab15690) were incubated overnight at 4ºC in 10% donkey serum and 0.5% Tween-20 in PBS. After several washes in PBST, the slices were incubated 3 hours at room temperature with Alexa Fluor fluorescent secondary antibodies. Slices were then washed and mounted with ProLong Gold (Molecular Probes, Cat# P36935).

Vglut-1 puncta quantification: Serial 10-micron coronal pre-frontal cortex sections stained for Vglut-1 were imaged at 63X using a Zeiss 510 confocal microscope. 8 Micron thick Z-stacks were imaged and analyzed for punta density using Volocity image analysis software.

Nissl Staining: 40µm sections were cut and stained with Cresyl Violet Solution (IHCWORLD, Cat#IW-3007A) as follows. Rehydrate slices in 1 min in 100% EtOH, 1 min in 95% EtOH, and 1 min in distilled water. Stain with Cresyl Violet Solution for 6 min at room temperature then rinse in distilled water. Differentiate stain in 95% EtOH for 2 min and dehydrate slices in 2 changes of 100% EtOH for 5 min each. The slices were then cleared in 2 changes of CitriSolv (Fisher) for 5 min each and mounted.

Neuronal counts: Nissl stained sections were imaged under 400X total magnification and images of layer 2/3 of the prefrontal cortex (Franklin and Paxinos, 2008) were taken from serial sections. Neurons from Naïve (N=35 ROIs each 150µm by 200µm, 1982 neurons) and Infected (N=34 ROIs each150µm by 200µm, 2073 neurons) sections were counted manually using strict morphological guidelines.

Microdialysis: Microdialysis was performed on uninfected and day 3, 7, 10, 14, 21, 28, 35, 42 post-infection C57BL/6 mice. Mice were placed in microdialysis cages

which allowed free movement and access to food and water. 1mm CMA 7 probes (CMA 000082) were implanted through the guide cannula and hooked to a microdialysis syringe pump. Artificial cerebral spinal fluid (CMA P000151) was perfused at a flow rate of 0.6 µl/min and collected in a 1.5ml eppendorf tube. Mice were perfused for 5 hours prior to sample collection to allow for equilibration of the CNS. Samples were then collected over a 3 hour period and placed on dry ice. Samples were sent to Sussex Research Laboratories for amino acid analysis via LC-MS. Data was then analyzed using a one-way ANOVA followed by a Dunnett's post test for each timepoint against naïve concentrations of each amino acid. Results reported as p-values for ANOVA and asterisks for the Dunnett's multiple comparison tests.

Dendritic Spine Analysis: 6 week infected C57BL/6 mice were sacrificed and perfused intracardically with PBS followed by 4% PFA. Brains were then extracted and post-fixed 2 hours in 4%PFA, then stored in PBS. 100µm coronal section were sliced using a vibratome and labeled using DiI coated tungsten particles administered through a gene gun. Dendritic spines in layer 2/3 of the prefrontal cortex were imaged using a Zeiss 510 confocal microscope at a magnification of 63X. 15µm Z-stacks were obtained and dendritic spine counts measured on Volocity 3D imager (Perkin Elmer).

Electroencephalography Recording and Analysis: Mice were connected to the MP150 EEG recording module (Biopac Systems inc.) and EEG traces recorded for 24 hours at a sampling rate of 4000 samples/ second using the AcqKnowledge 4.4 software. Raw EEG traces were filtered using a digital FIR band pass filter between 0.8hz and 30Hz. A fast Fourier transform followed by a power spectrum density analysis was

performed to measure power over the set frequency range of 8-10 30-minute traces for each experimental group. Percent power was calculated by dividing power at each frequency by total power (area under curve) and multiplying by 100. Data was then analyzed using a one-way ANOVA followed by a Bonferroni's multiple comparison's test. For entropy analysis, 7 filtered 2min traces for each group were analyzed for approximate entropy using the following parameters: epoch: 2s; order (m): 2 and filtering level (r): 0.2. All analysis was performed on AcqKnowledge 4.4 software.

Behavioral experiments: Naïve (N=13), 6 week infected (N=11) and 6 week infected and treated with Ceftriaxone for 1 week (N=11) C57B/6 mice were placed at the center of a standard elevated plus maze and recorded with an overhead camera for 5 minutes. The following day, the same cohort was placed at the center of an open field maze (22cm x 22cm) and recorded for 30 minutes. Videos were analyzed blindly with EthoWatcher software; distance travelled and velocity was measured for both the elevated plus maze and open field. Additionally, number of open arm entries and time spent in the open arms of the elevated plus maze was measured.

4.4 Results:

4.4.1 Infection induces profound and chronic astrocytic morphological and molecular changes:

In the brain, all glutamate is synthesized *de-novo* as no transporters exist on the BBB (Hertz et al., 1999); glutamate is then released at presynaptic sites during synaptic transmission. This extracellular glutamate is then carefully regulated by the actions of specific transporters present on astrocytes. Astrocyte activation and swelling has been previously observed following *Toxoplasma* infection (Wilson et al., 2009). To further assess astrocytic health during chronic infection, a series of morphological and molecular analyses were performed. Although we have previously observed astrocytic swelling during the chronic phase of infection (Wilson et al., 2009), to quantify the degree of morphological change in astrocytes in the prefrontal cortex, astrocytic endfeet were analyzed from serial transmission electron microscopy images from mice infected with *Toxoplasma* over the course of chronic infection. The beginning of the chronic stage of infection is characterized by an increase in cyst burden, CNS inflammation, and a decrease in the free tachyzoite form of the parasite and occurs around the third week post infection. Brain slices from naïve and infected mice were compared and astrocyte endfeet measured by electron microscopy. Due to the nature of this sampling it is not always clear if the astrocytes are juxtaposed to sites of infection although the tissue around cysts is clearly distorted **(Fig. 4-1A)**. For consistent measurements, only astrocytic processes enveloping small blood vessels (about 5 μm in diameter) were sampled. In the naïve brain, astrocytic endfeet are on average less than 0.5μm wide. By 3 weeks post-infection,

astrocytic endfeet are already significantly swollen. At 6 weeks post infection, well into the chronic phase, cyst burden has reached a plateau, and the immune response and parasite reactivation have reached a stable balance. Here, astrocytic endfeet width peaks to almost 6 fold higher than naïve (2.606± 0.1021μm; $p<0.0001$) **(Fig. 4-1A)**. The balance between cyst burden and the immune response is maintained for the remainder of the host's life. To test if astrocytic endfeet remain swollen after peak inflammation, endfeet were measured at 12 weeks post infection, late in the chronic phase. Although the endfeet width decreases to 1.562± 0.08404μm, they remain significantly swollen compared to naïve animals ($P<0.0001$) **(Fig. 4-1A)**.

This type of morphological change is frequently indicative of significant changes in the molecular and functional role of these cells. One of the major roles of astrocytes is to remove extracellular glutamate to prevent neuroexcitotoxicity (Rothstein et al., 1996). The main astrocytic glutamate transporter in the forebrain is GLT-1, with GLAST playing a smaller role (Danbolt, 2001). Once glutamate is taken up by the astrocyte, GS converts a portion to glutamine, which can then be safely released back to neurons for conversion to glutamate. Although profound peripheral inflammatory events including the circulation of high levels of the cytokines IFN-γ and TNF-α are occurring one-week post infection, GLT-1, GS and GLAST transcripts are not significantly different than naïve levels **(Fig. 4-1B)**. At 2 weeks post infection, coincident with parasites entering the CNS, a decrease in GS transcripts is observed. This reduction is maintained throughout the chronic and late chronic stages of infection. In contrast, GLT-1 transcripts are significantly reduced and continue to decline over the course of infection **(Fig. 4-1B)**.

Although GLT-1 is responsible for over 90% of glutamate uptake by astrocytes we also measured GLAST. This transporter showed no indication of reduction from naïve levels at any point during infection, remaining constant through the acute inflammation and the establishment of the CNS chronic phase **(Fig. 4-1B).**

4.4.2 Infection with *Toxoplasma* causes profound neuronal pathology:

The prefrontal cortex plays a large role in innate fear, anxiety and decision-making and is also the area of the brain most densely infected with *Toxoplasma* (Dellacasa-Lindberg et al., 2007). To understand the root of behavioral changes induced by infection, the prefrontal cortex was examined at 6 weeks post infection, well into the chronic phase, for changes in neuronal morphology (Conejero-Goldberg et al., 2003; Hermes et al., 2008). Immunohistochemistry staining for β-III tubulin, a cytoskeleton component of neurons, reveals a profound disruption in neuronal structure. Indeed, mice infected with *Toxoplasma* exhibit significantly fewer β-III tubulin positive cells ($p=0.0012$) **(Fig. 4-2A)**. To test if this lack of β-III tubulin was due to the absence of neurons and therefore neuronal death or merely an indicator of poor neuronal health, nissl staining was performed. Neuronal counts in layer II/III of the prefrontal cortex of naïve ($n=1982$ neurons) and infected ($n=2073$ neurons) reveal no significant differences in neuron density, suggesting that no neuronal death is occurring ($p=0.132$)**(Fig. 4-2B)**. To test if synaptic changes in the frontal cortex are occurring during infection with *Toxoplasma*, labeling of dendritic spines, postsynaptic sites of excitatory synapses, was performed using DiI delivered on tungsten particles by gene gun. Secondary dendrites in

layers II/III and IV were randomly selected from serial sections of the frontal cortex and spines counted blindly. Infection with *Toxoplasma* significantly reduces spine density in 6 week infected C57BL/6 mice compared to naïve (I=5.510±0.2474 spines per 10 μm and N=6.456±0.2122 spines per 10 μm; p=0.0046) **(Fig. 4-2C)**. To further test the extent of synaptic loss, IHC staining for the excitatory presynaptic marker Vglut-1 was conducted and reveals a dramatic loss of Vglut-1 positive presynaptic boutons in the brains of chronically infected animals (scale bar: 33 μm, insert scale bar: 10 μm) **(Fig. 4-2D)**. These data demonstrate that although the infection is categorized as asymptomatic, with no neuronal death observed, significant disruption in neuronal cytoskeleton and significant decreases in excitatory synapses occur during the chronic phase of the infection.

4.4.3 Glutamate extracellular concentrations increase during infection:

Global disruption of the cytoskeletal component β-III-tubulin and loss of dendritic spines may be a result of glutamate excitotoxicity. Interestingly, previous studies in *Toxoplasma* infected mice have also demonstrated a decrease in neuronal branching (Parlog et al., 2014), decreases in the dendritic marker MAP2 (Cekanaviciute et al., 2014) and the excitatory postsynaptic density marker PSD95 (Parlog et al., 2014). Excitotoxicity occurs when extracellular levels of glutamate increase to a pathological level; this is often measured in animal models of highly pathological and neurodegenerating diseases such as multiple sclerosis, Alzheimer's disease, Parkinson's disease, amyotrophic lateral sclerosis (ALS) and cerebral malaria (Gonsette, 2008; Foran

and Trotti, 2009; Lau and Tymianski, 2010; Miranda et al., 2010; Schallier et al., 2011). To measure extracellular levels of glutamate in the prefrontal cortex during infection with *Toxoplasma*, 1mm long microdialysis probes were positioned in the frontal cortex of C57BL/6 mice and the dialysate was collected over the course of infection. At the conclusion of the experiment, brains were harvested and histologically assessed for appropriate probe positioning and signs of necrotic tissue **(Fig. 4-3A)**. Using LC-MS, the extracellular concentration of all 20 amino acids was measured. As a positive control, a separate cohort was injected intraperitoneally with pentylenetetrazol (PTZ) (60mg/kg) and the dialysate collected. PTZ induces the depolarization of neurons and can cause seizures at high doses; therefore, a spike in extracellular glutamate is expected. Indeed, PTZ administration produced a large spike in both glutamate (E) and its analogue aspartic acid (D) within 5 minutes of administration **(Fig. 4-3B, arrows)** with little to no changes in other amino acids demonstrating successful microdialysis and measurement of glutamate in the murine frontal cortex.

Extracellular concentrations of amino acids were then measured at days 3, 7, 10, 14, 21, 28, 35 and 42-post infection with *Toxoplasma.* Extracellular glutamate levels remain low and constant during the first 3 weeks of infection however, consistent with our observations of astrocyte and neuronal morphologies, a significant increase is observed at and after 5 weeks and continues to increase over the course of infection **(Fig. 4-3C)**(one way ANOVA; $p=0.0003$).

The dysregulation of glutamate can occur through a number of mechanisms. As we have documented extreme swelling of astrocytes, one these mechanisms could be via

volume regulated anion channels (VRAC). However measurement of aspartate and glutamine did not exhibit the same pattern of increasing concentrations and therefore suggest that the non-specific dumping of amino acids as would occur through VRACs is a less likely mechanism. Further, glutamine is the most prevalent amino acid in the CNS and its extracellular concentration is not directly regulated by GLT-1, GS or GLAST. Although aspartate is co-transported with glutamate, its extracellular levels can be maintained independently of GLT-1 and GLAST. Both glutamine and aspartate exhibit non significant changes during the course of infection indicating that changes observed in glutamate are not due to an experimental artifact ($p=0.2023$, $p=0.2227$ respectively). Most of the essential amino acids (besides glutamate, aspartate and glutamine) exhibited a U-shaped curve, with extracellular levels sharply increasing in early acute infection, then decreasing back to naïve levels between days 10 and 28 only to increase again during the chronic stage **(Fig. 4-3D, S1)**. Using a one-way ANOVA, significant changes in extracellular levels of Tryptophan ($p=0.0071$), Histidine ($p=0.0403$), Lysine ($p=0.0243$), Phenylalanine ($p=0.0229$), Proline ($p=0.0168$), Serine ($p=0.04$), Threonine ($p=0.0052$) and Tyrosine ($p=0.0149$) were measured during the course of infection. A Dunnett's post-test was performed for all timepoints against naïve concentrations and significance shown as asterisks on Figure 3 and Supplemental Figure 1. One notable change is in arginine, which continuously decreases during the course of infection **(Fig. 4-3D)** ($p<0.0001$). Arginine is an important substrate for anti-microbial factors including nitric oxide, which is readily made during infection with *Toxoplasma.* Non-essential amino acids show a similar U-shaped response **(S1),** which suggest a global disruption of

brain metabolism during the course of infection. Thus, during *Toxoplasma* infection we can measure a specific and sustained dysregulation of glutamate over the course of infection.

4.4.4 Ceftriaxone does not alter the immune response to *Toxoplasma* infection:

The antibiotic Ceftriaxone has previously been reported to up-regulate GLT-1 in mouse models of ALS (Rothstein et al., 2005) and shown to be neuroprotective in a variety of CNS injury where increases in extracellular glutamate are also observed (Lipski et al., 2007; Verma et al., 2010). Ensuring that treatment with Ceftriaxone in this model is neuroprotective via an increase in GLT-1 and not a reduction in inflammation or parasite burden is critical. To address this potential caveat, we measured the immune response and parasite burden in Ceftriaxone treated and untreated infected mice 6 weeks post infection. Mice treated with Ceftriaxone had similar weights compared to untreated mice **(Fig. 4-4A)**, and exhibited similar inflammation in the meninges and in the perivascular space of the prefrontal cortex **(Fig. 4-4B)**. To test if Ceftriaxone altered immune cell infiltration, brain mononuclear cell extraction was performed at 6 weeks post infection and immune cells were counted; these typically include T-cells, macrophages and resident microglia. Mice treated with Ceftriaxone did not display a significantly different number of total immune cells when compared to untreated mice **(Fig. 4-4C)**. This indicates that treatment with Ceftriaxone does not impair or enhance immune cell infiltration in the CNS. Furthermore, flow cytometry reveals that the proportions of infiltrating CD8 and CD4 T-cells did not significantly differ from

Ceftriaxone treated and untreated mice **(Fig. 4-4D)**. To test whether Ceftriaxone can directly or indirectly kill *Toxoplasma*; parasite DNA was quantified from the frontal cortex of 6 week infected treated and untreated animals and revealed no significant differences between the two groups **(Fig. 4-4E)**. Finally, to test if Ceftriaxone inhibited the global astrocyte and microglial activation typically seen in *Toxoplasma* infections, brain slices were stained for the microglial marker Iba-1 and the astrocyte marker GFAP. Both the Ceftriaxone treated and the untreated infected mice exhibited widespread microglial and astrocytic activation **(Fig. 4-4F)**.

4.4.5 Ceftriaxone specifically rescues glutamate transporter GLT-1:

To determine if Ceftriaxone could rescue GLT-1 expression in *Toxoplasma* infected mice, chronically infected C57BL/6 mice were treated with 200mg/kg i.p for one week starting at 5 weeks post infection. At 6 weeks post infection, brains were harvested to measure RNA and protein expression of GLT-1. This treatment paradigm did not induce any significant changes in the transcript expression of GLT-1, GS or GLAST compared to untreated mice **(Fig. 4-5A)**. Mice infected with *Toxoplasma* exhibited a significant decrease in GLT-1 and GS protein compared to naïve mice **(Fig. 4-5B, Fig. 4-5C)**. These data corroborate the decrease in GS and GLT-1 transcripts over the course of infection **(Fig. 4-1B)**. When treated with Ceftriaxone for one week, GLT-1 protein, but not GS, is partially rescued **(Fig. 4-5B, Fig. 4-5C)**, confirming the specificity of Ceftriaxone in regulating GLT-1 expression(Rothstein et al., 2005). Finally, immunohistochemistry for GLT-1 on serial sagittal sections reveals large areas negative

for GLT-1 staining in the pre-frontal cortex of the untreated but not the Ceftriaxone treated mice **(Fig. 4-5D)**.

These data suggest that infection with *Toxoplasma* significantly decreases GLT-1 and GS protein levels and that Ceftriaxone treatment for one week partially rescue GLT-1 protein and prevent the formation of large GLT-1 negative patches in the cortex. These experiments were repeated on the BALB/C strain to test whether the dramatic loss of GLT-1 is specific to the susceptible C57BL/6. BALB/C mice infected with *Toxoplasma* suffer a significant loss in GLT-1 protein **(S2)** suggesting that GLT-1 loss is a global and common mechanism between mouse strains.

4.4.6 Ceftriaxone is neuroprotective during infection with *Toxoplasma*:

The elevated levels of ECS glutamate observed in infection could possibly offer one explanation for the profound neuronal damage observed. Treatment with Ceftriaxone and subsequent protection of GLT-1 loss is expected to have a protective effect on neurons. To assess the protective effects of Ceftriaxone on neuronal health during chronic infection with *Toxoplasma*, immunohistochemistry was performed for the neuronal nucleic marker NeuN. A marked decrease in staining intensity was observed in chronically infected mice when compared to naïve. Some areas of the cortex were devoid of NeuN staining, suggesting poor neuronal health **(Fig. 4-6A)**. Remarkably, mice treated with Ceftriaxone did not exhibit reduced NeuN staining in any cortical areas **(Fig. 4-6A)**. Higher magnification confocal imaging reveal dramatic differences in the pattern of NeuN staining between naïve and infected animals. While NeuN is strongly positive in

the nucleus of naïve neurons, it appears cytoplasmic in the infected animals. Treatment with Ceftriaxone protects the loss of nuclear NeuN **(Fig. 4-6A)**. These data suggest that infection with *Toxoplasma* is damaging to neurons and that treatment with Ceftriaxone is effective in preventing areas of neuronal damage.

Western blot for Vglut-1 in naïve, chronically infected and Ceftriaxone treated animals demonstrates a striking loss in excitatory synapses during infection ($p<0.0001$), which is not quantitatively rescued by a 7-day Ceftriaxone treatment ($p=0.0725$) **(Fig. 4-6B)**. This data suggest a loss of excitatory synapses during infection with *Toxoplasma,* possibly due to increased levels of extracellular glutamate. Although the 7-day Ceftriaxone treatment does not rescue Vglut-1 levels, the low p-value suggests that a longer treatment might allow greater time for recovery to occur.

To test if Ceftriaxone can protect total synaptic loss in the frontal cortex that are occurring during infection with *Toxoplasma*, dendritic spine labeling was performed using DiI and spines were blindly counted in naïve, infected and treated mice. Corroborating our previous experiment **(Fig. 4-2C)**, infection with *Toxoplasma* significantly reduces spine density in 6 week infected C57BL/6 mice compared to naïve (I=5.573±0.2288 spines per 10 μm and N=6.724±0.2572 spines per 10 μm; $p=0.0052$) **(Fig. 4-6C)**. Ceftriaxone treated mice did not exhibit any significant change in spine density when compared to naïve (C=6.922±0.2904 spines per 10 μm and N=6.724±0.2572 spines per 10 μm; $p=0.2026$) **(Fig. 4-6C)**, but did have significantly more spines than untreated infected mice (C=6.922±0.2904 spines per 10 μm and I=5.573±0.2288 spines per 10 μm; $p=0.0004$) **(Fig. 4-6C)**. These findings demonstrate

that during infection with *Toxoplasma,* neurons of the frontal cortex lose a significant number of spines, which can be rescued by treatment with Ceftriaxone.

4.4.7 Infection with *Toxoplasma* disrupts neuronal networks and changes behavior:

There are numerous correlations with *Toxoplasma* infection, human behavior and disease including an increase in risk seeking behavior, schizophrenia and Alzheimer's disease (Flegr et al., 2000; Yolken et al., 2001; Conejero-Goldberg et al., 2003; Torrey and Yolken, 2003; Webster et al., 2006; Flegr, 2007; Torrey et al., 2007; Flegr et al., 2009; Kusbeci et al., 2011; Torrey et al., 2012; Flegr, 2013b, a). Experiments in mice have demonstrated a highly specific effect of infection on olfaction and behavior towards bobcat urine (Vyas et al., 2007), postulated to relate to the need of the parasite to return to the definitive host, the cat. The mechanism, of what must be a highly specific modulation of neuronal activity has recently been described as epigenetic control of the arginine vasopressin promoter of the amygdala (Hari Dass and Vyas, 2014). However such specific alterations are less likely to lead to the wide range of human disorders correlated with infection. Other studies have described widespread changes in neuronal connectivity (Parlog et al., 2014), pathology, and behavior (Hermes et al., 2008). Our data demonstrates a significant and global dysregulation of the main excitatory neurotransmitter in the brain, which could translate to functional and behavioral abnormalities in infected mice.

To further test if and what neuronal changes are induced by chronic *Toxoplasma* infection, mice were subjected to the elevated plus maze anxiety tests (Gonzalez et al., 2007; Walf and Frye, 2007; Afonso et al., 2012) **(Fig. 4-7A)**. Following six weeks of infection, the time mice spent in the open arm of the elevated maze was assessed and compared to uninfected naïve, and Ceftriaxone treated mice. Consistent with experiments conducted in rats (Gonzalez et al., 2007) and mice (Afonso et al., 2012), mice placed on an elevated plus maze spent significantly more time in the open arms of the maze ($p=0.0002$) **(Fig. 4-7B)** and entered the open arms more frequently ($p=0.0005$) **(Fig. 4-7C)** when infected with *Toxoplasma*. Ceftriaxone treatment for one week does not rescue either phenotype. The observed increase in open arm activity is not due to an increase in the general activity of infected mice as there were no differences in the distance travelled or velocity compared to naïve mice ($p=0.9569$ and $p=0.9561$ respectively) **(Fig. 4-7D)**. In the open field test, performed to measure differences in activity between naïve, infected and Ceftriaxone treated mice, no significant differences were observed in both velocity and distance traveled over a 30min test **(S3)**. This confirms that the chronic stage of *Toxoplasma* infection causes profound and persistent behavioral changes in the mouse.

To test if Ceftriaxone treatment rescued extracellular levels of glutamate, microdialysis was performed on naïve, 6-week infected and ceftriaxone treated mice. Ceftriaxone treatment selectively rescues glutamate levels (N vs I: $p=0.0003$; I vs C: $p=0.0072$) **(Fig. 4-7E)**, with no significant changes in other amino acids **(Fig. 4-7E, S4)**.

If glutamate is dysregulated on a global scale, then we would expect to see abnormalities in the collective firing of neurons. To test if the changes in behavior are paralleled by changes in normal electrical activity of the brain, EEGs were performed on uninfected, chronically infected and Ceftriaxone treated mice. Ceftriaxone treatment began at 3 weeks post infection and continued throughout the experiments. The EEG probes, placed in the frontal cortex, measured brain activity for 24-hour periods and allowed for a detailed analysis of EEG waveform and power. Following 6 weeks post infection; the thalamo-cortical rhythmic waves (**Fig. 4-7F, arrows)** observed in naïve mice are disrupted in infected mice **(Fig. 4-7F)** suggesting a reduction or perturbation in synchronous neuronal firing. The degree of pattern in an EEG trace can be quantitatively measured using approximate entropy; this technique can quantify the level of unpredictability in a time series, with larger values representing less regularity. In line with Ceftriaxone's neuroprotective qualities and its rescue of dendritic spine density, treatment partially rescues these rhythms as measure by approximate entropy (Naïve vs Infected, $p<0.0001$; Infected vs Ceftriaxone, $p=0.0057$; Naïve vs Ceftriaxone, $p=0.0138$) **(Fig. 4-7F)**. EEG power over the entire physiological frequency range was then quantified as a measure of neuronal synchrony and normal brain functioning. A dramatic loss in EEG power over all frequencies is observed at 4, 5 and 6 weeks post infection compared to naïve (One way ANOVA: $p<0.0001$ Bonferroni's post test: $p<0.001$ between Naïve and Infected for week 4, 5 and 6) **(Fig. 4-7G)** and is not rescued by a one-week treatment with ceftriaxone (One way ANOVA: week 4, $p<0.0001$ Bonferroni's post test not significant between Infected vs Ceftriaxone). However, continued treatment with

ceftriaxone partially rescues EEG power at 5 (One way ANOVA: week 5, $p<0.0001$ Bonferroni's post test (I vs C): $p<0.001$) and 6 weeks (One way ANOVA: week 6, $p<0.0001$ Bonferroni's post test (I vs C): $p<0.05$) post infection **(Fig. 4-7G)**. To test whether the EEG power is allocated differentially across frequencies between the naïve, infected and treated groups, percent power was calculated **(Fig. 4-7H)**. Although the ceftriaxone treated group is particularly variable, no significant differences in power allocation was observed between all 3 groups across weeks 4, 5 and 6 post infection (One way ANOVA). These data suggest that a loss in signal, rather than a redistribution is occurring during the course of infection. These data demonstrate that infection with *Toxoplasma* alters neuron biology, electrical physiology and ultimately, behavior.

4.5 Discussion:

To this day, scientists are still unsure on the etiology of a variety of common neurodegenerative diseases. Although AD, dementia, cognitive impairment and some neuropsychiatric disorders all have genetic components, these are often not sufficient to explain the disease in all patients. It is now appreciated that epigenetic factors and insults acquired during the lifespan of the patient play an important role in predisposing humans to certain diseases (Masliah et al., 2013; Pezzi et al., 2014). An example examining early life infections with a variety of viruses report that CNS or systemic infections are a significant risk factor in the pathogenesis and pathophysiology of AD. Furthermore, the same study reports that chronic CNS infections are a significant risk factor of sporadic AD (Honjo et al., 2009). Although infection with *Toxoplasma* is largely asymptomatic, the chronicity and CNS localization of the parasitic infection warrants investigation of its effects on brain function. In light of the recent animal studies demonstrating the profound behavioral changes *Toxoplasma* infection induces in rodents, (Vyas et al., 2007; Vyas, 2013; Hari Dass and Vyas, 2014) as well as the many human studies suggesting infection with *Toxoplasma* being a significant risk factor in a variety of diseases (Torrey and Yolken, 2003; Miman et al., 2010; Kusbeci et al., 2011; Dickerson et al., 2014) and is correlated with risk-seeking behavior (Flegr et al., 1996; Flegr, 2007; Flegr et al., 2009; Flegr, 2013a), we suggest that treatment of CNS infections must be considered as an option when treating for these diseases.

In this report, we set out to characterize the CNS pathology and its effect on normal brain function during the chronic phase of infection. We have demonstrated that

infection with *Toxoplasma* causes profound changes in behavior and brain wave activity suggesting a significant modification of neuronal networks. We further show significant neuronal pathology in the pre-frontal cortex including decreases in dendritic spine density and disruption in a variety of neuronal proteins consistent with neuronal damage as a result of glutamate excitotoxicity. Microdialysis experiments then confirmed a robust increase in ECS glutamate and revealed dynamic changes in ECS amino acids during the course of infection. We also demonstrate a clear defect in glutamate regulation by astrocytes, which is rescued by the beta-lactam antibiotic Ceftriaxone. Restoring glutamate regulation rescues the neuronal pathology observed and some homeostatic brain function. These data suggest that although infected mice are nearly indistinguishable from their naïve counterparts, severe and chronic CNS pathology is occurring which could contribute to neurodegenerative disorders or to mental illness.

We have shown that infection with *Toxoplasma* specifically changes glutamate homeostasis in the brain. With no transporters for glutamate on the blood brain barrier, all CNS glutamate carbon skeletons are synthesized *de novo* from astrocytes. This specificity is due to the key astrocyte specific enzymes pyruvate decarboxylase and cytosolic malic enzymes responsible for glutamate carbon skeleton production and recycling of excess glutamate into the metabolic pathway (Hertz et al., 1999). Astrocytes are not only the only CNS cell type able to sustain *de-novo* production of glutamate; they also are critical in regulating its extracellular levels. The astrocytic glutamate transporters GLT-1 and GLAST are present at high densities in the forebrain and cerebellum respectively, and are responsible for over 90% of ECS glutamate uptake (Hertz et al., 1999; Danbolt, 2001;

Hertz and Zielke, 2004). These glutamate transporters use the sodium/ potassium gradients to co-transport glutamate into the astrocytic compartment against its concentration gradient. Indeed, glutamate is present in the astrocyte at an estimated 100-1000 times the concentration in the ECS (Hertz et al., 1999; Danbolt, 2001; Hertz and Zielke, 2004). Another astrocyte specific enzyme, glutamine synthetase, converts intracellular astrocytic glutamate to glutamine, thus stabilizing the intracellular glutamate concentrations. The specificity of glutamate synthesis and regulation by astrocytes leaves the CNS vulnerable to excitotoxicity by lack of compensatory mechanisms to regulate glutamate should astrocytes fail. This evidently occurs in most CNS injuries, infections and neurodegenerative diseases as many are characterized by an increase in CNS extracellular glutamate and an astrocytic dysregulation of glutamate (Obrenovitch and Urenjak, 1997; Werner and Engelhard, 2007; Gonsette, 2008; Zhang et al., 2008; Foran and Trotti, 2009; Lau and Tymianski, 2010; Miranda et al., 2010; Schallier et al., 2011). ECS glutamate can reach excitotoxic levels either by decreased glutamate uptake, increased secretion during neuronal transmission, or both. In *Toxoplasma* infection, we demonstrate a decrease uptake by GLT-1 leading to an increase in ECS glutamate most likely exacerbated by increased glutamate release through the glutamate/cysteine antiporter xc^- system expressed by microglia and other cells in the CNS during inflammatory events. Massive glutamate release has also been reported to occur through the astrocyte specific volume regulated anion channels (VRACs) during cell swelling (Feustel et al., 2004; Kimelberg et al., 2006; Haskew-Layton et al., 2008). Although we observe significant astrocytic swelling during the course of infection, it is unlikely that

glutamate is being released through VRACs as a parallel ECS increase in aspartic acid would be expected and is not observed (Feustel et al., 2004; Bowens et al., 2013). The sustained increase in ECS glutamate is associated with profound neuronal damage including decreased synaptic density and altered neuronal signaling as evidenced by EEG. These changes result in very specific behavioral modifications in rodents (Vyas et al., 2007; Vyas, 2013; Hari Dass and Vyas, 2014). However, *Toxoplasma* infection in humans is associated with a wide range of pathologies (Torrey and Yolken, 2003; Miman et al., 2010; Kusbeci et al., 2011; Dickerson et al., 2014) suggesting a possible disruption a basic mechanism affecting multiple parts of the brain.

Understanding the multifactorial etiology of neurodegenerative diseases is critical in our approach in developing therapeutics. To date, there are no comprehensive studies on the CNS pathology of *Toxoplasma* infection in humans. The CNS localization and the life-long presence of the parasite make it a good candidate as a risk factor for neurodegenerative diseases and with a global infection rate of 30%, the potential population at risk could be significant. As increasing numbers of publications report *Toxoplasma* infection as a risk factor in a multitude of diseases (Yolken et al., 2001; Miman et al., 2010; Kusbeci et al., 2011; Dickerson et al., 2014), we suggest that infection could act as a trigger for the observed pathology, possibly by dysregulation of glutamate homeostasis.

4.6 Figures and Legends:

Figure 4-1. Infection induces profound and chronic astrocytic morphological and molecular changes.

A) Scanning serial electron microscopy images (Renovo) were analyzed for astrocytic endfeet width (highlighted in yellow). A significant increase in endfoot width is observed during the course of infection (scale bar: 5μm, BV: blood vessel). The first panel depicts a *Toxoplasma* cyst inside a neuron (red) within the frontal cortex. B) Whole forebrain RNA RT-qPCR for GLT-1 and glutamine synthetase demonstrates a reduction in both transcripts over the course of infection with no changes in GLAST transcripts.

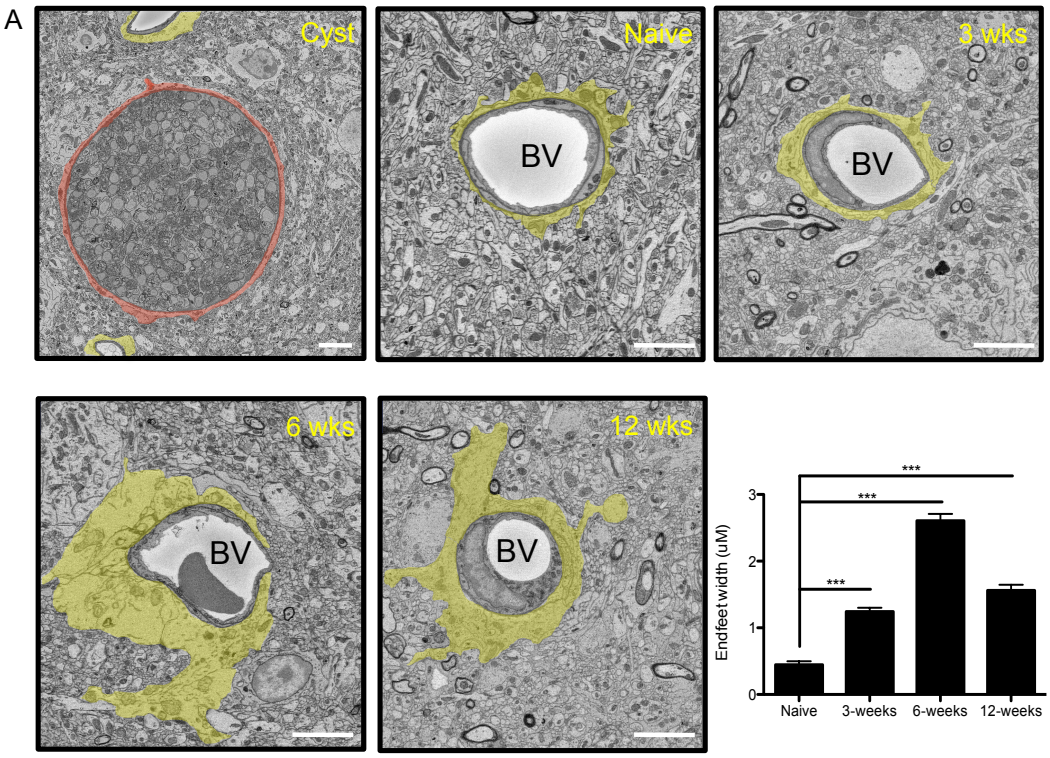
A
Cyst
Naive
3 wks
6 wks
12 wks
BV
BV
BV
BV
Endfeet width (uM)
***
***
***
Naive
3-weeks
6-weeks
12-weeks

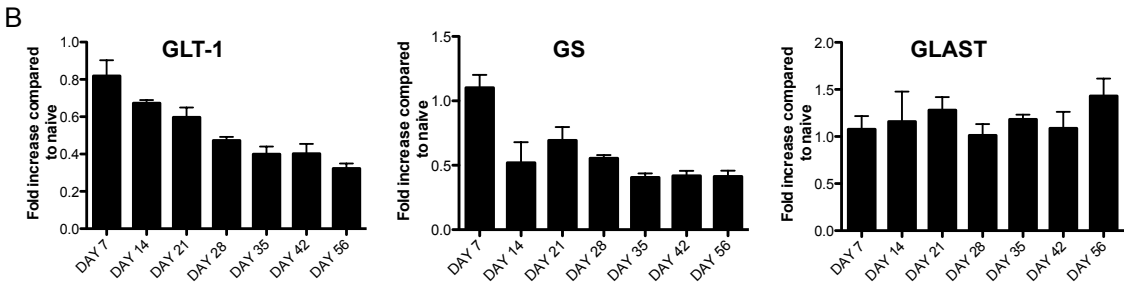
B
GLT-1
GS
GLAST
Fold increase compared to naive
DAY 7
DAY 14
DAY 21
DAY 28
DAY 35
DAY 42
DAY 56

Figure 4-2. Infection with *Toxoplasma* causes profound neuronal pathology.

A) Immunohistochemistry staining was performed on 12-micron sections of naïve and 6 week infected mice for ß-III Tubulin. A significant (p=0.0012) reduction in ß-III Tubulin positive cell count is present in the infected animals compared to naïve (scale bar: 90µm). B) Nissl stain of 40µm 6 week infected and naïve brain sections. Cortical layers labeled with roman numerals and representative ROI shown (square). No significant difference in neuronal counts between infected and naïve groups (Naïve: 34 ROIs, 1982 neurons; Infected: 35 ROIs, 2073 neurons; p=0.132) (scale bar 70µm and 18µm). C) DiI labeling of dendritic spines in the pre-frontal cortex of naïve and 6 week infected animals reveals a significant decrease in dendritic spine density in the infected mice (p=0.0046) (scale bar: 7µm). D) Immunohistochemistry for Vglut-1 in the pre-frontal cortex of naïve, chronically infected and Ceftriaxone treated mice. (Scale bar: 33µm; insert scale bar: 10µm).

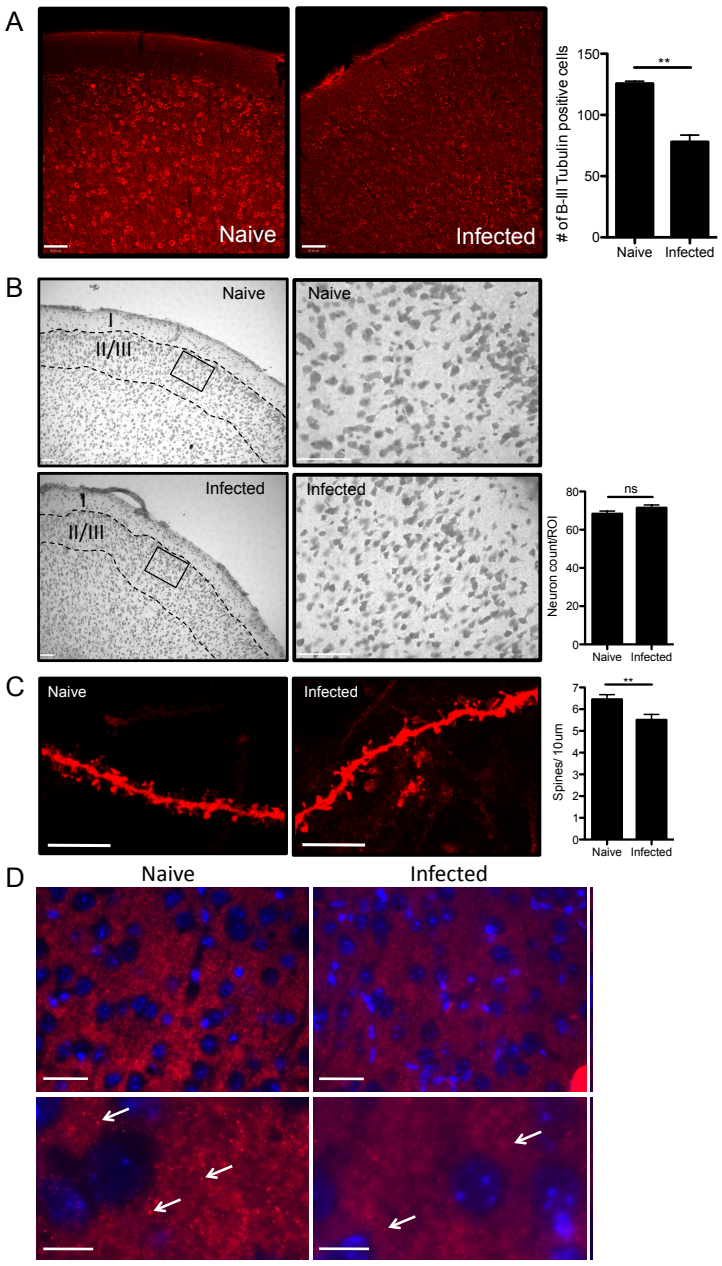
A
Naive
Infected
# of B-III Tubulin positive cells
150
100
50
0
**
Naive
Infected
B
Naive
Naive
I
II/III
Infected
Infected
I
II/III
Neuron count/ROI
80
60
40
20
0
ns
Naive
Infected
C
Naive
Infected
Spines/ 10um
7
6
5
4
3
2
1
0
**
Naive
Infected
D
Naive
Infected

Figure 4-3. Glutamate extracellular concentrations increase during infection.

A) Hematoxylin and eosin staining was performed to confirm microdialysis probe placement in the frontal cortex. B) Intraperitoneal injections of pentylenetetrazol were completed to confirm detection and changes in concentration of each amino acid. C,D) LC-MS analysis (Sussex) on microdialysis samples over the course of infection reveal dynamic changes in non-essential extracellular amino acid concentration in the CNS. A one-way ANOVA reveals significant changes in Glutamate ($p=0.0003$), Arginine ($p<0.0001$), Proline ($p=0.0168$), Serine ($p=0.04$), and Tyrosine ($p=0.0149$). A Dunnett's post-test was performed for all timepoints against naïve concentrations and significance shown as asterisks. Amino acids not listed did not change significantly.

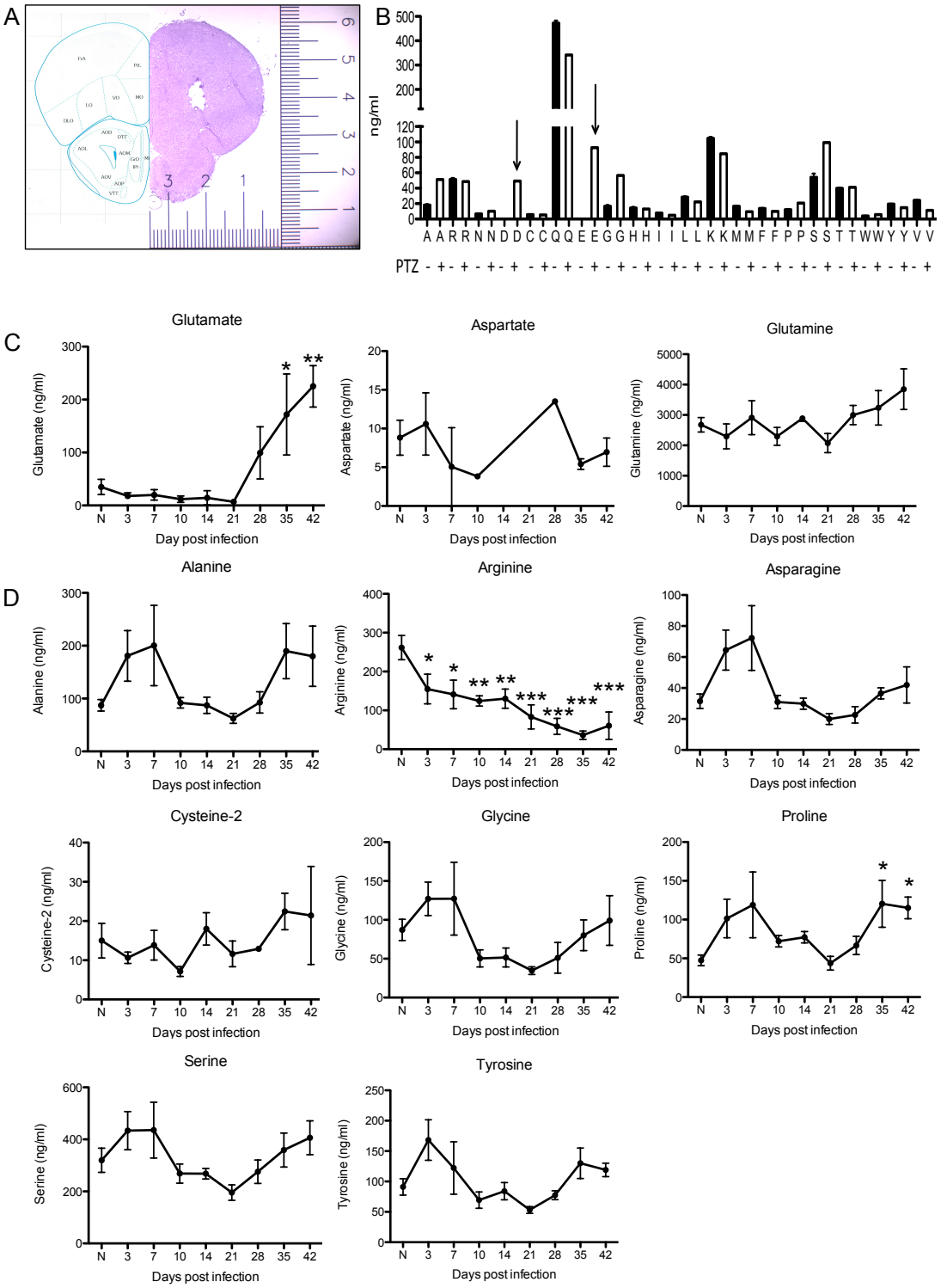
A
B
ng/ml
A A R R N N D D C C Q Q E E G G H H I I L L K K M M F F P P S S T T W W Y Y V V
PTZ - +
C
Glutamate
Glutamate (ng/ml)
Day post infection
Aspartate
Aspartate (ng/ml)
Days post infection
Glutamine
Glutamine (ng/ml)
Days post infection
D
Alanine
Alanine (ng/ml)
Days post infection
Arginine
Arginine (ng/ml)
Days post infection
Asparagine
Asparagine (ng/ml)
Days post infection
Cysteine-2
Cysteine-2 (ng/ml)
Days post infection
Glycine
Glycine (ng/ml)
Days post infection
Proline
Proline (ng/ml)
Days post infection
Serine
Serine (ng/ml)
Days post infection
Tyrosine
Tyrosine (ng/ml)
Days post infection

Figure 4-4. Ceftriaxone does not alter the immune response to *Toxoplasma* infection.

A) Infected mice treated and not treated with Ceftriaxone were weighed everyday between week 5 and 6 post-infection. No significant differences were observed between infected groups. B) Hematoxylin and eosin staining was performed and images of the prefrontal cortex (10X) and blood vessels (25X) within the prefrontal cortex were taken. Infiltrating cells are observed in both the treated and untreated infected animals. C) No significant difference was found in total brain mononuclear cell counts following treatment with Ceftriaxone. D) Flow cytometry reveals no differences in the composition and proportions of CD8 and CD4 T-cells infiltrating the CNS in infected and treated mice. D) Parasite DNA was amplified using qPCR in infected and Ceftriaxone treated mice. No significant difference in parasite burden was observed. E) Immunohistochemistry for the microglial marker Iba-1 and the astrocytic marker GFAP was performed on 12 micron thick frozen sections. Global microglial and astrocytic activation can be observed in both treated and untreated infected groups (scale bar: 80μm).

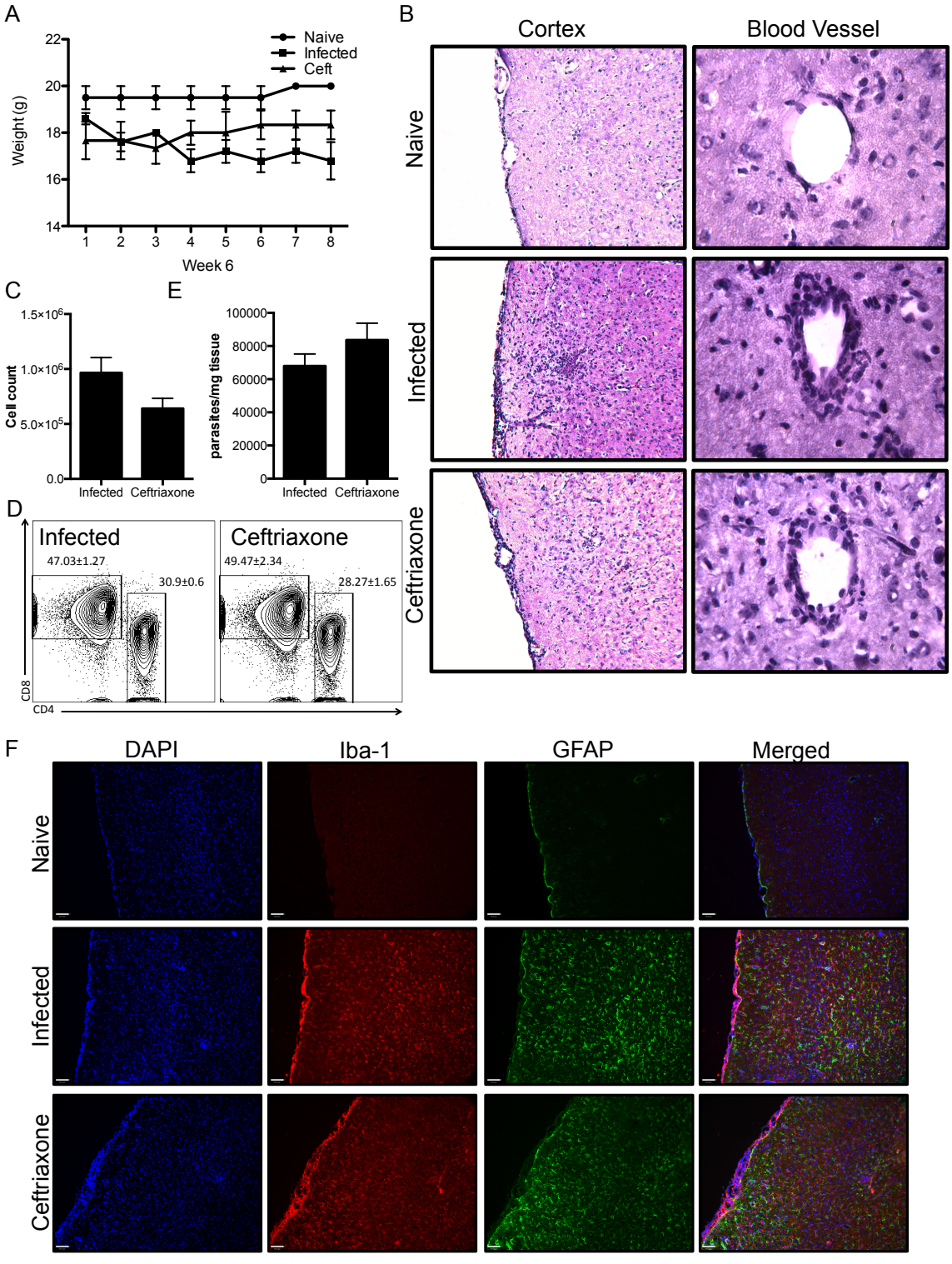
A
Naive
Infected
Ceft
Weight (g)
Week 6
B
Cortex
Blood Vessel
Naive
Infected
Ceftriaxone
C
Cell count
Infected
Ceftriaxone
E
parasites/mg tissue
Infected
Ceftriaxone
D
Infected
47.03±1.27
30.9±0.6
Ceftriaxone
49.47±2.34
28.27±1.65
CD8
CD4
F
DAPI
Iba-1
GFAP
Merged
Naive
Infected
Ceftriaxone

Figure 4-5. Ceftriaxone specifically rescues glutamate transporter GLT-1.

A) RT-qPCR was performed on whole forebrain RNA on naïve, infected and Ceftriaxone treated animals. No significant difference in transcripts of GLT-1, GS or GLAST was observed following treatment with Ceftriaxone. B) Whole forebrain western blots were conducted for GLT-1 and C) GS on naïve, infected and Ceftriaxone treated animals. Infection with *Toxoplasma* causes a significant decrease in GLT-1 and GS ($p=0.0144$ and $p=0.0002$ respectively). Treatment with Ceftriaxone significantly increases GLT-1 protein compared to infected group ($p=0.0172$). D) Immunohistochemistry for GLT-1 and GFAP demonstrates areas negative for GLT-1 but positive for GFAP. No such patches are observed in animals treated with Ceftriaxone for one week (scale bar: 80μm).

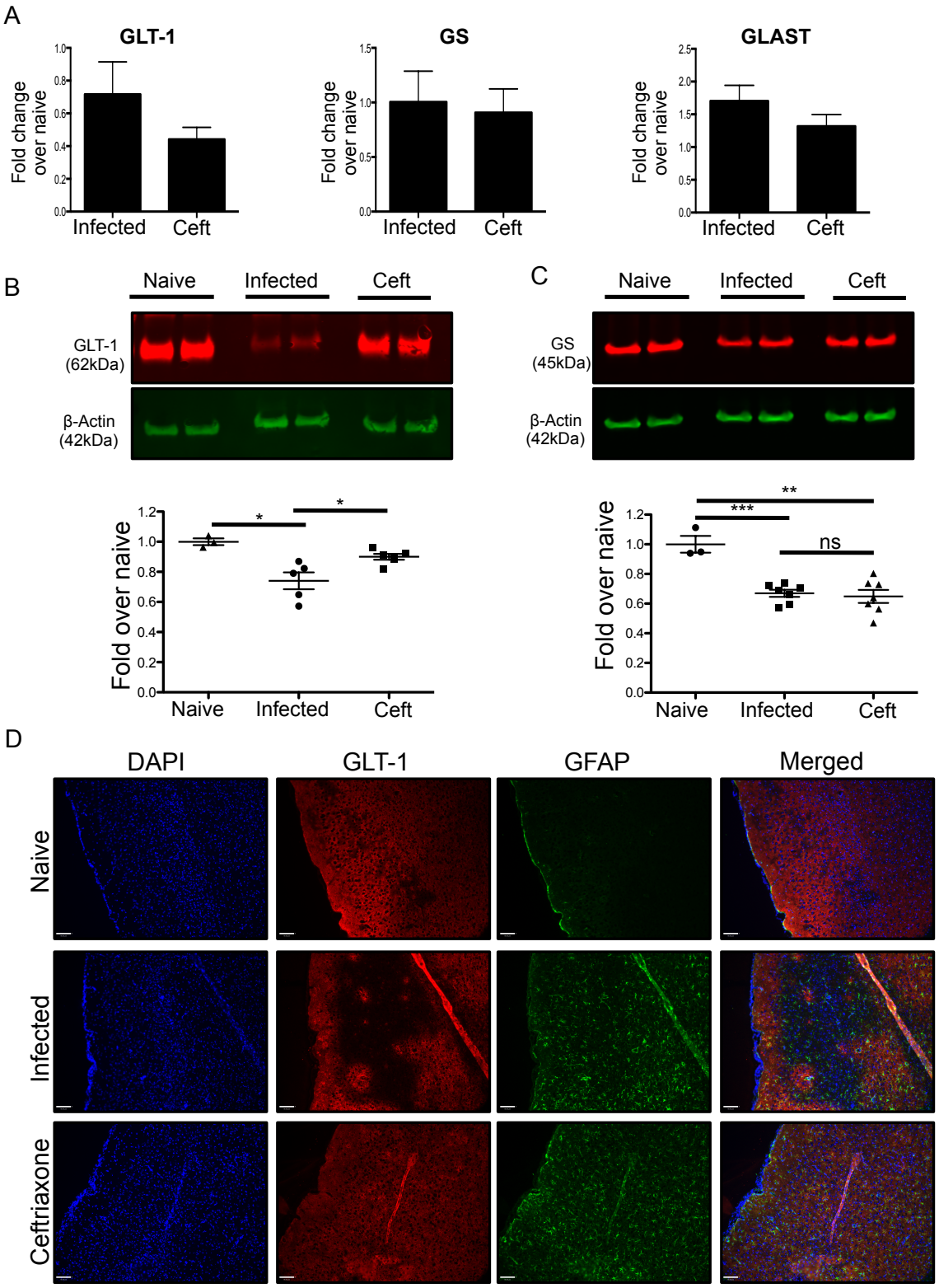
A
GLT-1
GS
GLAST
Fold change over naive
Infected
Ceft
B
Naive
Infected
Ceft
GLT-1 (62kDa)
β-Actin (42kDa)
Fold over naive
C
GS (45kDa)
ns
D
DAPI
GLT-1
GFAP
Merged
Naive
Infected
Ceftriaxone

Figure 4-6. Ceftriaxone is neuroprotective during infection with *Toxoplasma*.

A) Immunohistochemistry for NeuN reveals patchy staining in the infected group with overall decreased staining intensity. These patches are not visible in mice treated with Ceftriaxone for one week (scale bar: 80μm). Higher magnification of NeuN immunohistochemistry (scale bar: 54μm) reveal intracellular localization of NeuN. B) Western blot analysis for Vglut-1 in naïve, chronically infected and Ceftriaxone treated mouse cerebrums (Naïve vs. Infected, $p<0.0001$; Infected vs. Ceftriaxone, $p=0.0725$; Student T-Test) C) DiI labeling of dendritic spines was quantified and reveals a significant increase ($p=0.0004$) in dendritic spine density following Ceftriaxone treatment when compared to the infected group (scale bars: 9μm).

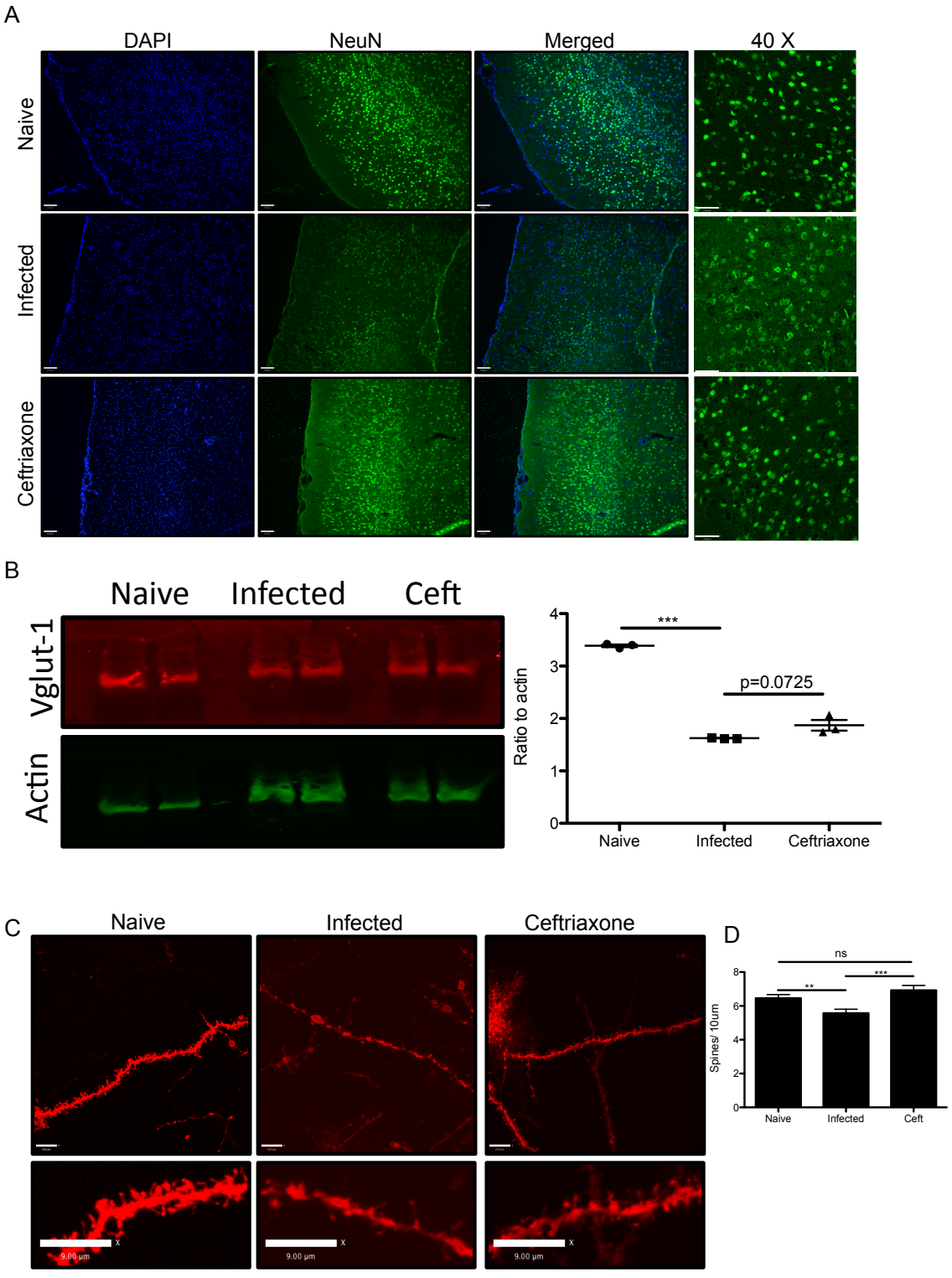
A
DAPI
NeuN
Merged
40 X
Naive
Infected
Ceftriaxone
B
Naive
Infected
Ceft
Vglut-1
Actin
Ratio to actin
***
p=0.0725
Naive
Infected
Ceftriaxone
C
Naive
Infected
Ceftriaxone
9.00 µm
D
ns
**
***
Spines/ 10um
Naive
Infected
Ceft

Figure 4-7. Infection with *Toxoplasma* disrupts neuronal networks and changes behavior.

A) Naïve (N=13), 6 week infected (N=11) and ceftriaxone treated (N=11) mice were placed in the center of an elevated plus maze and recorded for 5 minutes. B) Infected mice spend significantly (p=0.0002) more time in the open arms (arrows) of the maze. C) Frequency of open arm entry was measured between naive and infected animals (p=0.0005). D) Velocity and total distance traveled were also measured to assess overall activity. E) Glutamate and glutamine concentrations in the extracellular space of naïve, infected and ceftriaxone treated mice as measured by microdialysis (Student's T-test: N vs I: p=0.0003; I vs C: p=0.0072). F) EEG raw traces for naïve, 6 week infected and Ceftriaxone treated animals (scale bar: 1sec; arrows point to one full rhythmic cycle). Approximate entropies were measured and a student's T-test performed between all groups (Naïve vs Infected, p<0.0001; Infected vs Ceftriaxone, p=0.0057; Naïve vs Ceftriaxone, p=0.0138) G) EEG power density spectrum for naïve, 4, 5 and 6-week infected and ceftriaxone treated animals. Asterisks represented are Bonferonni's multiple comparison test (I vs N) and (C vs I) H) EEG percent power calculated from power density spectral analysis in G.

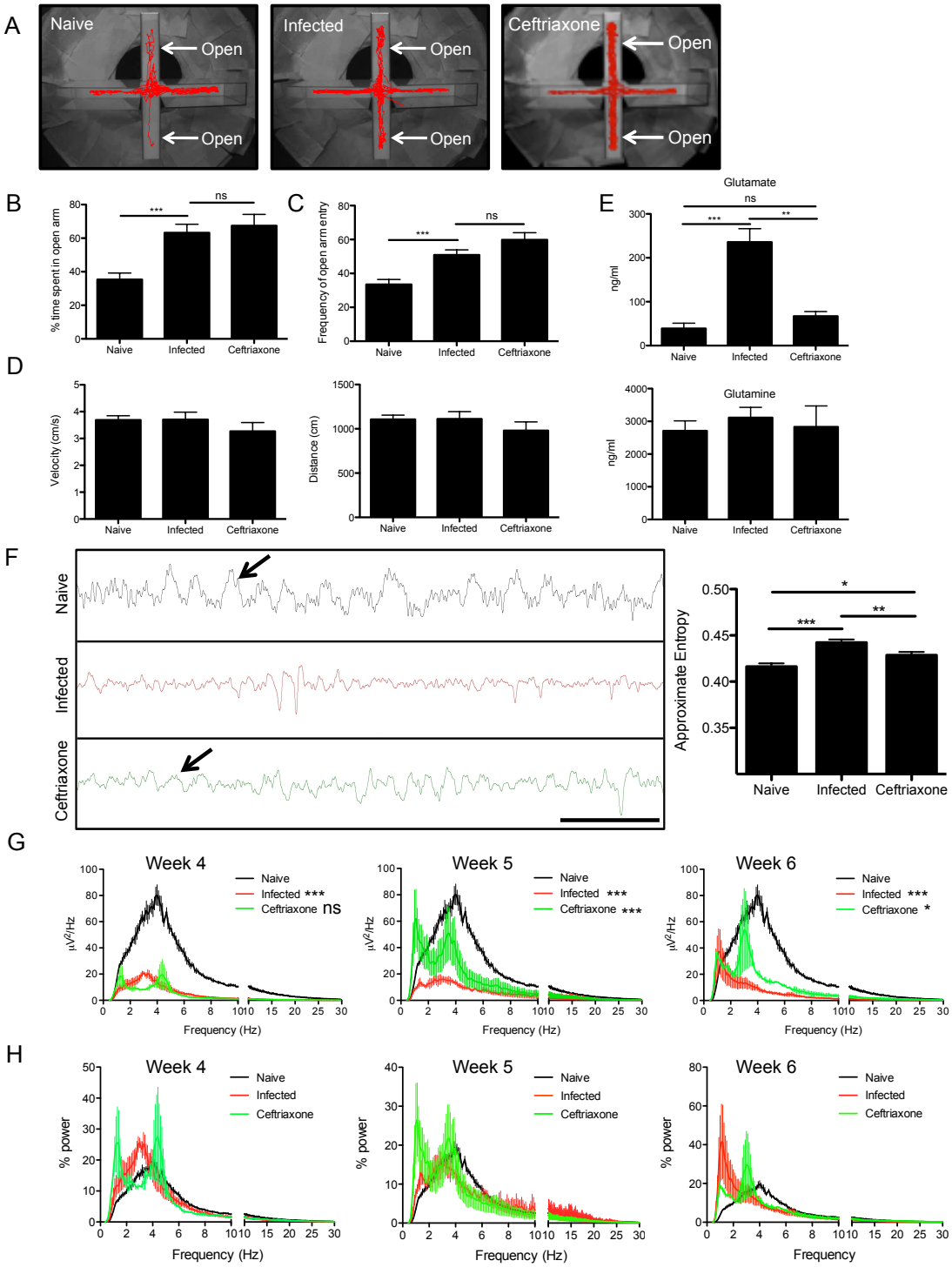
A
Naive
Open
Open
Infected
Open
Open
Ceftriaxone
Open
Open
B
% time spent in open arm
***
ns
Naive
Infected
Ceftriaxone
C
Frequency of open arm entry
***
ns
Naive
Infected
Ceftriaxone
E
Glutamate
ns
***
**
ng/ml
Naive
Infected
Ceftriaxone
D
Velocity (cm/s)
Naive
Infected
Ceftriaxone
Distance (cm)
Naive
Infected
Ceftriaxone
Glutamine
ng/ml
Naive
Infected
Ceftriaxone
F
Naive
Infected
Ceftriaxone
Approximate Entropy
*
**
***
Naive
Infected
Ceftriaxone
G
Week 4
Naive
Infected ***
Ceftriaxone ns
μV²/Hz
Frequency (Hz)
Week 5
Naive
Infected ***
Ceftriaxone ***
μV²/Hz
Frequency (Hz)
Week 6
Naive
Infected ***
Ceftriaxone *
μV²/Hz
Frequency (Hz)
H
Week 4
Naive
Infected
Ceftriaxone
% power
Frequency (Hz)
Week 5
Naive
Infected
Ceftriaxone
% power
Frequency (Hz)
Week 6
Naive
Infected
Ceftriaxone
% power
Frequency

Supplemental Figure 4-1: Infection with *Toxoplasma* induces dynamic changes in essential amino acids.

LC-MS analysis (Sussex) on microdialysis samples over the course of infection reveal dynamic changes in extracellular essential amino acid concentration in the CNS. A one-way ANOVA reveals significant changes in Tryptophan ($p=0.0071$), Histidine ($p=0.0403$), Lysine ($p=0.0243$), Phenylalanine ($p=0.0229$) and Threonine ($p=0.0052$). A Dunnett's post-test was performed for all timepoints against naïve concentrations and significance shown as asterisks. Amino acids not listed did not change significantly.

A

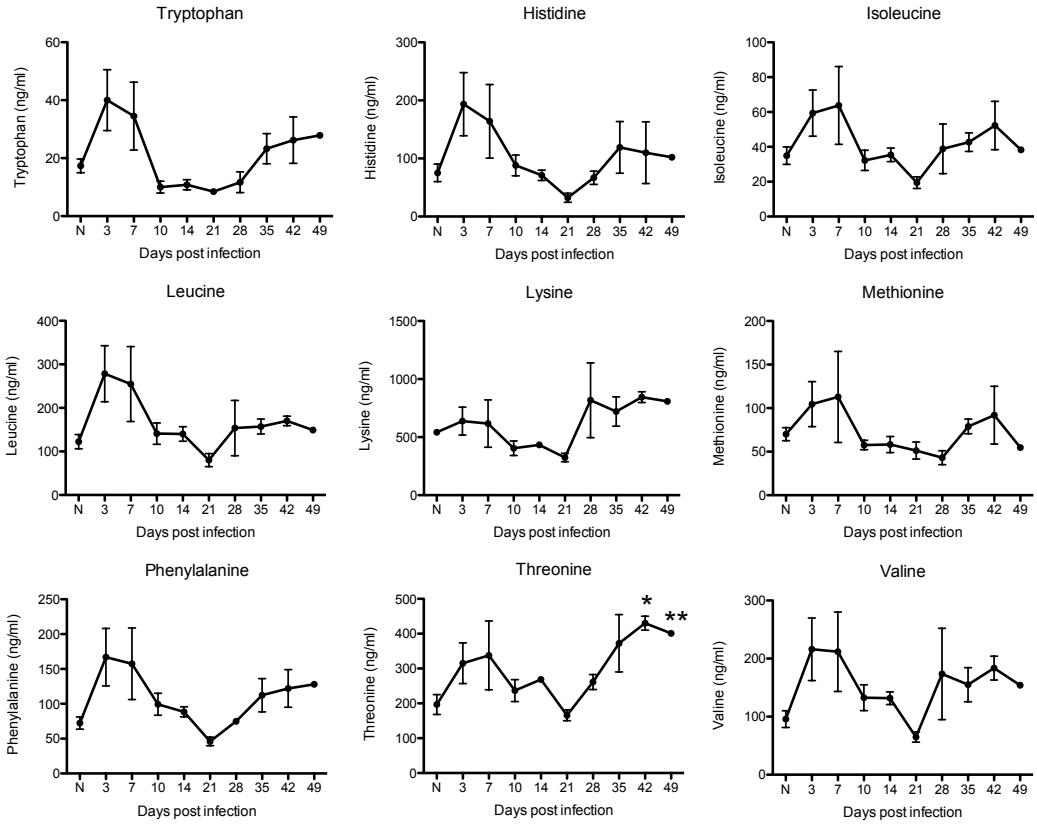
Tryptophan
Tryptophan (ng/ml)
Histidine
Histidine (ng/ml)
Isoleucine
Isoleucine (ng/ml)
Leucine
Leucine (ng/ml)
Lysine
Lysine (ng/ml)
Methionine
Methionine (ng/ml)
Phenylalanine
Phenylalanine (ng/ml)
Threonine
Threonine (ng/ml)
*
**
Valine
Valine (ng/ml)
N 3 7 10 14 21 28 35 42 49
Days post infection

Supplemental Figure 4-2: Infection with *Toxoplasma* induces a loss in GLT-1 in the resistant BALB/c mouse.

A) 6 week Me49 infected BALB/c mice show significant weight loss compared to naïve mice (student's T test: p=0.0112). B) Whole forebrain western blots were conducted and quantified for GLT-1 (Student's T test: p=0.0081).

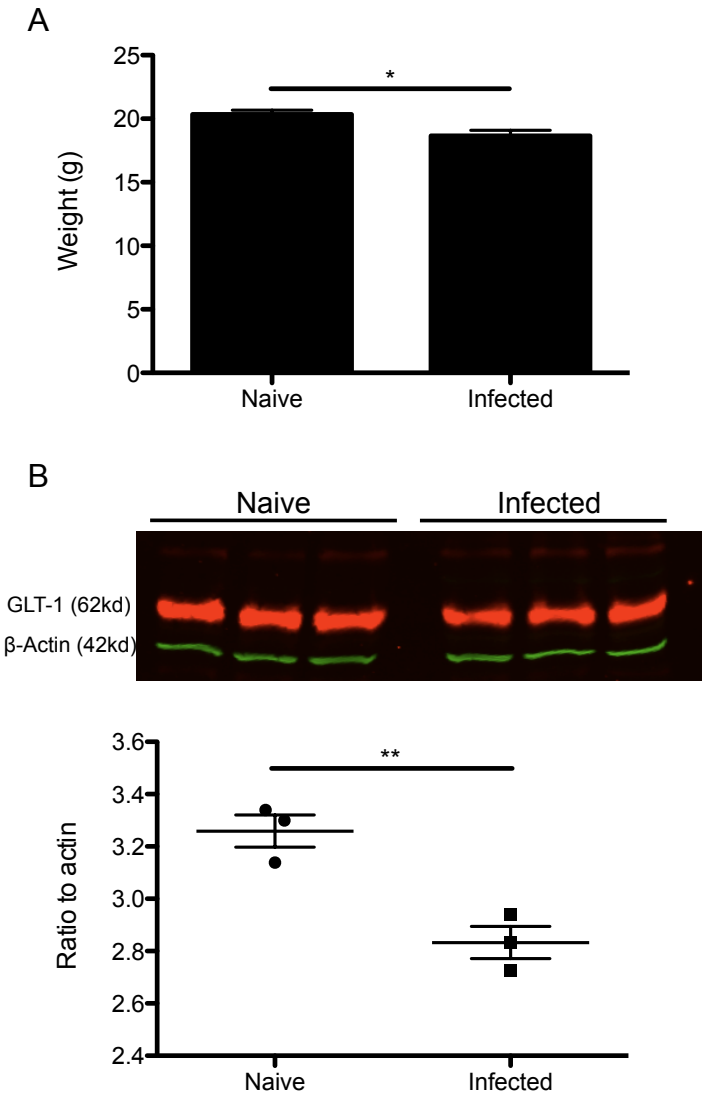
A
25
20
15
10
5
0
Weight (g)
*
Naive
Infected
B
Naive
Infected
GLT-1 (62kd)
β-Actin (42kd)
3.6
3.4
3.2
3.0
2.8
2.6
2.4
Ratio to actin
**
Naive
Infected

Supplemental Figure 4-3: Infection with *Toxoplasma* does not affect motility.

A) Naïve (N=13), 6 week infected (N=11) and ceftriaxone treated (N=11) mice were placed in the center of an open field arena and recorded for 30 minutes. No significant changes were measured in velocity or distance traveled.

A

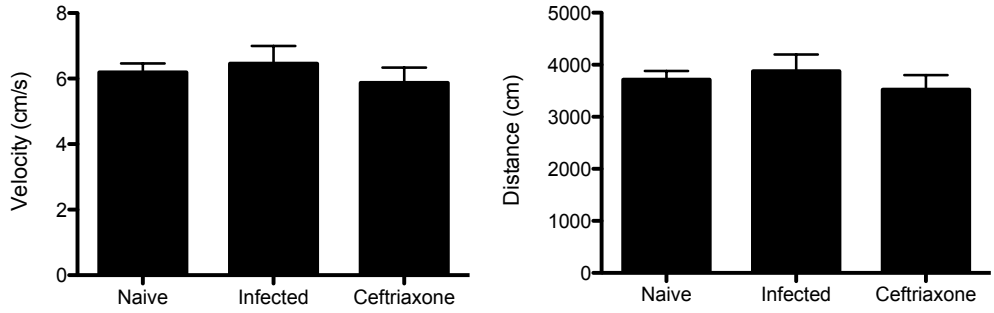
Velocity (cm/s)
0
2
4
6
8
Naive
Infected
Ceftriaxone
Distance (cm)
0
1000
2000
3000
4000
5000
Naive
Infected
Ceftriaxone

Supplemental Figure 4-4: Treatment with Ceftriaxone does not alter extracellular amino acid concentrations.

A) Microdialysis of naïve, 6-week Me49 infected and Ceftriaxone treated mice reveals no significant changes in extracellular amino acids following treatment with ceftriaxone.

A

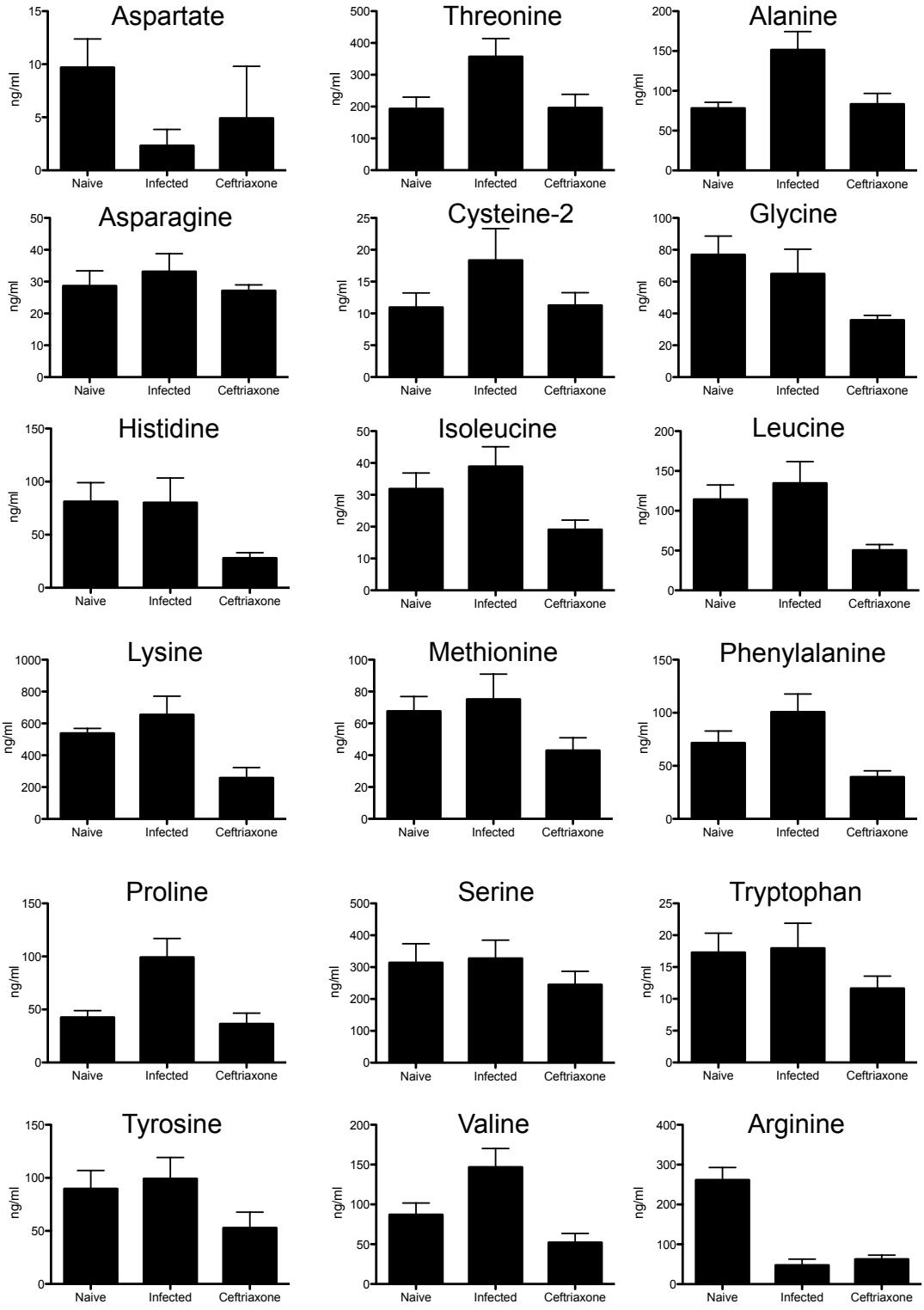
Aspartate
Threonine
Alanine
Asparagine
Cysteine-2
Glycine
Histidine
Isoleucine
Leucine
Lysine
Methionine
Phenylalanine
Proline
Serine
Tryptophan
Tyrosine
Valine
Arginine
ng/ml
Naive
Infected
Ceftriaxone

4.7 References:

1 Afonso C, Paixao VB, Costa RM (2012) Chronic Toxoplasma infection modifies the structure and the risk of host behavior. PLoS One 7:e32489.

2 Amiry-Moghaddam M, Frydenlund DS, Ottersen OP (2004) Anchoring of aquaporin-4 in brain: molecular mechanisms and implications for the physiology and pathophysiology of water transport. Neuroscience 129:999-1010.

3 Bowens NH, Dohare P, Kuo YH, Mongin AA (2013) DCPIB, the proposed selective blocker of volume-regulated anion channels, inhibits several glutamate transport pathways in glial cells. Mol Pharmacol 83:22-32.

4 Cekanaviciute E, Dietrich HK, Axtell RC, Williams AM, Egusquiza R, Wai KM, Koshy AA, Buckwalter MS (2014) Astrocytic TGF-beta Signaling Limits Inflammation and Reduces Neuronal Damage during Central Nervous System Toxoplasma Infection. J Immunol 193.

5 Conejero-Goldberg C, Torrey EF, Yolken RH (2003) Herpesviruses and Toxoplasma gondii in orbital frontal cortex of psychiatric patients. Schizophr Res 60:65-69.

6 Danbolt NC (2001) Glutamate uptake. Prog Neurobiol 65:1-105.

7 Dellacasa-Lindberg I, Hitziger N, Barragan A (2007) Localized recrudescence of Toxoplasma infections in the central nervous system of immunocompromised mice assessed by in vivo bioluminescence imaging. Microbes Infect 9:1291-1298.

8 Dickerson F, Stallings C, Origoni A, Vaughan C, Katsafanas E, Khushalani S, Yolken R (2014) Antibodies to Toxoplasma gondii in individuals with mania. Bipolar Disord 16:129-136.

9 Fagard R, Tan HV, Creuzet C, Pelloux H (1999) References : Differential Development of Toxoplasma gondii in Neural Cells. Parasitology 15.

10 Feustel PJ, Jin Y, Kimelberg HK (2004) Volume-regulated anion channels are the predominant contributors to release of excitatory amino acids in the ischemic cortical penumbra. Stroke 35:1164-1168.

11 Flegr J (2007) Effects of toxoplasma on human behavior. Schizophr Bull 33:757-760.

12 Flegr J (2013a) Influence of latent Toxoplasma infection on human personality, physiology and morphology: pros and cons of the Toxoplasma-human model in studying the manipulation hypothesis. J Exp Biol 216:127-133.

13 Flegr J (2013b) How and why Toxoplasma makes us crazy. Trends Parasitol 29:156-163.

14 Flegr J, Kodym P, Tolarova V (2000) Correlation of duration of latent Toxoplasma gondii infection with personality changes in women. Biol Psychol 53:57-68.

15 Flegr J, Lenochova P, Hodny Z, Vondrova M Fatal attraction phenomenon in humans: cat odour attractiveness increased for toxoplasma-infected men while decreased for infected women. PLoS Negl Trop Dis 5:e1389.

16 Flegr J, Zitkova S, Kodym P, Frynta D (1996) Induction of changes in human behaviour by the parasitic protozoan Toxoplasma gondii. Parasitology 113 (Pt 1):49-54.

17 Flegr J, Klose J, Novotna M, Berenreitterova M, Havlicek J (2009) Increased incidence of traffic accidents in Toxoplasma-infected military drivers and protective effect RhD molecule revealed by a large-scale prospective cohort study. BMC Infect Dis 9:72.

18 Flegr J, Preiss M, Klose J, Havlicek J, Vitakova M, Kodym P (2003) Decreased level of psychobiological factor novelty seeking and lower intelligence in men latently infected with the protozoan parasite Toxoplasma gondii Dopamine, a missing link between schizophrenia and toxoplasmosis? Biol Psychol 63:253-268.

19 Foran E, Trotti D (2009) Glutamate transporters and the excitotoxic path to motor neuron degeneration in amyotrophic lateral sclerosis. Antioxid Redox Signal 11:1587-1602.

20 Giraudon P, Bernard A (2009) Chronic viral infections of the central nervous system: Aspects specific to multiple sclerosis. Rev Neurol (Paris) 165:789-795.

21 Gonsette RE (2008) Neurodegeneration in multiple sclerosis: the role of oxidative stress and excitotoxicity. J Neurol Sci 274:48-53.

22 Gonzalez LE, Rojnik B, Urrea F, Urdaneta H, Petrosino P, Colasante C, Pino S, Hernandez L (2007) Toxoplasma gondii infection lower anxiety as measured in the plus-maze and social interaction tests in rats A behavioral analysis. Behav Brain Res 177:70-79.

23 Halonen SK, Taylor GA (2001) Gamma Interferon-Induced Inhibition of Toxoplasma gondii in Astrocytes Is Mediated by IGTP. Society 69:5573-5576.

24 Hari Dass SA, Vyas A (2014) Toxoplasma gondii infection reduces predator aversion in rats through epigenetic modulation in the host medial amygdala. Mol Ecol.

25 Haskew-Layton RE, Rudkouskaya A, Jin Y, Feustel PJ, Kimelberg HK, Mongin AA (2008) Two distinct modes of hypoosmotic medium-induced release of excitatory amino acids and taurine in the rat brain in vivo. PLoS One 3:e3543.

26 Hermes G, Ajioka JW, Kelly KA, Mui E, Roberts F, Kasza K, Mayr T, Kirisits MJ, Wollmann R, Ferguson DJ, Roberts CW, Hwang JH, Trendler T, Kennan RP, Suzuki Y, Reardon C, Hickey WF, Chen L, McLeod R (2008) Neurological and behavioral abnormalities, ventricular dilatation, altered cellular functions, inflammation, and neuronal injury in brains of mice due to common, persistent, parasitic infection. J Neuroinflammation 5:48.

27 Hertz L, Zielke HR (2004) Astrocytic control of glutamatergic activity: astrocytes as stars of the show. Trends Neurosci 27:735-743.

28 Hertz L, Dringen R, Schousboe A, Robinson SR (1999) Astrocytes: glutamate producers for neurons. J Neurosci Res 57:417-428.

29 Honjo K, van Reekum R, Verhoeff NP (2009) Alzheimer's disease and infection: do infectious agents contribute to progression of Alzheimer's disease? Alzheimers Dement 5:348-360.

30 Hyzinski-Garcia MC, Vincent MY, Haskew-Layton RE, Dohare P, Keller RW, Jr., Mongin AA (2011) Hypo-osmotic swelling modifies glutamate-glutamine cycle in the cerebral cortex and in astrocyte cultures. J Neurochem 118:140-152.

31 Kimelberg HK, Macvicar BA, Sontheimer H (2006) Anion channels in astrocytes: biophysics, pharmacology, and function. Glia 54:747-757.

32 Kimelberg HK, Rutledge E, Goderie S, Charniga C (1995) Astrocytic swelling due to hypotonic or high K+ medium causes inhibition of glutamate and aspartate uptake and increases their release. J Cereb Blood Flow Metab 15:409-416.

33 Kusbeci OY, Miman O, Yaman M, Aktepe OC, Yazar S (2011) Could Toxoplasma gondii have any role in Alzheimer disease? Alzheimer Dis Assoc Disord 25:1-3.

34 Lafferty KD, Shaw JC (2013) Comparing mechanisms of host manipulation across host and parasite taxa. J Exp Biol 216:56-66.

35 Lau A, Tymianski M (2010) Glutamate receptors, neurotoxicity and neurodegeneration. Pflugers Arch 460:525-542.

36 Lee M, McGeer E, McGeer PL (2013) Neurotoxins released from interferon-gamma-stimulated human astrocytes. Neuroscience 229:164-175.

37 Lipski J, Wan CK, Bai JZ, Pi R, Li D, Donnelly D (2007) Neuroprotective potential of ceftriaxone in in vitro models of stroke. Neuroscience 146:617-629.

38 Masliah E, Dumaop W, Galasko D, Desplats P (2013) Distinctive patterns of DNA methylation associated with Parkinson disease: identification of concordant epigenetic changes in brain and peripheral blood leukocytes. Epigenetics 8:1030-1038.

39 Miman O, Kusbeci OY, Aktepe OC, Cetinkaya Z (2010) The probable relation between Toxoplasma gondii and Parkinson's disease. Neurosci Lett 475:129-131.

40 Miranda AS, Vieira LB, Lacerda-Queiroz N, Souza AH, Rodrigues DH, Vilela MC, Gomez MV, Machado FS, Rachid MA, Teixeira AL (2010) Increased levels of glutamate in the central nervous system are associated with behavioral symptoms in experimental malaria. Braz J Med Biol Res 43:1173-1177.

41 Nagelhus EA, Mathiisen TM, Ottersen OP (2004) Aquaporin-4 in the central nervous system: cellular and subcellular distribution and coexpression with KIR4.1. Neuroscience 129:905-913.

42 Neely JD, Amiry-Moghaddam M, Ottersen OP, Froehner SC, Agre P, Adams ME (2001) Syntrophin-dependent expression and localization of Aquaporin-4 water channel protein. Proc Natl Acad Sci U S A 98:14108-14113.

43 Obrenovitch TP, Urenjak J (1997) Is high extracellular glutamate the key to excitotoxicity in traumatic brain injury? J Neurotrauma 14:677-698.

44 Pappas G, Roussos N, Falagas ME (2009) Toxoplasmosis snapshots: global status of Toxoplasma gondii seroprevalence and implications for pregnancy and congenital toxoplasmosis. Int J Parasitol 39:1385-1394.

45 Parlog A, Harsan LA, Zagrebelsky M, Weller M, von Elverfeldt D, Mawrin C, Korte M, Dunay IR (2014) Chronic murine toxoplasmosis is defined by subtle changes in neuronal connectivity. Dis Model Mech 7:459-469.

46 Parpura V, Scemes E, Spray DC (2004) Mechanisms of glutamate release from astrocytes: gap junction "hemichannels", purinergic receptors and exocytotic release. Neurochem Int 45:259-264.

47 Pezzi JC, Ens CM, Borba EM, Schumacher-Schuh AF, de Andrade FM, Chaves ML, Fiegenbaum M, Camozzato AL (2014) DNA methyltransferase haplotype is associated with Alzheimer's disease. Neurosci Lett 579:70-74.

48 Rothstein JD, Dykes-Hoberg M, Pardo CA, Bristol LA, Jin L, Kuncl RW, Kanai Y, Hediger MA, Wang Y, Schielke JP, Welty DF (1996) Knockout of glutamate transporters reveals a major role for astroglial transport in excitotoxicity and clearance of glutamate. Neuron 16:675-686.

49 Rothstein JD, Patel S, Regan MR, Haenggeli C, Huang YH, Bergles DE, Jin L, Dykes Hoberg M, Vidensky S, Chung DS, Toan SV, Bruijn LI, Su ZZ, Gupta P, Fisher PB (2005) Beta-lactam antibiotics offer neuroprotection by increasing glutamate transporter expression. Nature 433:73-77.

50 Schallier A, Smolders I, Van Dam D, Loyens E, De Deyn PP, Michotte A, Michotte Y, Massie A (2011) Region and age-specific changes in glutamate transport in the AbetaPP23 mouse model for Alzheimer's disease. J Alzheimers Dis 24:287-300.

51 Strack A, Asensio VC, Campbell IL, Schluter D, Deckert M (2002) Chemokines are differentially expressed by astrocytes, microglia and inflammatory leukocytes Neuropathol 103:458-468.

52 Takaki J, Fujimori K, Miura M, Suzuki T, Sekino Y, Sato K (2012) L-glutamate expression in neuroinflammation: the 'collusion' hypothesis for increased 9:275.

53 Torrey EF, Yolken RH (2003) Toxoplasma gondii and schizophrenia. Emerg Infect Dis 9:1375-1380.

54 Torrey EF, Bartko JJ, Yolken RH (2012) Toxoplasma gondii and other risk factors for schizophrenia: an update. Schizophr Bull 38:642-647.

55 Torrey EF, Bartko JJ, Lun ZR, Yolken RH (2007) Antibodies to Toxoplasma gondii in patients with schizophrenia: a meta-analysis. Schizophr Bull 33:729-736.

56 Verma R, Mishra V, Sasmal D, Raghubir R (2010) Pharmacological evaluation of glutamate transporter 1 (GLT-1) mediated neuroprotection following cerebral ischemia/reperfusion injury. Eur J Pharmacol 638:65-71.

57 Vyas A (2013) Parasite-augmented mate choice and reduction in innate fear in rats infected by Toxoplasma gondii. J Exp Biol 216:120-126.

58 Vyas A, Kim SK, Giacomini N, Boothroyd JC, Sapolsky RM (2007) Behavioral changes induced by Toxoplasma infection of rodents are highly specific to aversion of cat odors. Proc Natl Acad Sci U S A 104:6442-6447.

59 Walf AA, Frye CA (2007) The use of the elevated plus maze as an assay of anxiety-related behavior in rodents. Nat Protoc 2:322-328.

60 Webster JP, Lamberton PH, Donnelly CA, Torrey EF (2006) Parasites as causative agents of human affective disorders? The impact of anti-psychotic, mood-stabilizer and anti-parasite medication on Toxoplasma gondii's ability to alter host behaviour. Proc Biol Sci 273:1023-1030.

61 Werner C, Engelhard K (2007) Pathophysiology of traumatic brain injury. Br J Anaesth 99:4-9.

62 Wilson EH, Hunter Ca (2004) The role of astrocytes in the immunopathogenesis of toxoplasmic encephalitis. International journal for parasitology 34:543-548.

63 Wilson EH, Harris TH, Mrass P, John B, Tait ED, Wu GF, Pepper M, Wherry EJ, Dzierzinski F, Roos D, Haydon PG, Laufer TM, Weninger W, Hunter Ca (2009) Behavior of parasite-specific effector CD8+ T cells in the brain and visualization of a kinesis-associated system of reticular fibers. Immunity 30:300-311.

64 Yolken RH, Bachmann S, Ruslanova I, Lillehoj E, Ford G, Torrey EF, Schroeder J (2001) Antibodies to Toxoplasma gondii in individuals with first-episode schizophrenia. Clin Infect Dis 32:842-844.

65 Zhang Y, Zhang H, Feustel PJ, Kimelberg HK (2008) DCPIB, a specific inhibitor of volume regulated anion channels (VRACs), reduces infarct size in MCAo and the release of glutamate in the ischemic cortical penumbra. Exp Neurol 210:514-520.

CHAPTER FIVE

Conclusions and Perspectives.

5.1 Conclusion and Future Directions:

Far from being limited to the passive, structural role they were initially labeled with; glial cells have emerged as complex, active, and essential components of the CNS. From the small, spatially tiled microglia, which constantly sample their environment for signs of damage (Nimmerjahn et al., 2005), to the large, interconnected astrocytes which maintain ion and neurotransmitter homeostasis while guarding the brain's vasculature (Attwell et al., 2010; Sofroniew and Vinters, 2010); glial cells are truly multifunctional units of the CNS. The true significance of these cells is evidenced by the neuropathological consequences of a deleterious gain or loss of their function; such as by DNA mutation, a lack of glutamate homeostasis, or deficient ion buffering during disease (Hertz and Zielke, 2004; Sofroniew and Vinters, 2010). In the context of glioma, genetic mutations in astrocytes are primarily responsible for the characteristic uncontrolled growth and capacity for profound invasion, resulting in rapid degeneration and low survival rates (Friedman et al., 2000; Furnari et al., 2007). Non-glioma astrocytes exacerbate the inherent properties of gliomas by altering the environment through increases in extracellular matrix remodeling, a decrease paracrine apoptotic factors and an increase in all survival and angiogenic factors (Le et al., 2003; Charles et al., 2011; Biasoli et al., 2014). Traditional chemotherapy with Temozolomide continues to be the most commonly used method for GBM treatment, yet is largely ineffective. Indeed, only 50% of GBM patients respond to Temozolomide treatment at all, and those who do respond are graced with an increase in survival of only 18 months (Friedman et al., 2000; Stupp et al., 2002; Hegi et al., 2005; Stupp et al., 2005; Mutter and Stupp, 2006; Ajaz et

al., 2014). Until a more potent chemotherapeutic is discovered, the exploration of new types of therapies remains a high priority.

One avenue currently being investigated is the modulation of the immune system to combat gliomablastomas. As discussed previously, GBMs have a large immune component, with up to 50% of some tumors being comprised of alternatively activated macrophages (Solinas et al., 2009). The presence and density of alternatively activated macrophages in tumors is positively correlated with poorer prognosis (Bingle et al., 2002; Zhang et al., 2011). Targeted destruction of alternatively activated macrophages in GBMs would be an exciting avenue for future GBM treatments. Within the same concept, targeting the permissive tumor environment would be an interesting and potentially effective way of cutting off a tumor's energy supply, stinting its growth, and finally killing it. Such a therapy has been briefly touched on in Chapter 2: using Stabilin-1 positive macrophages to remove the extracellular SPARC and decrease tumor infiltration. SPARC levels are normally low in the cerebrum, but significantly increased during GBMs (Framson and Sage, 2004). SPARC is abnormally expressed in all grades of GBMs but particularly localized at the sites of tumor proliferation (Rempel et al., 1998). Some studies have already demonstrated that a decrease in SPARC expression using siRNA has significantly reduced tumor proliferative capabilities (Shi et al., 2007). This study, however, focuses solely on an *in-vitro* approach, and the treatment of cells with siRNA is not easily applicable to the human patient population. An elegant solution would be to use Stabilin-1 positive macrophages to remove extracellular SPARC in and around the tumor in an effort to stop its proliferation and survival. Such an approach

would be possible if: 1) we could successfully modify the phenotype of TAMs to induce Stabilin-1 expression, 2) such expression proved not only functional, but sustainable and 3) we could demonstrate that no other extracellular matrix remodeling protein compensates for the loss of SPARC. An alternative, already under investigation by several research groups, demonstrates great potential by targeting the cytokine milieu and increasing the proportion of Th-1 response. Since the tumors induce a strong M2 phenotype to promote survival and growth, the induction of a strong Th-1 response by INF-γ has the potential to decrease the effects of M2 cells. A study by Fritzell et al. has demonstrated that in a rat model of GBM, a steady increase in INF-γ, along with an increase in proliferating CD8+ T-cells during GBM, results in a dramatic increase in survival, with 85% of the treated mice not succumbing to GBM (Smith et al., 2009; Fritzell et al., 2013). Although any one therapy has its advantages and disadvantages, it is critical to remember that combination therapies tend to be most successful in treating brain gliomas. Surgical removal of the bulk of the tumor combined with chemotherapy/radiotherapy (Friedman et al., 2000; Stupp et al., 2002), dietary restriction (Safdie et al., 2012) and immune therapy is likely to be more effective than any one alone.

As discussed previously, astrocytes are responsible for maintaining a multitude of homeostatic functions. For example, they provide metabolic support, clear excess potassium from areas of high neuronal activity and maintain low extracellular levels of glutamate in the CNS (Danbolt, 2001; Dienel and Cruz, 2006; Sofroniew and Vinters, 2010). The loss of any of these functions can be extremely detrimental to the brain. As

discussed in detail in Chapter 4, the disruption in glutamate homeostasis through the loss of the transporter GLT-1, results in widespread neuropathology characterized by decreases in NeuN, ß-III Tubulin, and synaptic density in the pre-frontal cortex as well as abnormal electrophysiological recordings. Although no neuronal death is observed, profound changes in neuronal cytoskeletal components, morphology and electrical signaling suggests poor health. While not all of these changes can be directly linked to the loss of GLT-1, treatment with Ceftriaxone—an antibiotic which upregulates GLT-1—has rescued most of the observed pathological phenotypes. Because the loss of GLT-1 and the resulting increase in extracellular glutamate is associated with multiple neurodegenerative and psychiatric disorders (see Ch.4), the ability to increase its expression gives hope to relieving the symptoms associated with these diseases. This hope is exactly what drove researchers to conduct clinical trials with Ceftriaxone as a treatment for ALS patients (Cudkowicz et al., 2014). Based on exhaustive and successful mouse studies, it was hypothesized that treatment with Ceftriaxone could decrease extracellular levels of glutamate through an increase in GLT-1 expression and relieve patients of the severe symptoms associated with ALS (Rothstein et al., 2005). Unfortunately, although very successful in mouse models, the human clinical trials were a failure. Future studies should focus on the benefits of the rescue of extracellular glutamate homeostasis on not only the morphological and molecular health of neurons but also of the restoration of their network. Extensive EEG, slice electrophysiology, and behavioral studies could aid in modulating the length and intensity of Ceftriaxone treatment until the restoration of the normal electrical signature can be achieved.

As the human population grows exponentially and ages older with each generation, it is critical to find treatments for disorders of the CNS. Identifying the molecular catalysts of disease will allow direct targeting of the cause, as opposed to a simple treatment of symptoms. Within the CNS, it is vital that we consider the important functions of glial cells as extensive contributors to disease; they should be seen as integral components of any new therapeutic targets.

5.2 References:

1 Ajaz M, Jefferies S, Brazil L, Watts C, Chalmers A (2014) Current and investigational drug strategies for glioblastoma. Clin Oncol (R Coll Radiol) 26:419-430.

2 Attwell D, Buchan AM, Charpak S, Lauritzen M, Macvicar BA, Newman EA (2010) Glial and neuronal control of brain blood flow. Nature 468:232-243.

3 Biasoli D, Sobrinho MF, da Fonseca AC, de Matos DG, Romao L, de Moraes Maciel R, Rehen SK, Moura-Neto V, Borges HL, Lima FR (2014) Glioblastoma cells inhibit astrocytic p53-expression favoring cancer malignancy. Oncogenesis 3:e123.

4 Bingle L, Brown NJ, Lewis CE (2002) The role of tumour-associated macrophages in tumour progression: implications for new anticancer therapies. The Journal of pathology 196:254-265.

5 Charles NA, Holland EC, Gilbertson R, Glass R, Kettenmann H (2011) The brain tumor microenvironment. Glia 59:1169-1180.

6 Cudkowicz ME et al. (2014) Safety and efficacy of ceftriaxone for amyotrophic lateral sclerosis: a multi-stage, randomised, double-blind, placebo-controlled trial. Lancet Neurol 13:1083-1091.

7 Danbolt NC (2001) Glutamate uptake. Prog Neurobiol 65:1-105.

8 Dienel Ga, Cruz NF (2006) Astrocyte activation in working brain: energy supplied by minor substrates. Neurochemistry international 48:586-595.

9 Framson PE, Sage EH (2004) SPARC and tumor growth: where the seed meets the soil? Journal of cellular biochemistry 92:679-690.

10 Friedman HS, Kerby T, Calvert H (2000) Temozolomide and treatment of malignant glioma. Clin Cancer Res 6:2585-2597.

11 Fritzell S, Eberstal S, Sanden E, Visse E, Darabi A, Siesjo P (2013) IFNgamma in combination with IL-7 enhances immunotherapy in two rat glioma models. J Neuroimmunol 258:91-95.

12 Furnari FB, Fenton T, Bachoo RM, Mukasa A, Stommel JM, Stegh A, Hahn WC, Ligon KL, Louis DN, Brennan C, Chin L, DePinho RA, Cavenee WK (2007) Malignant astrocytic glioma: genetics, biology, and paths to treatment. Genes Dev 21:2683-2710.

13 Hegi ME, Diserens AC, Gorlia T, Hamou MF, de Tribolet N, Weller M, Kros JM, Hainfellner JA, Mason W, Mariani L, Bromberg JE, Hau P, Mirimanoff RO, Cairncross JG, Janzer RC, Stupp R (2005) MGMT gene silencing and benefit from temozolomide in glioblastoma. N Engl J Med 352:997-1003.

14 Hertz L, Zielke HR (2004) Astrocytic control of glutamatergic activity: astrocytes as stars of the show. Trends Neurosci 27:735-743.

15 Le DM, Besson A, Fogg DK, Choi KS, Waisman DM, Goodyer CG, Rewcastle B, Yong VW (2003) Exploitation of astrocytes by glioma cells to facilitate invasiveness: a mechanism involving matrix metalloproteinase-2 and the urokinase-type plasminogen activator-plasmin cascade. J Neurosci 23:4034-4043.

16 Mutter N, Stupp R (2006) Temozolomide: a milestone in neuro-oncology and beyond? Expert Rev Anticancer Ther 6:1187-1204.

17 Nimmerjahn A, Kirchhoff F, Helmchen F (2005) Resting microglial cells are highly dynamic surveillants of brain parenchyma in vivo. Science 308:1314-1318.

18 Rempel SA, Golembieski WA, Ge S, Lemke N, Elisevich K, Mikkelsen T, Gutierrez JA (1998) SPARC: a signal of astrocytic neoplastic transformation and reactive response in human primary and xenograft gliomas. J Neuropathol Exp Neurol 57:1112-1121.

19 Rothstein JD, Patel S, Regan MR, Haenggeli C, Huang YH, Bergles DE, Jin L, Dykes Hoberg M, Vidensky S, Chung DS, Toan SV, Bruijn LI, Su ZZ, Gupta P, Fisher PB (2005) Beta-lactam antibiotics offer neuroprotection by increasing glutamate transporter expression. Nature 433:73-77.

20 Safdie F, Brandhorst S, Wei M, Wang W, Lee C, Hwang S, Conti PS, Chen TC, Longo VD (2012) Fasting enhances the response of glioma to chemo- and radiotherapy. PLoS One 7:e44603.

21 Shi Q, Bao S, Song L, Wu Q, Bigner DD, Hjelmeland aB, Rich JN (2007) Targeting SPARC expression decreases glioma cellular survival and invasion associated with reduced activities of FAK and ILK kinases. Oncogene 26:4084-4094.

22 Smith KE, Fritzell S, Badn W, Eberstal S, Janelidze S, Visse E, Darabi A, Siesjo P (2009) Cure of established GL261 mouse gliomas after combined immunotherapy with GM-CSF and IFNgamma is mediated by both CD8+ and CD4+ T-cells. Int J Cancer 124:630-637.

23 Sofroniew MV, Vinters HV (2010) Astrocytes: biology and pathology. Acta Neuropathol 119:7-35.

24 Solinas G, Germano G, Mantovani a, Allavena P (2009) Tumor-associated macrophages (TAM) as major players of the cancer-related inflammation. Journal of leukocyte biology 86:1065-1073.

25 Stupp R, Dietrich PY, Ostermann Kraljevic S, Pica A, Maillard I, Maeder P, Meuli R, Janzer R, Pizzolato G, Miralbell R, Porchet F, Regli L, de Tribolet N, Mirimanoff RO, Leyvraz S (2002) Promising survival for patients with newly diagnosed glioblastoma multiforme treated with concomitant radiation plus temozolomide followed by adjuvant temozolomide. J Clin Oncol 20:1375-1382.

26 Stupp R, Mason WP, van den Bent MJ, Weller M, Fisher B, Taphoorn MJ, Belanger K, Brandes AA, Marosi C, Bogdahn U, Curschmann J, Janzer RC, Ludwin SK, Gorlia T, Allgeier A, Lacombe D, Cairncross JG, Eisenhauer E, Mirimanoff RO (2005) Radiotherapy plus concomitant and adjuvant temozolomide for glioblastoma. N Engl J Med 352:987-996.

27 Zhang B, Yao G, Zhang Y, Gao J, Yang B, Rao Z, Gao J (2011) M2-Polarized tumor-associated macrophages are associated with poor prognoses resulting from accelerated lymphangiogenesis in lung adenocarcinoma. Clinics 66:1879-1886.